Title
Improving Titer and Infectivity of Lentiviral Vectors for Gene and Cell Therapy

Author
Han, Jiaying

Publication Date
2021

Peer reviewed|Thesis/dissertation

UNIVERSITY OF CALIFORNIA

Los Angeles

Improving Titer and Infectivity of Lentiviral Vectors for Gene and Cell Therapy

A dissertation submitted in partial satisfaction of the

requirements for the degree Doctor of Philosophy

in Molecular and Medical Pharmacology

by

Jiaying Han

2021

ABSTRACT OF THE DISSERTATION

Improving Titer and Infectivity of Lentiviral Vectors for Gene and Cell Therapy

by

Jiaying Han

Doctor of Philosophy in Molecular and Medical Pharmacology

University of California, Los Angeles, 2021

Professor Donald Barry Kohn, Chair

Lentivirus is a type of retrovirus that can integrate viral genetic information into the DNA of the host cell. Lentivirus has gone through generations of engineering to become a safe robust gene delivery vehicle for gene and cell therapies, known as the lentiviral vectors (LVs). LVs demonstrate advantages over other gene delivery methods including effective infections of both dividing and non-dividing cells, long-term stable expression of the transgene, and relatively safe integration profile. Autologous hematopoietic stem cell transplant (HSCT) in combination with gene therapy has successfully treated multiple genetic blood diseases, such as sickle cell disease and severe combined immunodeficiency, in clinical trials. In this approach, the patient's own HSCs are collected from either bone marrow or mobilized peripheral blood, genetically modified with LVs in a cell-culture plate, and transplanted back to the same patient, thereby avoiding many immune complications associated with allogeneic HSCT. The genetically modified HSCs with the therapeutic gene can self-renew and differentiate into different blood cells, therefore providing life-long therapeutic benefits for patients.

The success of lentiviral gene therapy relies on several intrinsic properties of the LVs. The first property is the viral titer, the concentration of transduction units (TU) per milliliter (mL). We and others have observed that titer decreases with increasing vector length, making it difficult to produce LVs with high titers for diseases that require large transgenes. Next, infectivity or the gene transfer capacity is a measure of how well the vector can transfer its genome into HSCs at a given dose of TU/mL. Some LVs have limited gene transfer capacity that the copies of the integrated genome do not further increase with additional TU and cannot achieve the minimum copy number required for therapeutic benefits.

Although the vector length is a well-known factor that affects titer and infectivity, how the vector genome limits the lentiviral lifecycle remains elusive. In Chapter 2, we compared a "well-behaved" clinical LV, EFS-ADA (4 kb), and a "poorly-performing" β-globin LV, Lenti/βAS3-FB (8.9 kb), at different steps of lentiviral lifecycle and identified several rate-limiting steps. We observed that the viral RNA (vRNA) of Lenti/βAS3-FB, but not vRNA of EFS-ADA, was heavily truncated. These truncated vRNAs failed to be reverse transcribed and subsequently cannot be integrated into the host cell genome. We also demonstrated that virion particle formation, measured by p24 ELISA, was impaired in Lenti/βAS3-FB and other reverse-oriented LVs, as they triggered certain cellular antiviral responses. Our findings uncovered two rate-limiting steps, vRNA truncation and defective virion formation, in the lentiviral lifecycle leading to low titer and infectivity.

We then developed strategies to overcome these two roadblocks. In Chapter 3, we focused on overcoming cellular restriction factors (RF) in the packaging cells by conducting a targeted CRISPR Cas9 screen to knock out potential RFs. We created a new packaging cell line **C**RISPRed **HE**K293T to **D**isrupt **A**ntiviral **R**esponses (CHEDAR) by knocking out OAS1, LDLR,

and PKR. In Chapter 4, we explored several methods to improve vRNA production, such as shortening the vector length, packaging with Tat, and overexpressing transcription elongation factors. The strategies described in Chapters 3 and 4 worked additively to increase titer and infectivity of different LVs, especially those with low titer or reverse-oriented transgene cassettes.

In summary, the work described in this thesis elucidates the rate-limiting steps in lentiviral production and demonstrates multiple strategies to increase titer and infectivity of LVs. We hope this work help to advance the field of gene and cell therapy by improving the production technology and reducing the cost to make the therapy more effective and accessible for patients.

The dissertation of Jiaying Han is approved.

Samson Chow

Matteo Pellegrini

Ting-Ting Wu

Donald Barry Kohn, Committee Chair

University of California, Los Angeles

2021

DEDICATION

To my dearest parents, Zhihong and Xianglan, for giving me everything in the world that I have ever wanted.

To the love of my life, Cheddar the Corgi, for patiently yet grumpily waiting for me to get home while watching her favorite Roku fish tank screensaver.

TABLE OF CONTENTS

LISTS OF FIGURES AND TABLES

CHAPTER 1

CHAPTER 2

CHAPTER 3

CHAPTER 4

ACKNOWLEDGEMENTS

First and foremost, I would like to thank my mentor, Dr. Donald Kohn. Don not only taught me how to practice science but also what it means to be an amazing human being. The first lesson he taught me was persistence. When I first emailed him to rotate in his lab, he said no because he had already taken in four other rotation students. Awkward as usual, I emailed him again and again (and maybe a few more times after that). Ultimately, he responded back saying that “Persistence is a good thing and should be rewarded. Let’s have a meeting.” From working in his lab for four years, I have witnessed that no matter how busy and successful he is, he never lets anything stop him from helping his patients, mentoring his students, and cracking jokes at lab meetings. I guess that is the second thing he taught me—never forget your initial goal. The word “cure” is a seemingly taboo word in science that researchers avoid using with regards to their research. However, Don has cured hundreds of patients who were otherwise deemed incurable. I feel so fortunate to have entered the realm of gene therapy under the guidance of Don. Don has and will forever be an important role model in my life.

I would also like to thank Dr. Roger Hollis. Roger is a real-world Doraemon, a manga character who solves all the problems in the world by taking out magical tools from his 4D pocket. He always has the perfect solutions to my infinite questions, just like how he always has candies in his locker for the lab. He gave me so many instructions and inspirations on how to design experiments, what experiments to do, where to find things, how to write grants/paper... As long as it’s science related, there is nothing Roger doesn’t know. When I first started in the lab and couldn’t say anything right, he would patiently listen to me practice presentations and explain data. He taught me how to tactfully walk people through my data and conclusions. I feel like I have infinite things to learn from Roger whenever I talk to him. Roger is so knowledgeable and resourceful that I could not ask for a better desk mate and mentor.

I appreciate the advice and help from my doctoral committee: Dr. Sam Chow, Dr. Ting-Ting Wu, and Dr. Matteo Pellegrini. I remember on my interview super day, Sam walked with me to Terasaki. I found myself thinking what a nice professor! I am so grateful for the kindness that Sam has shown me throughout my PhD to make me feel that this foreign land could be

home. The first time I received reverse transcription kinetics data, Sam had an insightful discussion with me and taught me how to analyze the data. Ting-Ting has provided me tons of great suggestions during our committee meetings and the virology seminar. She gave me the idea to knock out ZAP and many other antiviral genes to increase titer. Matteo asked me challenging questions about next-generation sequencing, which I cannot be more appreciative of as I really have so much to learn.

I want to thank Curtis and Kevin, who are my former mentees, current technicians, and my younger brothers. Many years have passed since I gave Kevin the scary quiz when I interviewed him. He really demonstrated his intelligence and work ethic and defeated all the other candidates. Adopting Kevin and Curtis was one of the best decisions I have made in my PhD. Both Curtis and Kevin helped me so much throughout my PhD and completed so much work in this thesis. I hope our friendship will continue, and in the future when my family is sick, I know who to go to because I know they will without a doubt be brilliant doctors! I am certain that Curtis and Kevin will have bright futures.

It has been wonderful to work alongside my lab mates—Dr. Caroline Kuo, Dr. Zulema Romero, Ralph Crisostomo, Marlene Ruiz, Paul Ayoub, Jason Quintos, Dr. David Gray, Edward Trope, Joseph Long, Shantha Senadheera, Dr. Kathryn Bradford, Dr. Kate Masiuk, Dr. Richard Morgan, Ryan Wong and many more. Caroline was my mentor during my rotation project and taught me many invaluable skills. Three years ago I told Caroline I wanted to be her when I grow up, which probably made her cringe, but I still think the same way today! She is so successful as a female scientist and doctor, and coupled with her great sense of humor and interpersonal skills, she is still my inspiration. I am also very grateful for the help I received from Marlene, Jason and Shantha. Thank you to all my lab mates for the help and support in the past four years. I also appreciate the opportunity to buy Ralph coffees every week in exchange for fun conversations. Let’s hang out in the Bay! And yes, my Overwatch buddies Paul and Jason, you guys brought me so much joy and laughter (and stress) during COVID. In 50 years, we can tell our grandchildren we survived COVID by playing Overwatch.

To my amazing friends—Lisa Ta, Dr. Diane Kim, Zhiyuan Mao, Jiaji Yu, Yuchen Wang, Feiyang Ma, Vivian Lu, and many more! Forgive me that I cannot mention all of you. Thank you for the amazing support, laughter, and love you have given me. I came to the United States by myself when I was eighteen. My undergrad years were difficult because of the culture shock and language barrier. You are the light in my graduate school. You have demonstrated time and time again that I am not alone and have gifted me with so many meaningful memories. I hope our friendship will last forever.

To Dr. Francesca Cole, thank you for encouraging and supporting me in so many ways in my pursuit of a PhD. You were one of my first mentors in science—you set an example of how to be a great mentor and female scientist. Without your support, I would not have been able to get in to graduate school, let alone complete my degree.

I want to thank Steven Fang for taking care of me in every single way and for putting up with my sloppiness. Although I have spent almost a third of my life in the United States, I still struggle every day to survive in this land where felt I didn't belong. You helped me improve my English and taught me the culture, giving me a sense of belonging. Thank you for visiting my mom with me every week, eating dinner with me every day, and cooking for Cheddar (no one has done that before)! Life is a one-way bus ride. The people we meet are the passengers who come and go. I am grateful that you are the one sitting next to me on this journey.

Lastly, I would like to thank my family—Zhihong Han, Xianglan Guan, and Cheddar Han. My parents have given me the world. Everything I have ever wanted, my parents made sure I had and more. I am so sorry that I could not be with you these past 10 years. My dad was my original inspiration to pursue a career in biomedical science and taught me the importance of hard work. I hope one day I can be as successful as my dad. Thank you Mom for your eternal love and support. You always wait for me to come home, no matter how late, and ladle me a bowl of hot soup, which warms my heart. I didn't fully understand what your love meant until I had Cheddar. Thank you Cheddar for teaching me the meaning of love and being a perpetual source of happiness.

VITA

EDUCATION

University of California, Los Angeles (UCLA) Los Angeles, CA
PhD, Molecular and Medical Pharmacology 09/2016-expected 06/2021

Rice University
Houston, TX
BA, Biochemistry and Cell Biology 08/2012-05/2016
BA, Visual and Dramatic Arts

RESEARCH EXPERIENCE

Kohn Lab | UCLA Los Angeles, CA
Graduate Student Researcher 06/2017-Present
- Elucidated novel mechanisms of viral titer and infectivity reduction of lentiviral vectors (LV)
- Developed strategies to improve the production technology of LVs, reducing vector production cost by 97%

Cole Lab | University of Texas MD Anderson Cancer Center Smithville, TX
Researcher Assistant 06/2015-08/2015
- Defined the role of mammalian Exonuclease 1 in meiotic homologous recombination in the mouse model
- Conducted immunocytological analysis of the enzyme complex that resolves double Holliday Junctions

PROFESSIONAL EXPERIENCE

Technology Development Group Los Angeles, CA
Business Development Fellow 06/2019-03/2021
- Assisted in managing the intellectual property portfolio and licensing activities via market analysis and licensee identification
- Synthesized deliverables for the licensing of UCLA technologies by assessing novelty, integrity of data, and commercial potential

Tianxin Pharmaceutical Company Jiangxi, China
Quality Control Intern 06/2014-08/2014
- Increased QC workflow efficiency by identifying redundancy in workflows and personnel
- Presented key findings to the c-suites after examining 180 QC reports overseeing $5MM in Vitamin B_6

LEADERSHIP

UCLA Advanced Degree Consulting Club Los Angeles, CA
Vice President 09/2019-Present
- Successfully initiated pro bono consulting cases by synthesizing and pitching proposals to potential clients
- Redesigned the club's marketing strategy to focus on reaching students across multiple online platforms

UCLA Department of Molecular Pharmacology Los Angeles, CA
Student Representative 10/2017-11/2019
- Spearheaded planning of 10+ departmental events

• Restructured the annual retreat to prioritize science quality and professional development

PUBLICATIONS

- **Han, J.**, Tam, K., Ma, F., Tam, C., Aleshe, B., Wang, X., Quintos, J.P., Morselli, M., Pellegrini, M., Hollis, R.P., et al. (2021). β-Globin Lentiviral Vectors Have Reduced Titers due to Incomplete Vector RNA Genomes and Lowered Virion Production. Stem Cell Reports. DOI: 10.1016/j.stemcr.2020.10.007
- **Han J.**, Tam K., Tam C., Hollis R.P., & Kohn D.B. (2021). Improved Lentiviral Vector Titers from a Multi-Gene Knock-out Packaging Line. In preparation.
- Zelazowski, M. J., Sandoval, M., Paniker, L., Hamilton, H. M., **Han, J**., Gribbell, M. A., Kang, R., & Cole, F. Age-Dependent Alterations in Meiotic Recombination Cause Chromosome Segregation Errors in Spermatocytes. *Cell*. 2017;171(3):601–614.e13. doi:10.1016/j.cell.2017.08.042

ORAL PRESENTATIONS

- **Han J**., Tam K., Tam C., Hollis R.P., Kohn D.B. Improved Lentiviral Vector Titers from a Multi-Gene Knock-out Packaging Line. American Society of Gene and Cell Therapy Annual Conference. May 2021.
- **Han J.**, Tam K., Aleshe B., Hollis R.P., & Kohn D.B. Developing Strategies to Improve the Titers and Gene Transfer of Complex Lentiviral Vectors. American Society of Gene and Cell Therapy Annual Conference. Washington, DC. May 2019.
- **Han J.**, Tam K., Aleshe B., Hollis R.P., & Kohn D.B. Developing Strategies to Improve the Titers and Gene Transfer of Complex Lentiviral Vectors. UCLA AIDS Institute Virology Seminar. Los Angeles, CA. 2019.
- **Han J.**, Tam K., Aleshe B., Hollis R.P., & Kohn D.B. Developing Strategies to Improve the Titers and Gene Transfer of Complex Lentiviral Vectors. UCLA Molecular Medical Pharmacology Seminar. Los Angeles, CA. 2019.

POSTER PRESENTATIONS

- **Han J**, Tam K., Tam C., Hollis R.P., & Kohn D.B. β-Globin Lentiviral Vectors Have Reduced Titers Due to Incomplete Vector RNA Genomes and Lowered Virion Production. Broad Stem Cell Research Center Symposium. Los Angeles, CA. 2020.
- **Han J**, Tam K., Tam C., Hollis R.P., & Kohn D.B. β-Globin Lentiviral Vectors Have Reduced Titers Due to Incomplete Vector RNA Genomes and Lowered Virion Production. UCLA Molecular Medical Pharmacology Retreat. Huntington Beach, CA. 2019.
- **Han J**, Tam K., Hollis R.P., & Kohn D.B. Developing Strategies to Improve the Titers and Gene Transfer of Complex Lentiviral Vectors. UCLA Molecular Medical Pharmacology Retreat. Huntington Beach, CA. 2018.
- **Han J**, Hamilton HM, Sandoval M, Cole F. Defining the Role of EXO1 in Meiotic Homologous Recombination. *Summer Undergraduate Research Poster Symposium*. Houston, TX, August, 2015.
- Hamilton HM, **Han J**, Sandoval M, Zelazowski M, Gribbell M, Paniker L, Cole F. Defining the Roles of Exo1 in Regulating Mouse Meiotic Recombination. *EMBO Meiosis Meeting.* Oxford, UK, August, 2015.

AWARDS

- NIH Virology and Gene Therapy Training Grant 09/2018-09/2019
  (Ruth L. Kirschstein National Research Service Award AI060567)
- American Society of Gene and Cell Therapy Conference Meritorious Travel Award 05/2019

CHAPTER 1

INTRODUCTION

The Development of Lentiviral Vectors in Gene and Cell Therapy

INTRODUCTION

Gene therapy enables the addition, deletion, or modification of a person's genome with the intention of treating diseases, such as those caused by genetic deficiencies. Moreover, gene therapy can endow a cell with a new capability that doesn't exist in the natural state. An example is the adoptive T cell therapy for treating cancers, which enables T cells to recognize antigens that the endogenous T cell receptors cannot recognize.

Retroviral vectors are typically used as gene delivery vehicles because they result in a stable integration of the gene of interest to be expressed in the host cells. There are two types of retroviral vectors, γ-retroviruses derived from murine leukemia viruses (MLV) and lentiviruses derived from HIV-1[1]. There has been a general tendency to switch from using MLV vectors to lentiviral vectors (LV) since the mid-2000s for several reasons: 1) unlike MLV which can only transduce dividing cells, lentiviruses can transduce both dividing and non-dividing cells; 2) lentiviruses tend to have safer integration profile compared to MLV vectors[2].

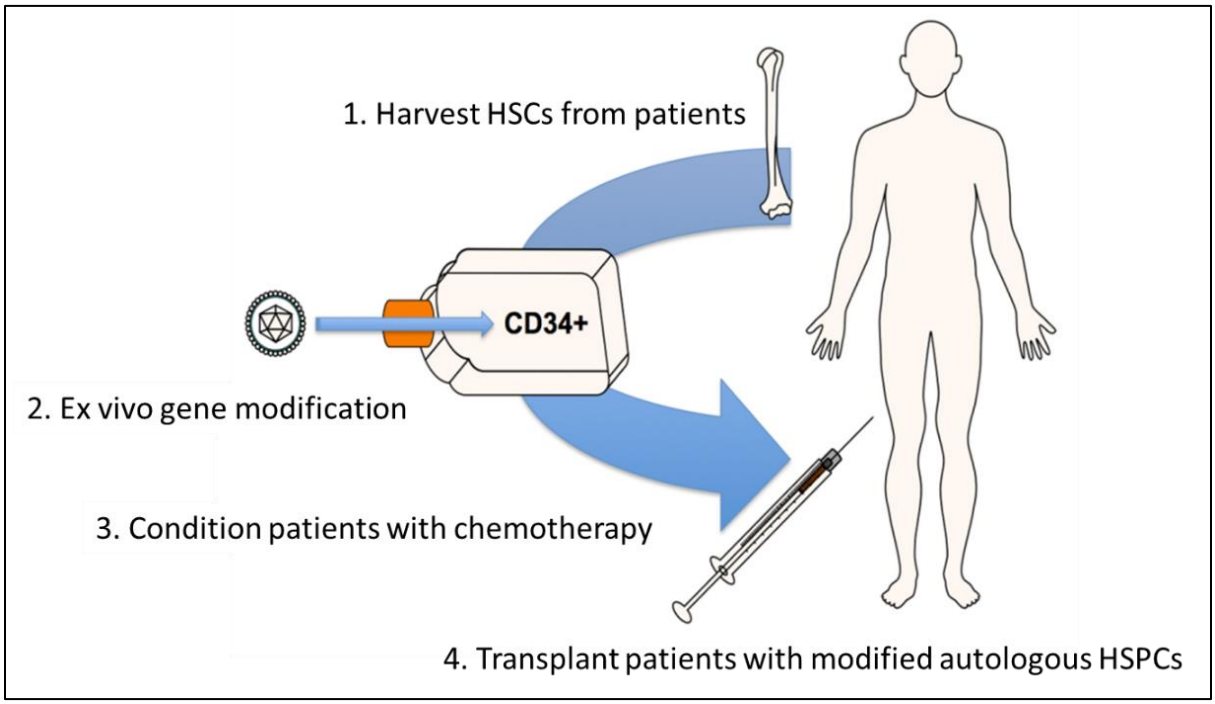

Figure 1. Autologous HSC transplant in combination with ex vivo gene therapy

In the past, patients with blood cell genetic diseases, such as sickle cell disease, severe combined immunodeficiency, chronic granulomatous disease, and many more, had limited treatment options. The only cure available for these patients was an allogenic HSC transplant from an immunologically matching donor. Although allogenic HSC transplant has been successful, many patients could not find an immunologically matching donor. Even when donors are available, the recipients face many immunological complications, including graft versus host disease and graft rejection. In contrast, autologous hematopoietic stem cell transplant in combination with gene therapy uses patients' own HSCs for *ex vivo* gene modification and subsequently reinfuses the cells back to the same patients, thereby avoiding many immune complications (Fig. 1). Hematopoietic stem cell (HSC) transplant in combination with lentiviral-based gene therapy has successfully treated various genetic blood cell diseases in clinical trials[3–6].

With the advances of clinical successes, several gene and cell therapy drug products have been approved by FDA for commercial uses. CAR T-cell therapies, Yescarta and Kymriah, were approved by FDA to treat aggressive B-cell lymphomas, B-cell leukemia, and relapsed or refractory mantle cell lymphoma. The production capability of clinical-grade LVs is a critical issue for the implementation of these novel therapies to become standard of care. Thus, this chapter discusses lentiviral biology, and the development of lentiviral vectors, and the clinical applications of LVs.

LENTIVIRAL BIOLOGY

LV is derived from the single-stranded RNA retrovirus, HIV-1. The basic viral genes required for lentiviral survival and functions are the *gag*, *pol*, and *env* genes[7]. *Gag* encodes the structural polyprotein, matrix, capsid, and nucleocapsid proteins, for the assembly of the viral

particles. *Pol* encodes several critical enzymes for lentiviral activity, including reverse transcriptase, integrase, and protease. *Env* encodes the viral surface glycoprotein gp160 that is cleaved into two segments: gp120 mediates viral binding to cells, and gp41 regulates the fusion of viral particles and cellular membrane. These components enable LVs to retain the essential functions of HIV-1.

In addition to these essential genes, the lentiviral genome also contains auxiliary genes, such as *vpr*, *vif*, *vpu*, and *nef*, as well as regulatory genes, such as *tat* and *rev*[7,8]. Vpr promotes cell-cycle arrest and assists the infection of non-dividing cells. Vif inhibits the host cell antiviral factor APOBEC3G and promotes a more stable reverse transcriptase complex. Vpu facilitates the release of virions. Nef prevents cell suicide and enhances viral infectivity, contributing to the progress of HIV. Tat enhances viral RNA transcription by regulating RNA polymerase II. Lastly, Rev binds to the rre sequence on viral RNA and promotes the nuclear export of the transcripts. These components, except Rev, were generally considered to be optional for the production of lentiviral vectors in the third generation of the packaging system.

The lentiviral lifecycle begins when the viral envelope glycoprotein binds to the specific receptor on the cellular membrane. After the initial interaction, viral transmembrane proteins change conformation to allow the membrane fusion of the virus and host cell. Upon entering the cell, the structural proteins uncoat to release the viral RNA and proteins into the cytoplasm. The viral RNA is reverse transcribed into double-stranded viral DNA. The viral DNA is then imported into the nucleus and integrated into the host cell genome. The integrated proviral genome is transcribed and translated using the host cell machinery, producing essential viral proteins and viral RNA for the assembly of new viral particles. The viral progenies are subsequently released into the extracellular space from the host cell through a process known as budding. The viral progenies can infect other cells and repeat this lifecycle to replicate.

DEVELOPMENT OF LENTIVIRAL VECTORS

Packaging Systems

In an attempt to make lentivirus safer and less pathogenic, three generations of LV production system by transient transfection were developed (Fig. 2)[23]. The first generation of packaging system has all of the HIV-1 genes except the envelope. The second generation of packaging system further removes all the auxiliary genes, such as *vpr*, *vif*, *vpu*, and *nef*. To date, the third-generation packaging system remains to be the most widely used system for R&D and clinical purposes. It is a four-plasmid system, including the transfer plasmid encoding the viral RNA, envelope plasmid encoding the structural envelope protein, packaging plasmid encoding gag and pol, and lastly regulatory protein-encoding rev. The nonoverlapping split genome constructs reduce the potential of recombination, which could result in the generation of replication-competent lentivirus[8]. Tat is also deleted in the third-generation packaging system. Tat enhances transcription by binding to the U3 promoter of the 5' long-terminal repeats (LTR), which has been replaced by a constitutively active promoter, such as cytomegalovirus (CMV)

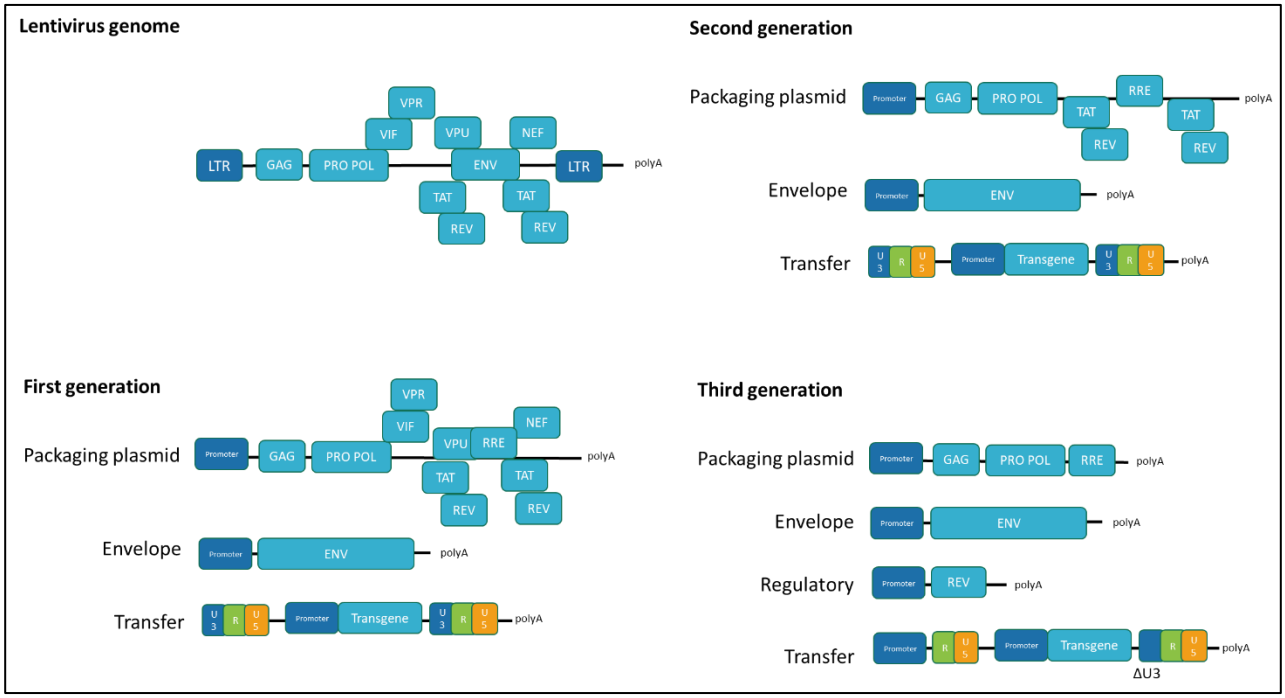

Figure 2. Different generations of lentiviral packaging plasmids

promoter [9–11] or Rous Sarcoma Virus (RSV) promoter[8]. The deletions of the enhancers and promoter in U3 also prevent the self-activation of the LV in target cells so that no full-length viral RNA can be transcribed after integration. These advancements in vector development minimize the possibility of recombination and prevent the insertional activation of cellular oncogenes or transcriptional interferences by the integrated viral genomes.

Lentiviral Vector Production

A common way to produce LVs is through transient transfection of HEK293T cells. The workflow is outlined in Fig. 3. HEK293T are plated in tissue culture-treated plates 24 hours before transfection. ~70% of confluent cells are transfected with the various plasmids discussed above. Different transfection reagents have been tested, including calcium phosphate[12], polyethylenimine[13], and lipofectamine[14]. ~20 hours after transfection, cells are incubated in D10 with 10 mM sodium butyrate and 20 mM HEPES for 6-8 hours. Sodium butyrate treatment leads to histone hyperacetylation, which transforms the chromatin structure into a more relaxed state and increases the gene transcription level. Cells are allowed to transcribe viral components for assembly into viral particles. LVs can be collected either as raw supernatant or concentrated virus. Typical raw lentiviral titer range from 10^5 to 10^7 transduction unit per mL.

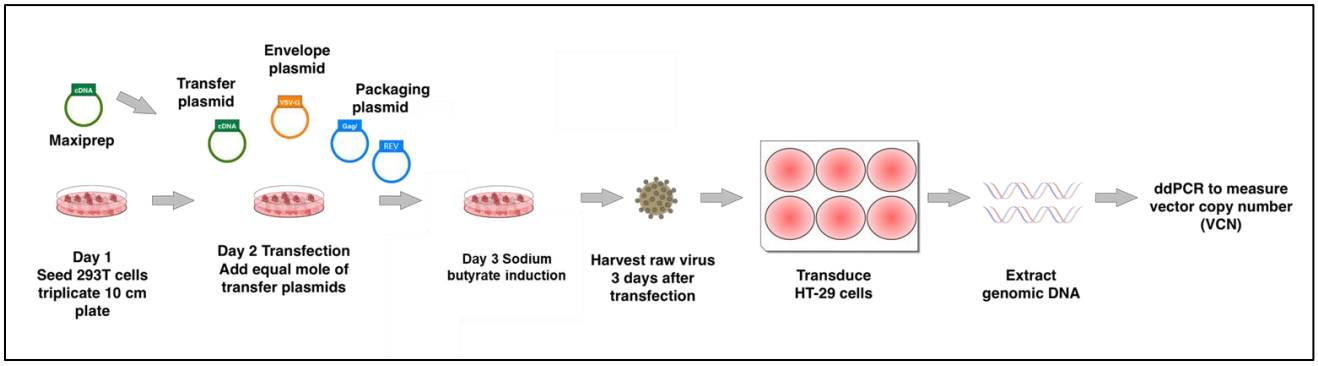

Figure 3. Workflow of packging and titering

Increased titers for *in vivo* applications can be achieved by techniques, such as ultracentrifugation and ultrafiltration. Ultracentrifugation is a technique used to spin LVs at a high speed (26,000 rpm for 90 minutes at 4^{o}C) to isolate the smaller sized infectious particles and remove the excess media. Ultrafiltration uses the fluid pressure to drive the migration of the undesired smaller molecules through an ultrafiltration membrane with the retention of desired bigger molecules. LVs pseudotyped with VSVG glycoprotein have been shown to be compatible with both ultracentrifugation and ultrafiltration without significant loss in titer[15,16]. Then the LVs are typically titered in a cell line to determine the transduction units per mL. We typically use the LVs to transduce HT-29 colorectal adenocarcinoma cells and measure the vector copy number 3 days after transduction by droplet digital PCR (ddPCR).

HEK293T is commonly used for LV production because of the fast cell growth rate and high transfection efficiency in comparison to the parental HEK293 cells[17]. The parental HEK293 cells were transformed into HEK293T cells by the introduction of human adenovirus 5 (hAd5) DNA and the expression of the large T antigen (TAg) of simian virus 40 (SV40). The TAg and adenovirus E1A inactivates the cellular tumor suppressor p53 and inhibits interferon (IFN) responses by suppressing IRF3 and other IFN-dependent transcription[18–20]. However, HEK293T cells are relatively limited in scalability because of the adherent nature of these cells. Hence, several adherent cell lines, like 293T, 293FT, and 293SF-3F6, have been modified into suspension cells by selecting them in chemically defined media (Freestyle 293 and F17)[21–23]. These suspension cells can be cultured in bioreactors, and therefore enable the industrial large-scale production of LVs.

LENTIVIRAL VECTOR APPLICATIONS AND CHALLENGES

Functioning as a powerful and versatile vehicle for gene delivery, LV has enabled a broad range of applications, from biological research to human gene therapy. LVs are commonly used in research labs to express the gene of interest in the desired cells or express small interfering/short hairpin RNAs to suppress gene expressions. LVs have moved beyond the preclinical stage into clinical trials since the mid-2000s and have been used to effectively and safely treat multiple disorders. The diseases that have been treated with LVs in clinical trials include adenosine deaminase severe combined immune deficiency, X-linked severe combined immune deficiency, Wiskott-Aldrich Syndrome, chronic granulomatous disease, leukocyte adhesion deficiency, sickle cell disease, beta-thalassemia, Gaucher Disease, Fanconi anemia, and etc[24]. Using autologous HSCs for genetic modification avoids GVHD and reduces the amounts of conditioning chemotherapy required for the engraftment of HSCs, allowing improved safety profiles. Despite these early clinical successes, there are many challenges to overcome in order to translate gene and cell therapy into clinics.

We and others have observed that the titer and infectivity of LVs decrease with increasing proviral length. Low titer leads to low yield and increased production cost. Current platforms of vector production and purification process are not capable to package enough viruses for the treatment of diseases that affect many patients, such as leukemia, B-cell lymphoma, and sickle cell disease. Low infectivity means a larger dose of LVs is needed to achieve the therapeutic effect, further increasing the cost of the therapy. Moreover, a larger dose of LVs can potentially lead to greater side effects and elicit more intense immune responses in the transduced cells. In our clinical trial for sickle cell disease with the 8.9-kb Lenti/βAS3FB, we observed suboptimal gene transfer (average 0.3 vector genomes/cell) in the patient and unfortunately did not achieve a sufficiently high copy number to correct the disease. The mechanisms of how increased proviral length leads to decreased titer and infectivity

remained elusive. Chapter 2 explores some of the mechanisms that cause low titer and infectivity and provides insights into how to overcome these hurdles.

Another challenge of the clinical use of LVs is that each disorder requires its specific vector with optimal expression, titer, and gene transfer efficiency. The vector development process takes years, as one parameter is typically optimized at the expense of the others. We have observed that the expression of the vector improves with increasing transgene length, while titer and gene transfer efficiency suffer. While finding a balance between the parameters is possible, vector development is an extremely time-consuming and expensive process. Therefore, in Chapter 3, we created a novel packaging cell line that can be applied to improve titers of different LVs so that expression can be prioritized in the vector development process. Our cell line may enable the applications of LVs with compromised titer but high expressions. Chapter 4 discusses several strategies to improve viral RNA production to improve titer and infectivity.

Despite the bright future that gene and cell therapy hold for treating various difficult diseases, many roadblocks prevent market access and large-scale applications of gene and cell therapy. Bluebird sets a $1.8 million price for its sickle cell disease gene therapy drug. From an R&D and clinical perspective, the high price is understandable because gene therapy development is much more costly than a conventional small molecule drug development. However, most patients cannot afford these gene and cell therapies without insurance coverage.

Improving titer and infectivity serves to decrease the production and treatment cost. The work in this thesis elucidated the mechanisms leading to low titer and infectivity and proposed several strategies to overcome those rate-limiting steps, resulting in improved titer and infectivity of LVs. We further created a versatile packaging cell line that can be readily applied to improve

the production of different LVs. We hope this work paves the way to decrease the cost and bring this technology to more patients.

REFERENCES

1. Delenda, C. (2004). Lentiviral vectors: Optimization of packaging, transduction, and gene expression. J. Gene Med. *6*.

2. Montini, E., Cesana, D., Schmidt, M., Sanvito, F., Bartholomae, C.C., Ranzani, M., Benedicenti, F., Sergi, L.S., Ambrosi, A., Ponzoni, M., et al. (2009). The genotoxic potential of retroviral vectors is strongly modulated by vector design and integration site selection in a mouse model of HSC gene therapy. J. Clin. Invest. *119*, 964–975.

3. Kohn, D.B., Booth, C., Shaw, K.L., Xu-Bayford, J., Garabedian, E., Trevisan, V., Carbonaro-Sarracino, D.A., Soni, K., Terrazas, D., Snell, K., et al. (2021). Autologous Ex Vivo Lentiviral Gene Therapy for Adenosine Deaminase Deficiency. N. Engl. J. Med., NEJMoa2027675.

4. Aiuti, A., Cattaneo, F., Galimberti, S., Benninghoff, U., Cassani, B., Callegaro, L., Scaramuzza, S., Andolfi, G., Mirolo, M., Brigida, I., et al. (2009). Gene therapy for immunodeficiency due to adenosine deaminase deficiency. N. Engl. J. Med. *360*, 447–58.

5. De Ravin, S.S., Wu, X., Moir, S., Anaya-O'Brien, S., Kwatemaa, N., Littel, P., Theobald, N., Choi, U., Su, L., Marquesen, M., et al. (2016). Lentiviral hematopoietic stem cell gene therapy for X-linked severe combined immunodeficiency. Sci. Transl. Med. *8*.

6. Cartier, N., Hacein-Bey-Abina, S., Von Kalle, C., Bougnères, P., Fischer, A., Cavazzana-Calvo, M., and Aubourg, P. (2010). [Gene therapy of x-linked adrenoleukodystrophy using hematopoietic stem cells and a lentiviral vector]. Bull. Acad. Natl. Med. *194*, 255–64; discussion 264-8.

7. Milone, M.C., and O'Doherty, U. (2018). Clinical use of lentiviral vectors. Leukemia *32*, 1529–1541.

8. Dull, T., Zufferey, R., Kelly, M., Mandel, R.J., Nguyen, M., Trono, D., and Naldini, L. (1998). A Third-Generation Lentivirus Vector with a Conditional Packaging System. J. Virol. *72*, 8463–8471.

9. Kim, V.N., Mitrophanous, K., Kingsman, S.M., and Kingsman, A.J. (1998). Minimal Requirement for a Lentivirus Vector Based on Human Immunodeficiency Virus Type 1. J. Virol. *72*, 811–816.

10. Miyoshi, H., Blömer, U., Takahashi, M., Gage, F.H., and Verma, I.M. (1998). Development of a Self-Inactivating Lentivirus Vector. J. Virol. *72*, 8150–8157.

11. Zufferey, R., Dull, T., Mandel, R.J., Bukovsky, A., Quiroz, D., Naldini, L., and Trono, D. (1998). Self-Inactivating Lentivirus Vector for Safe and Efficient In Vivo Gene Delivery. J. Virol. *72*, 9873–9880.

12. Marino, M.P., Luce, M.J., and Reiser, J. (2003). Small- to large-scale production of lentivirus vectors. Methods Mol. Biol. *229*, 43–55.

13. Boussif, O., LezoualC'H, F., Zanta, M.A., Mergny, M.D., Scherman, D., Demeneix, B., and Behr, J.P. (1995). A versatile vector for gene and oligonucleotide transfer into cells in culture and in vivo: Polyethylenimine. Proc. Natl. Acad. Sci. U. S. A. *92*, 7297–7301.

14. Pham, P.L., Kamen, A., and Durocher, Y. (2006). Large-scale transfection of mammalian cells for the fast production of recombinant protein. In Molecular Biotechnology (Mol Biotechnol), pp. 225–237.

15. Bartz, S.R., and Vodicka, M.A. (1997). Production of high-titer human immunodeficiency virus type 1 pseudotyped with vesicular stomatitis virus glycoprotein. Methods A Companion to Methods Enzymol. *12*, 337–342.

16. Cooper, A.R., Patel, S., Senadheera, S., Plath, K., Kohn, D.B., and Hollis, R.P. (2011). Highly efficient large-scale lentiviral vector concentration by tandem tangential flow filtration. J. Virol. Methods *177*, 1–9.

17. Gama-Norton, L., Botezatu, L., Herrmann, S., Schweizer, M., Alves, P.M., Hauser, H., and Wirth, D. (2011). Lentivirus production is influenced by sv40 large t-antigen and chromosomal integration of the vector in hek293 cells. Hum. Gene Ther. *22*, 1269–1279.

18. Ronco, L. V., Karpova, A.Y., Vidal, M., and Howley, P.M. (1998). Human papillomavirus 16 E6 oncoprotein binds to interferon regulatory factor-3 and inhibits its transcriptional activity. Genes Dev. *12*, 2061–2072.

19. Fonseca, G.J., Thillainadesan, G., Yousef, A.F., Ablack, J.N., Mossman, K.L., Torchia, J., and Mymryk, J.S. (2012). Adenovirus evasion of interferon-mediated innate immunity by direct antagonism of a cellular histone posttranslational modification. Cell Host Microbe *11*, 597–606.

20. Juang, Y.T., Lowther, W., Kellum, M., Au, W.C., Lin, R., Hiscott, J., and Pitha, P.M. (1998). Primary activation of interferon A and interferon B gene transcription by interferon regulatory factor 3. Proc. Natl. Acad. Sci. U. S. A. *95*, 9837–9842.

21. Witting, S.R., Li, L.H., Jasti, A., Allen, C., Cornetta, K., Brady, J., Shivakumar, R., and Peshwa, M. V. (2012). Efficient large volume lentiviral vector production using flow electroporation. Hum. Gene Ther. *23*, 243–249.

22. Ansorge, S., Lanthier, S., Transfiguracion, J., Durocher, Y., Henry, O., and Kamen, A. (2009). Development of a scalable process for high-yield lentiviral vector production by transient transfection of HEK293 suspension cultures. J. Gene Med. *11*, 868–876.

23. Merten, O.W., Hebben, M., and Bovolenta, C. (2016). Production of lentiviral vectors. Mol. Ther. - Methods Clin. Dev. *3*, 16017.

24. Morgan, R.A., Gray, D., Lomova, A., and Kohn, D.B. (2017). Hematopoietic Stem Cell Gene Therapy: Progress and Lessons Learned. Cell Stem Cell *21*, 574–590.

25. Biffi, A., Bartholomae, C.C., Cesana, D., Cartier, N., Aubourg, P., Ranzani, M., Cesani, M., Benedicenti, F., Plati, T., Rubagotti, E., et al. (2011). Lentiviral vector common integration sites in preclinical models and a clinical trial reflect a benign integration bias and not oncogenic selection. Blood *117*, 5332–5339.

26. Cartier, N., Hacein-Bey-Abina, S., Bartholomae, C.C., Bougnres, P., Schmidt, M., Von Kalle, C., Fischer, A., Cavazzana-Calvo, M., and Aubourg, P. (2012). Lentiviral hematopoietic cell gene therapy for X-linked adrenoleukodystrophy. In Methods in Enzymology (Academic Press Inc.), pp. 187–198.

CHAPTER 2

β-Globin Lentiviral Vectors Have Reduced Titers Due to Incomplete Vector RNA Genomes and Lowered Virion Production

ABSTRACT

Lentiviral vectors (LV) commonly used for the treatment of hemoglobinopathies carry long, genomic β-globin sequences to achieve high-level erythroid-specific expression; the β-globin gene is in reverse-orientation to retain critical intronic sequences. These complex vectors often have low titers and suboptimal gene transfer efficiency, hindering clinical translation and commercialization for *ex vivo* gene therapy of hemoglobinopathies. Our overall objectives are to elucidate the mechanism(s) of the titer and infectivity reduction in complex vectors and to develop strategies to improve the vector design and production to create effective LVs for gene therapy. A systematic study of lentiviral lifecycle was conducted to compare a "well-behaved" simple vector, EFS-ADA (4 kb), and a "poorly-performing" complex β-globin vector, CCL-βAS3 (8.9 kb). Many steps of the lentiviral lifecycle were examined: 1) viral RNA production in packaging cells, 2) viral RNA incorporation into the virions, 3) physical particle formation, and 4) reverse transcription. Viral RNA of the complex vector, Lenti/βAS3FB, were significantly more truncated in both packaging cells and LVs than viral RNAs of the simple vector, EFS-ADA. Only 9% vRNA of the complex vector were complete vRNA that can be fully reverse transcribed and integrated into the host cell genomes compared to the 73% for EFS-ADA. Next-generation RNA sequencing was deployed to unbiasedly uncover the coverage of the full transcript. A gradual decrease in coverage toward the 3' end was observed in the viral RNA of the 8.9-kb β-globin vector but not in the 6-kb β-globin vector, suggesting that the truncation may be caused by poor processivity of RNA polymerase (Pol) II. Furthermore, we observed that the complex vector with a reverse-orientation β-globin gene cassette had defective viral particle formation with reduced p24 production. Our findings uncovered an important role of complete vRNAs as substrates for each step of the lentiviral lifecycle and revealed that reverse-oriented Lenti/βAS3-FB had defective particle formation. The identification of the two rate-limiting steps in the lentiviral lifecycle provides insight into new strategies to improve titer and infectivity of lentiviral vectors.

INTRODUCTION

In multiple clinical trials, autologous hematopoietic stem cell (HSCs) transplantation in combination with gene therapy has produced clinical benefits with desirable long-term engraftment of gene corrected HSC and stable gene expression[1–4]. Despite these early successes, the lengthy and complex nature of some LVs has led to several challenges for clinical translation. We and others observed that titers of LVs decrease substantially with increasing proviral length[5,6]. The reduction in titer, especially in the vectors with complex expression cassettes, creates a barrier for scaling up Good Manufacturing Practices (GMP)-grade vector production and significantly increases the production cost for clinical trials and commercialization[7]. Additionally, even when adjusted to matching transduction units, the complex vectors do not efficiently transduce HSCs, which are relatively resistant to LV infection, as efficiently as the simple vectors, often failing to achieve high vector copy number (VCN) and transgene expression to provide therapeutic benefits[8]. Low titer and infectivity associated with complex LVs present hurdles to the use of these LVs to treat diseases with complex transgene cassettes, like Duchenne muscular dystrophy (~15-kb proviral length) and sickle cell disease (~9-kb proviral length)[9,10].

Sickle cell disease (SCD) is one of the most common monogenic disorders worldwide with >250,000 new patients each year[11]. SCD is caused by a point mutation in the sixth codon of the β-globin gene, resulting in an abnormal hemoglobin molecule that aggregates at low oxygen tension, leading to rigid sickle-shaped red blood cells that occlude small blood vessels [12–14]. Using a dominant anti-sickling β-globin gene (e.g. T87Q or βAS3-globin) integrated into the patient's own hematopoietic stem cells which are then reinfused back to the patient can potentially provide healthy non-sickling erythrocytes to patients throughout life. However, the development of β-globin LVs that allows efficient gene transfer into hematopoietic stem and progenitor cells (HSPCs) while maintaining stable, high-level, and lineage-specific expression of

the β-globin gene has been historically challenging[15]. Many regulatory elements from the β-globin locus, such as 5' and 3' untranslated regions, introns, and parts of the β-globin locus control region (LCR), are necessary to maintain stable, high-level expression of the therapeutic gene. In addition, the β-globin gene cassette is typically placed in the anti-sense orientation relative to the direction of genome transcription during packaging, to prevent splicing of introns in the transgene. The complex nature of the β-globin LV, namely the long genome length and reverse orientation of the β-globin cassette, lowers the viral titer and infectivity.

Small molecule transduction enhancers have been reported to improve the transduction efficiency of HSPCs[16–18]. Nonetheless, transduction enhancers do not affect the intrinsic infectious properties of the LVs, such as viral RNA transcription and infectious particle production. New methods to increase titer and gene transfer that can be used in combination with transduction enhancers will lead to additional clinical and commercial benefits.

Although the main reason for poor infectivity and low titer has been attributed to the increased proviral length, the effects of complex proviral construct on lentiviral lifecycle have not been fully explored. Therefore, a systematic study of the lentiviral lifecycle was conducted to compare a "well-behaved" simple vector, EFS-ADA (4 kb), and a "poorly-performing" complex β-globin vector, Lenti/βAS3-FB (8.9 kb). Several steps of the lentiviral lifecycle were examined: 1) viral RNA production in packaging cells, 2) viral RNA incorporation into virions, 3) physical vector particle formation, and 4) reverse transcription.

Our results showed that the viral RNAs of long complex vectors in packaging cells were predominantly incomplete at the 3' end and failed reverse transcription in target cells at the first strand transfer step, thus reducing the amount of vector DNA available for integration. In addition, we observed that the Lenti/βAS3 vector with its β-globin gene expression unit in reverse orientation yielded fewer virion particles (measured by p24 Gag) than were produced with forward-oriented vectors and even with empty vectors lacking any genome. These findings

may facilitate vector development and production not only with β-globin vectors but also with many complex vectors with low titer and infectivity.

RESULTS

Complex vectors had low titer and deficient gene transfer

Lenti/βAS3-FB is an 8.9-kb LV carrying a complex anti-sickling β-globin gene cassette, as previously described by Romero et al[10]. The β-globin gene is driven by the endogenous β-globin promoter and enhancers in the anti-sense (reverse) orientation, with the expression regulated by a "mini" locus control region (LCR) comprised of portions of the β-globin locus DNAse hypersensitive sites (HS) HS2, HS3, and HS4, as shown in Fig. 1A. In addition, Lenti/βAS3-FB contains the Woodchuck Hepatitis Virus post-transcriptional regulatory element (wPRE) and a 77-bp insulator in the U3 region of the 3' LTR, termed as FB (FII-BEAD). EFS-ADA is a 4-kb LV for treating adenosine deaminase severe combined immunodeficiency (ADA-SCID) that is capable of high-level and consistent ADA gene transfer and expression[19,20]. The EFS-ADA vector consists of the human elongation factor-α gene "short" promoter (EFS) driving the expression of a codon-optimized human ADA gene cassette followed by the wPRE, all in the sense (forward) orientation. Both vectors consist of a pCCL backbone and differ only by the internal promoters and transgene cassettes[21]. We defined Lenti/βAS3-FB as a complex LV

because of the lengthy viral genome, additional enhancer elements for lineage-specific expression, and anti-sense orientation of the transgene cassette.

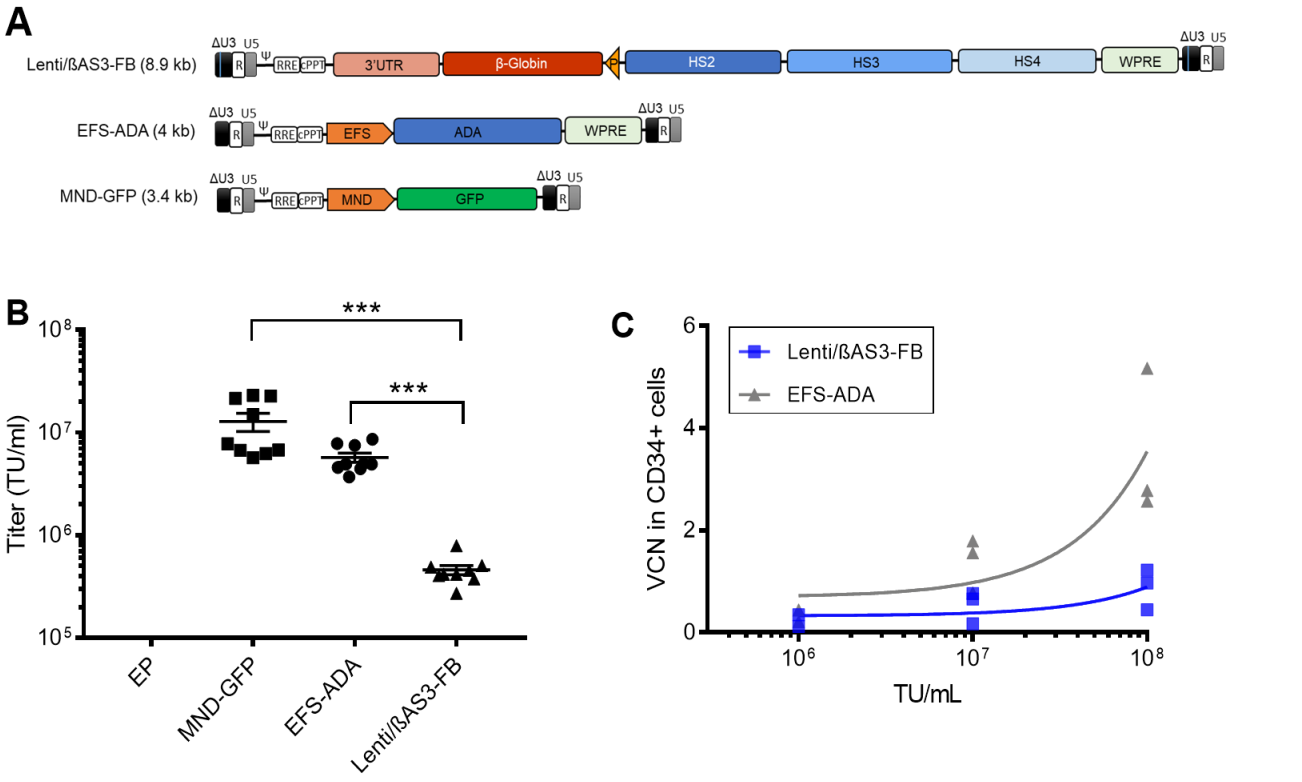

Figure 1. Complex ß-globin vector, Lenti/ßAS3-FB, had low titer and infectivity in human bone marrow CD34+ hematopoietic stem and progenitor cells (HSPCs). (A) Maps of the proviral forms of EFS-ADA and Lenti/ßAS3-FB lentiviral vectors (LV). Both vectors consist of a pCCL backbone and differ only by the internal promoters and transgene cassettes. LVs are flanked by the 5' and 3' long terminal repeats (LTR). The EFS-ADA provirus contains the mutated Woodchuck hepatitis virus post-transcriptional regulatory element (WPRE) and codon-optimized adenosine deaminase (ADA) gene cassette driven by the EFS promoter. The Lenti/ßAS3-FB provirus contains the human ß-globin promoter (P) and the locus control region (LCR) hypersensitive sites (HS), HS2, HS3, and HS4 in anti-sense orientation driving the expression of the ß-globin gene cassette with 3' untranslated region (UTR) enhancer. The 3' LTR of Lenti/ßAS3-FB contains the 77 bp FB (FII-BEAD) insulator. (B) Viral titers of unconcentrated LVs (bars represent mean with SEM; n=6-9 from 3 independent experiments; wilcoxon rank sum test; $p<0.001$). LVs in viral supernatant were assayed for titer by transducing HT29 cells at 10-fold serial dilution and vector copy number (VCN) measured by ddPCR. The MND-GFP (3.4 kb) provirus contains the GFP gene cassette driven by a ubiquitous, gamma-retroviral promoter, MND. Empty particle (EP) are vectors packaged without vector transfer plasmids. (C) Transduction of human bone marrow (BM) CD34+ HSPCs by LVs at three doses of transduction units (TU) per mL (bars represent mean with SEM; n=3 independent donors from 3 independent experiments; linear regression, comparison of slopes, $p<0.01$). 1e6 cells/mL of human BM CD34+ HSPCs cells were pre-stimulated with cytokines for 24 h and transduced with LVs at three doses of TU at MOI=1, 10, 100 for an additional 24 h. Cells were cultured in an in vitro myeloid differentiation condition, and VCN was measured 12 days after transduction.

To evaluate the viral titer of the Lenti/βAS3-FB LV in comparison to the EFS-ADA vector, LVs were packaged concurrently in 293T cells, and the titers of the unconcentrated viral supernatants were tested in parallel with the HT-29 cell line. The titer of Lenti/βAS3-FB was ~12-fold lower than the titer of EFS-ADA ($p<0.001$, Wilcoxon rank-sum test) (Fig. 1B).

To characterize the gene transfer efficiency of these vectors in clinically relevant target cells, prestimulated human BM CD34+ HSPCs from healthy donors were transduced at three doses of transduction units (TU), and the integrated VCN was measured by ddPCR 12 days after transduction. Lenti/βAS3-FB displayed less efficient gene transfer to human BM CD34+ cells than EFS-ADA (comparison of the slopes by linear regression, $p=0.006$), especially at higher doses (Fig. 1C). At the highest dose tested, $1x10^8$ TU/mL, the average VCN of Lenti/βAS3-FB was 0.88 ± 0.23 versus 3.51 ± 0.83 for EFS-ADA in three independent donors, resulting in a 4-fold difference in transduction between the two LVs despite the use of the same MOIs. We subsequently used Lenti/βAS3-FB and EFS-ADA as examples of complex and simple LVs to study different steps of the lentiviral lifecycle, identify the blocks that restrict the performance of complex vectors and develop strategies to improve the titer and infectivity of complex vectors.

Viral RNA of the complex vectors was truncated in packaging cells and vector particles

To quantify RNA species at different stages of transcription, we designed multiple ddPCR primers and probes along with the viral RNA. Because transcription of vector plasmids starts at the 5' LTR driven by the CMV promoter, RNA is transcribed in the following order: R/U5, primer binding site (PBS), transgene, and U3/R. R/U5 primers and probe were used to quantify Initial RNA, PBS primers and probe were used to quantify Intermediate RNA, and U3/R primers and probes were used to quantify Complete RNA (Fig. 2A). RNA was extracted from

both packaging cells and vector particles three days post-transfection in the packaging process. Equal masses of viral RNA were treated with DNAse and reverse transcribed with random primers. Amplifications of R/U5, PBS and U3/R regions were conducted to quantify the Initial, Intermediate, and Complete viral RNA by ddPCR. The sequences of the primers and probes were listed in Table 1.

As shown in Fig. 2B, two simple vectors, EFS-ADA and MND-GFP, displayed similar levels of all three RNA species. The complex vector, Lenti/βAS3-FB, had similar levels of Initial and Intermediate RNA as EFS-ADA. Lenti/βAS3-FB had 15.4-fold fewer Complete RNA species than EFS-ADA. Only ~9.2% of Lenti/βAS3-FB RNA transcripts initiated at the 5' LTR have intact 3' LTR RNA detected by the U3/R primers and probe, whereas ~72.9% viral RNA was complete in EFS-ADA (Fig. 2C). The amplification efficiencies by the three sets of primers and probes were assessed using plasmids and gave similar efficiency, suggesting that the decrease in Complete RNA in Lenti/βAS3-FB was not a PCR artifact (Fig. 3A, B, C).

We further quantified the viral RNA content in vector particles to assess whether the RNA truncation was also observed in vector particles. EFS-ADA and MND-GFP displayed minor decreases in the RNA content from 5' to 3', whereas Lenti/βAS3-FB showed a substantial decrease in the level of Complete RNA, resulting in 42.9-fold lower Complete RNA in Lenti/βAS3-FB than in EFS-ADA (Fig. 2D). Lenti/βAS3-FB consisted of only 8% Complete viral RNAs in contrast to the 35.9% Complete RNA in EFS-ADA demonstrating that the RNA truncation was observed in both packaging cells and vector particles (Fig. 2E).

The R/U5 primer and probes for quantification of Initial RNA may additionally pick up read-through transcripts through the 3' LTR and introduce a systematic enrichment of R/U5 sequences. To investigate the extent of transcription readthrough, we quantified the abundance of the sequences from the 3' LTR U5 region to the SV40 polyadenylation site of the plasmid backbone by high-throughput RNA sequencing of the viral RNA (Fig. 3D). The read-through to

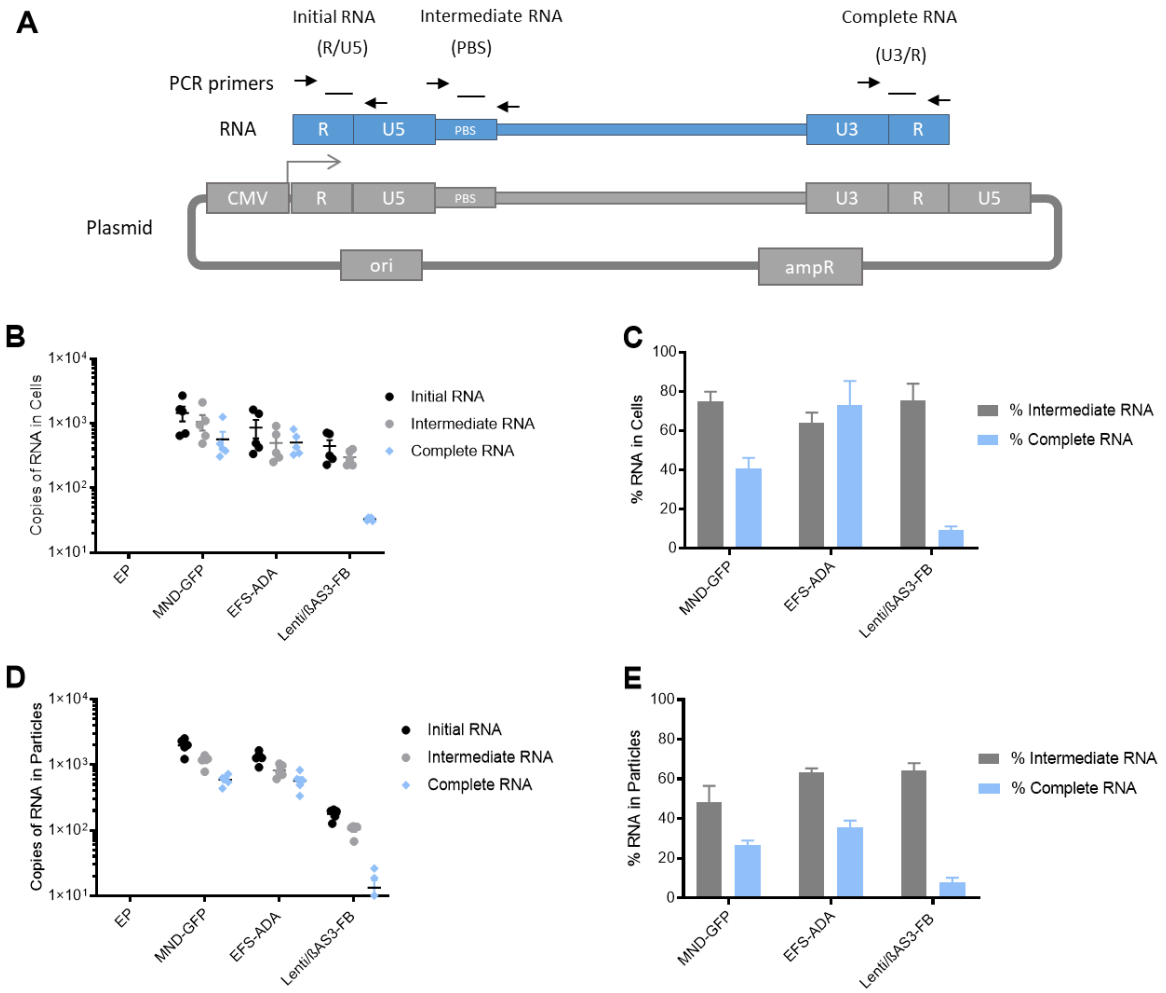

Figure 2. Lenti/ßAS3-FB had reduced levels of Complete RNA in packaging cells and vector particles. (A) Schematic representation of viral RNA and the PCR primers and probes used to quantify each RNA species by ddPCR. Transcription starts at the 5' LTR driven by the CMV promoter, and RNA is transcribed in the following order: R/U5, PBS and U3/R. R/U5 primers were used to quantify Initial RNA, PBS primers quantify Intermediate RNA, and U/3R primers quantify Complete RNA. (B) The absolute quantification of viral RNA in 293T packaging cells measured by ddPCR and (C) the percentages of Intermediate and Complete viral RNA in 293T cells. Cells were harvested three days post transfection. Total RNA was extracted from 293T cells, treated with DNAse and reverse transcribed with random primers. The amounts of viral RNA species were quantified by ddPCR. The percentage of Intermediate RNA was calculated as Intermediate RNA/Initial RNA*100%, and the percentage of Complete RNA was calculated as Complete RNA/Initial RNA*100%. (D) The absolute quantification of viral RNA in unconcentrated viral supernatant measured by ddPCR and (E) the percentages of Intermediate and Complete RNA in vector particles (bars represent mean with SEM; n=5 dishes of identical cultures treated and analyzed in two independent experiments).

U5 was relatively low compared to transcription through the 5'LTR and therefore should not significantly over-estimate the R/U5 reads from the 5'LTR. In addition, the read-through

transcription would be a consistent systematic bias that should not affect the overall conclusions.

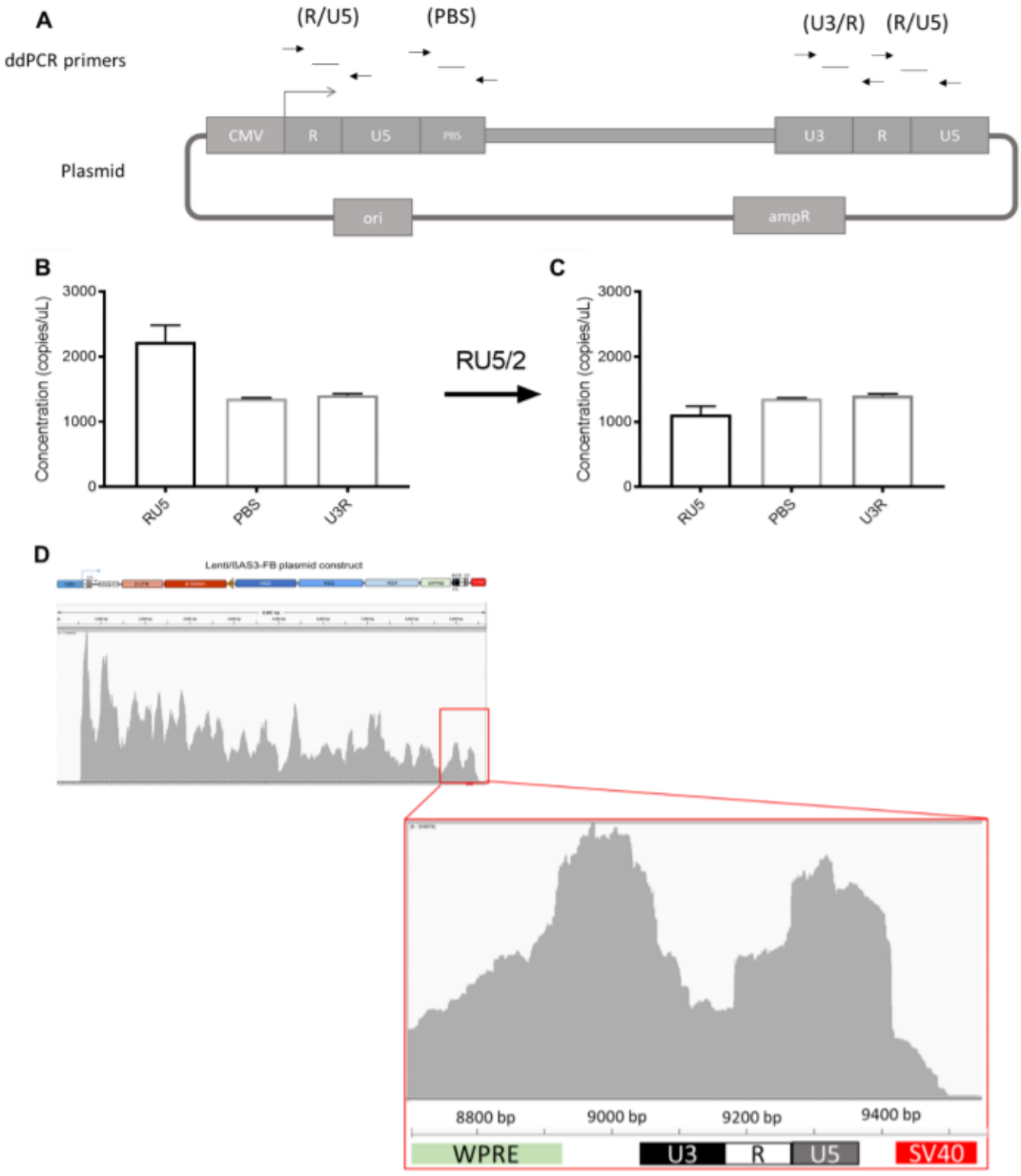

Figure 3. Quantification of ddPCR primer amplification efficiencies and viral RNA transcription readthrough. (A) Schematic representation of primer binding sites in vector plasmids. (B) Copy number/ul by R/U5, PBS, and U3/R primers and probes in Lenti/ßAS3-FB plasmids (n=2 independent experiments). (C) Normalized copy number/ul. R/U5 copy number was divided by two because plasmids contain two copies of R/U5 (bars represent mean with SEM; n=2 independent experiments). (D) Alignment of RNA-seq reads to 3'LTR to SV40 polyadenylation sites in Integrative Genomics Viewers.

Table 1. Sequences of primers and probes

Name	**Sequence 5'→3'**
R/U5 FWD	GCTAACTAGGGAACCCACTGCT
R/U5 REV	GGGTCTGAGGGATCTCTAGTTACCA
R/U5 Probe	FAM- CTTCAAGTAGTGTGTGCCCGTCTGT-31ABFQ
PBS FWD	AAGTAGTGTGTGCCCGTCTG
PBS REV	CCTCTGGTTTCCCTTTCGCT
PBS Probe	FAM-CCCTCAGACCCTTTTAGTCAGTGTGGAAAATCTCTAG-31ABFQ
U3/R FWD	AGCAGTGGGTTCCCTAGTTAG
U3/R REV	GGGACTGGAAGGGCTAATTC
U3/R Probe	FAM-AGAGACCCAGTACAAGCAAAAAGCAG-31ABFQ
Psi FWD	CTTGAAAGCGAAAGGGAAACC
Psi REV	CGCACCCATCTCTCTCCTTCT
Psi Probe	FAM-AGCTCTCTCGACGCAGGACTCGGC-31ABFQ
SDC4 FWD	CAGGGTCTGGGAGCCAAGT
SDC4 REV	GCACAGTGCTGGACATTGACA
SDC4 Probe	FAM - CCCACCGAACCCAAGAAACTAGAGGAGAAT - TAMRA

RNA-seq to examine the frequency of the viral RNA sequences across the entire transcript

We next explored the relationship between vector proviral length and viral RNA transcript completeness. A series of β-globin LVs of different lengths were packaged and titered concurrently, and the levels of Complete RNA in the unconcentrated viral supernatant were quantified. The proviral maps of the vectors used were listed in Figure 4.

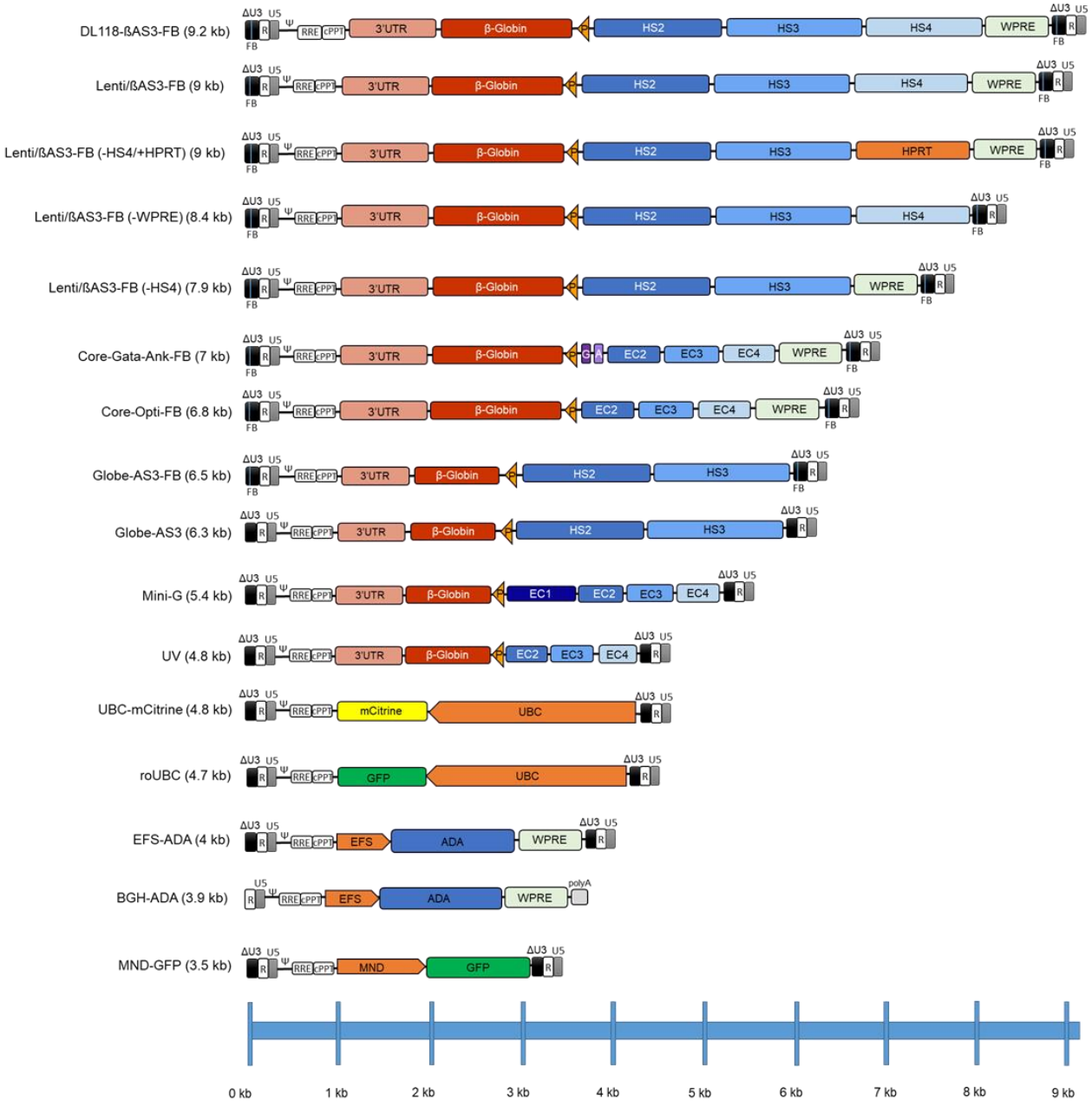

Figure 4. Maps of the lentiviral vector proviruses. All vectors consist of a pCCL backbone and differ only by the internal promoters and transgene cassettes. ΔU3, R, U5 are long terminal repeats (LTR). FB, FII-BEAD insulator. Ψ, packaging signal. RRE, Rev response element. cPPT, central polypurine tract. 3' UTR, ß-globin gene 3' UTR enhancer elements. P, promoter. G, Gata1 erythroid transcription factor binding site. A, ankyrin-1 barrier insulator element. HS2, HS3, HS4, ß-globin locus hypersensitive sites 2, 3 and 4. EC2, EC3, EC4, enhancer core elements. WPRE, mutated woodchuck hepatitis virus post-transcriptional regulatory element. ß-Globin, ß-Globin gene cassette. UBC, ubiquitin C promoter. EFS, elongation factor 1 alpha promoter. ADA, codon-optimized adenosine deaminase cDNA. BGH-ADA is shown in its RNA form because it is a truncated vector that cannot integrate.

As expected, the titer of the LVs negatively correlated with the vector length (Pearson correlation, r^2=0.81, p<0.01) (Fig. 5A). The concentration of Complete RNA also decreased with increasing vector length in all LVs (Pearson correlation, r^2=0.68, p<0.05) (Fig. 5B). The decrease in Complete RNA in complex LVs could be caused by the presence of specific sequences, which lead to discrete termination of vector transcripts, such as cryptic polyadenylation signals or splice signals. Alternatively, there may be progressive termination of transcription in a length-dependent manner, consistent with a previous study that demonstrated that inefficient transcription of the HIV provirus is associated with premature termination of viral RNA, attributed to poor processivity of RNA Polymerase (Pol) II[22]. To identify the mechanisms that truncate viral RNA, we characterized the frequency of the viral RNA sequences across the entire transcripts using Illumina RNA sequencing.

Viral RNA was extracted from unconcentrated viral supernatants packaged from three independent experiments, and sequencing library preparations were produced and sequenced by the UCLA Technology Center for Genomics & Bioinformatics. Two β-globin LVs of different lengths, Globe-AS3-FB (6.4-kb) and Lenti/βAS3-FB (8.9-kb), and the EFS-ADA LV (4.2-kb) were analyzed. Reads were aligned to the vector genome and plotted as the percentage of maximum reads versus the mapping position of the vector genome (Fig. 5C). All LVs had the most abundant reads at the 5' LTR which progressively decreased in abundance toward the 3' end. No discrete termination of viral transcripts was observed, suggesting the termination was not caused by the presence of specific problematic sequences. The reads of both Globe-AS3-FB and EFS-ADA maintained at ~50% of the maximum reads at the 3' LTR, whereas

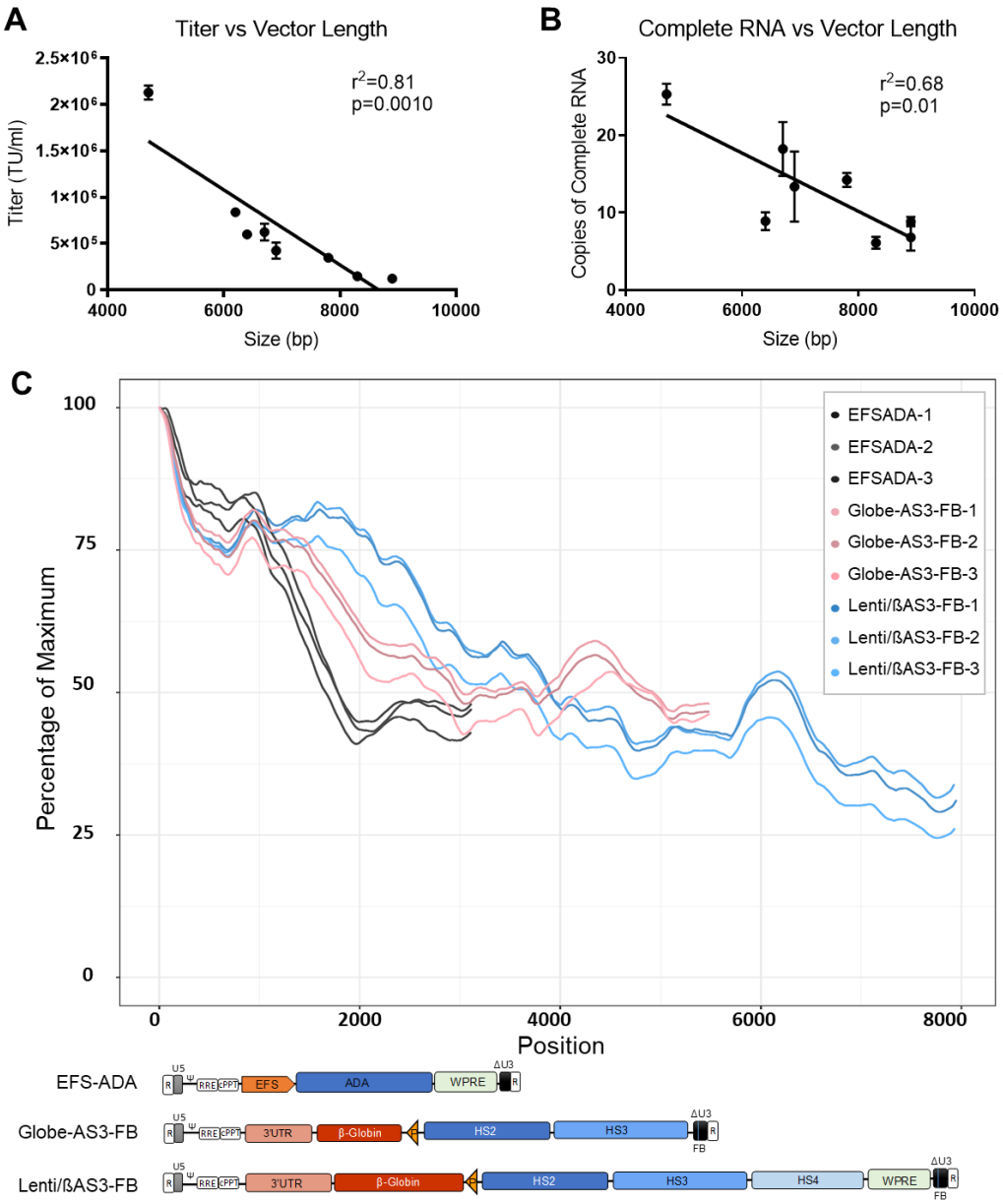

Figure 5. Viral RNA of LVs showed length-dependent decrease in completeness and coverage in RNA sequencing. (A) Comparison of titer vs vector length (bars represent mean with SEM; n=3 independent experiments; Pearson correlation, r=-0.86, p<0.01) and (B) complete RNA vs vector length in a panel of ß-globin vectors of different lengths (Bars represent mean with SEM; n=3 independent experiments; Pearson correlation exclude Globe-AS3, r=-0.67, p<0.05). All ß-globin vectors were packaged and assayed concurrently. Viral RNA was extracted from vector particles. (C) Percentage of maximum reads of EFS-ADA, Globe-AS3-FB, and Lenti/ßAS3-FB vs vector length (n=3 independent experiments). Schematic representation of the viral RNA is displayed below. LVs were packaged in three independent experiments. Total RNA was extracted from 140 µL unconcentrated viral supernatant followed by DNAse treatment. RNA was fragmented to an average of 400 bp, reverse transcribed by random priming, and sequencing adaptors ligated. The library was sequenced on illumina HiSeq 3000.

Lenti/βAS3-FB experienced a further decrease after 6-kb, resulting in ~25% RNA with 3' LTR.

The decrease in coverage from 6 to 9 kb in the two β-globin vectors with similar sequences but different lengths suggested that the RNA truncation is length-dependent and is likely to be caused by poor processivity of RNA Pol II.

Truncated RNA failed reverse transcription at the first strand transfer

We next investigated the reverse transcription kinetics of Lenti/βAS3-FB and EFS-ADA in target cells to elucidate the inhibitory effect of truncated RNA. The steps of reverse transcription, locations of ddPCR primers and probes, and the reverse transcribed products are illustrated in Figure 6A. A tRNA serves as a primer and binds to a complementary sequence on the 5' end of the viral RNA genome termed as the primer binding site (PBS) to initiate reverse transcription (first strand priming). First strand synthesis proceeds from 5' to 3' to make the single-stranded DNA copy of the R and U5 regions, and then RNAse H degrades the R and U5 regions on the 5' end of the viral RNA. The newly formed first strand viral DNA then finds the complementary R on the 3' end of the viral genome (first strand transfer) and resumes the first strand synthesis from 5' to 3' using the viral RNA as a template. First strand viral DNA elongates to generate the U3 region first and, in the end, the Psi region. Therefore, primer and probes spanning the R/U5 region were designed to quantify early reverse transcribed products (first strand priming), primer and probes spanning the U3/R region were designed to quantify intermediate reverse transcribed products (first strand transfer), and primer and probes spanning the Psi region were designed to quantify late reverse transcribed products (first strand elongation). Since the R sequence in the 3' LTR is absent in truncated RNA, we hypothesized that incomplete RNA in Lenti/βAS3-FB failed reverse transcription at the first strand transfer step (Fig. 6B).

A primitive human hematopoietic myeloid progenitor cell line, KG1a, was chosen as the target cells because of its relative resistance to LV transduction, similar to that of primary human

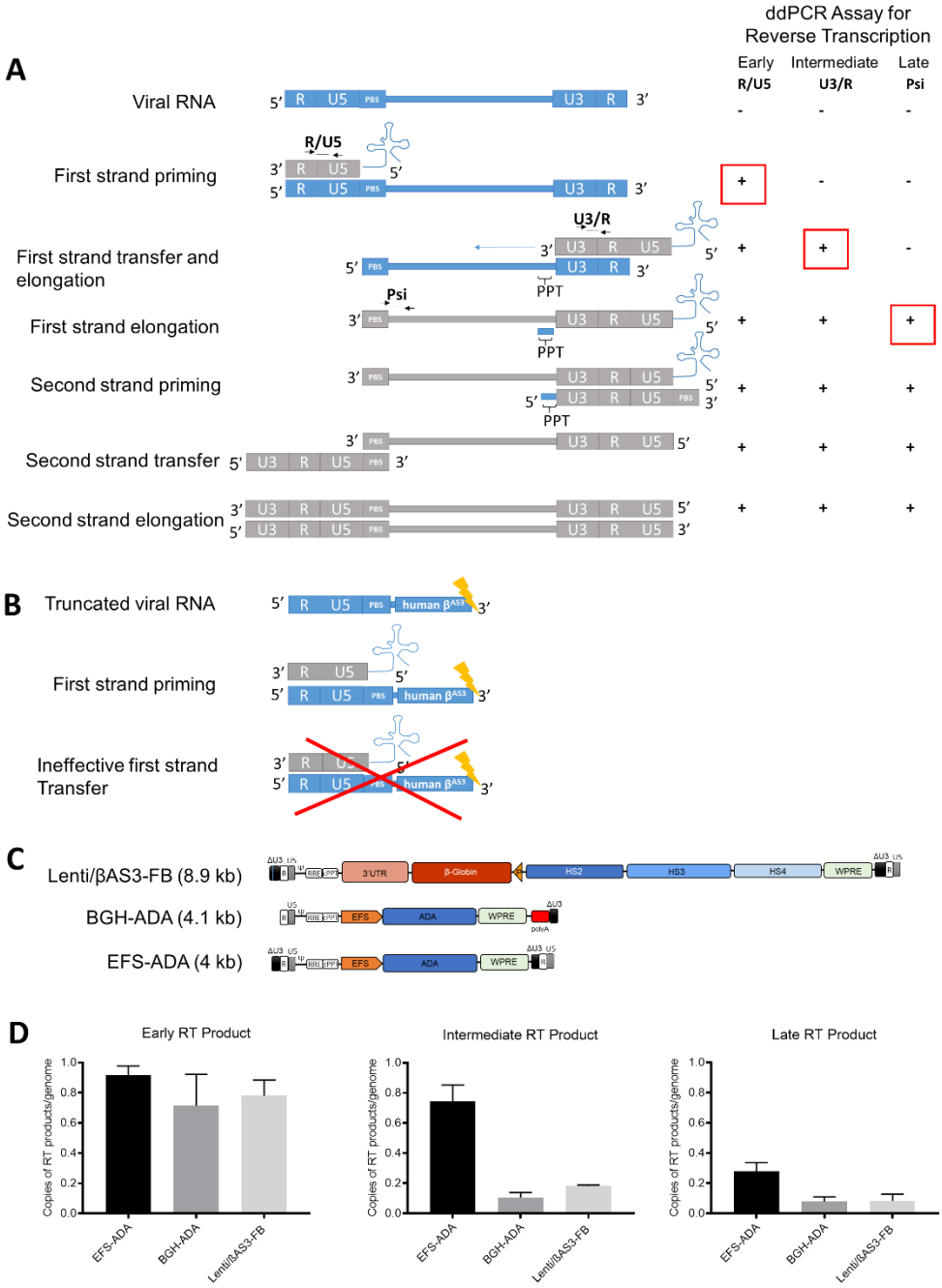

Figure 6. Lenti/ßAS3-FB failed reverse transcription at the first strand transfer step. (A) Schematic representation of the mechanism of reverse transcription (RT) and the ddPCR assay used to quantify reverse transcribed products. The ddPCR primers and probes were designed to quantify different stages of RT when RT products become detectable. The R/U5 primers quantify initial reverse transcribed products, the U3/R primers quantify intermediate reverse transcribed products, and the Psi primers quantify late reverse transcribed products. Blue box: viral RNA. Gray box: viral DNA. (B) Proposed mechanism of truncated RNA failing reverse transcription at the first strand transfer step. (C) Schematic representation of the vector RNA of EFSADA and the truncated version BGHADA. (D) Quantification of reverse transcribed products of Lenti/ßAS3-FB, EFS-ADA and BGH-ADA LVs in KG1a cells (bars represent mean with SEM; n=5 dishes of identical cultures from 2 independent experiments; unpaired t test, *p<0.05, **p<0.01, ***p<0.001). BGH-ADA is a truncated form of EFSADA LV with the Bovine Growth Hormone (BGH) polyadenylation signal between WPRE and 3'LTR. KG1a cells were transduced with Lenti/ßAS3-FB, EFS-ADA, or BGH-ADA LVs at equal levels of Initial RNA in the presence of PGE2, poloxamer, and benzonase. Cells were harvested at 24 h for gDNA extraction. Reverse transcription products were quantified by ddPCR with R/U5, U3/R, Psi, and SDC4 primers.

CD34+ HSPC[23]. A control vector, BGH-ADA, was a truncated version of EFS-ADA made by inserting the bovine growth hormone polyadenylation signal upstream of the 3'LTR (Fig. 6C). KG1a cells were transduced with equal amounts of Initial viral RNA of Lenti/βAS3-FB, EFS-ADA, and BGH-ADA vector particles and collected 24 hours after infection for analysis of serial reverse transcription products.

As expected, all three vectors displayed similar kinetics for the production of early reverse transcribed products, because equal amounts of Initial RNA were used to infect cells (Fig. 6D). Interestingly, compared to EFS-ADA, Lenti/βAS3-FB produced 4-fold fewer intermediate reverse transcribed products and 3-fold fewer late reverse transcribed products, similar to the truncated vector BGH-ADA. These data strongly suggest that truncated RNA failed to find the complementary R at the 3' LTR of the viral RNA and resulted in premature termination of reverse transcription at the first strand transfer step. BGH-ADA displayed low levels of intermediate and late reverse transcribed products. It was likely to be caused by the transcriptional read-through of the polyadenylation signal, and full-length RNA was produced at a low level.

Lenti/βAS3-FB had defective particle formation

Although EFS-ADA and Lenti/βAS3-FB had similar levels of Initial and Intermediate RNA in 293T packaging cells, Lenti/βAS3-FB had substantially reduced Initial and Intermediate RNA species in viral supernatant compared to EFS-ADA, as shown in Fig. 2B and Fig. 2D. We, therefore, assessed the RNA export efficiency as indicated by the ratios of copies of Initial RNA in vector particles to copies of Initial RNA in packaging cells (Fig. 7A). Surprisingly, the export efficiency was 4.6-fold higher for EFS-ADA than for Lenti/βAS3-FB. We next assessed the physical vector particle production by measuring the p24 concentration in the viral supernatant.

Surprisingly, despite the fact that equal amounts of GAG/POL plasmids were used at packaging, the p24 concentration of Lenti/βAS3-FB was considerably lower than the p24 concentrations of the three controls, including empty particles, which were packaged without vector transfer plasmids (Fig. 7B). When we normalized viral RNA export efficiency to p24 concentration, EFS-ADA and Lenti/βAS3-FB had nearly equal RNA export efficiency from cells to particles, suggesting that RNA export was not the primary limiting factor (Fig. 7C). Instead, physical particle formation by Lenti/βAS3-FB seemed to be impaired.

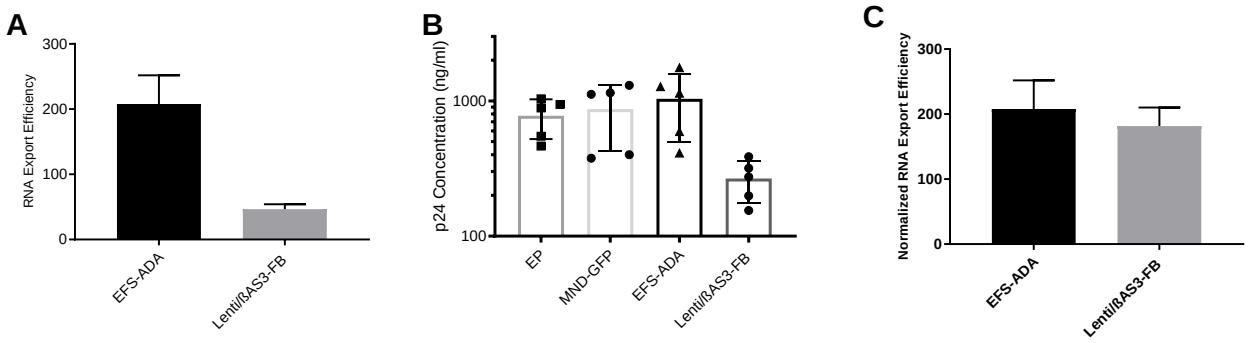

Figure 7. Lenti/βAS3-FB had defective physical particle formation. (A) The export efficiency of Initial RNA from cells to vector particles of EFS-ADA and Lenti/ßAS3-FB (bars represent mean with SEM; n=5 dishes of identical cultures from 2 independent experiments). RNA export efficiency was defined as the ratios of copies of Initial RNA in vector particles to copies of Initial RNA in packaging cells. (B) p24 concentration quantified by ELISA of EP (empty particle), MND-GFP, EFS-ADA and Lenti/ßAS3-FB unconcentrated viral supernatant (bars represent mean with SEM; n=5 dishes of identical cultures from 2 independent experiments). (C) The export efficiency normalized for the fold difference in p24 concentration (bars represent mean with SEM; n=5 dishes of identical cultures from 2 independent experiments).

DISCUSSIONS

The advances in clinical and scientific understanding of lentiviral gene therapy in the past decades have enabled the first wave of clinical gene therapy successes for multiple diseases[1–4]. However, low titer and poor gene transfer of complex vectors remain critical challenges for the successful clinical application of these vectors. Viral titer is a critical factor in the costs of production, and the titers of complex vectors are typically 1-2 log-orders lower than the titers of simple vectors. Additionally, even when adjusted to the same TU, transduction of HSPCs with

complex vectors results in lower VCNs that barely increase with the use of more infectious particles. The low titer and poor gene transfer may be caused by the lengthy and complex nature of the genome, but the exact mechanisms that restrict complex vectors to perform as efficiently as simple GFP vectors have remained elusive. Herein, we demonstrated that viral RNA and protein production were impaired in complex vectors such as Lenti/βAS3-FB.

The majority of viral RNA of Lenti/βAS3-FB was truncated and was not fully reverse transcribed, thus resulting in fewer complete linear forms of viral DNA for nuclear translocation and integration. The RNA truncation was observed in a length-dependent manner, suggesting that the truncation may be caused by the poor processivity of RNA Pol II during transcription elongation. Multiple studies demonstrated that inefficient transcription of the HIV provirus is associated with premature termination of transcription[22,24–27]. Future studies to improve RNA Pol II processivity or to identify additional problematic sequences that truncate RNA are needed.

We also observed that Lenti/βAS3-FB had low p24 production compared to the control vectors. Our observations were consistent with others that bidirectional vectors had low titer due to the formation of dsRNA[28]. One hypothesis is that specific cellular factors are activated to inhibit protein translation for bidirectional vectors. A potential restriction factor is protein kinase R, which was explored in Chapter 4.

In summary, the complex and lengthy nature of the viral genome of Lenti/βAS3-FB led to RNA truncation in a length-dependent manner and triggered specific cellular responses to inhibit viral protein production during the packaging phase. This study elucidates the mechanisms of low titer and infectivity caused by the long proviral length and provides insights into overcoming current limitations with the complex LV. This study may further support the clinical translation of novel lentiviral autologous gene therapy for treating genetic blood cell disorders.

METHODS

LV production and titration

LVs used in this study included EFS-ADA, Lenti/βAS3-FB, GLOBE-AS3, Lenti/βAS3-FB (-HS4/+HPRT), Lenti/βAS3-FB (-HS4), CoreGA-AS3-FB, Core-AS3-FB, UV-AS3, Mini-G, MND-GFP, and a version of EFS-ADA designed to not generate any full-length LV genomes by inserting the bovine growth hormone polyadenylation sequence (BGH-ADA) upstream of the 3' LTR (Fig. 4)[6,10,19,29–31].

The packaging protocol was previously described in Masiuk et al[16]. Briefly, LVs were packaged by transient transfection of 293T cells with fixed amounts of HIV Gag/Pol, Rev, and VSV-G expression plasmids and equimolar amounts of each of the different vector transfer plasmids using TransIT-293 (Mirus Bio, Madison, WI). To determine the titers of the LVs, the HT-29 human colon carcinoma cell line was transduced with different dilutions of the LVs and harvested ~60 hours after transduction. Genomic DNA was extracted using the PureLink Genomic DNA Mini Kit (Invitrogen, Waltham, MA). VCN was measured by Droplet Digital PCR (ddPCR), as previously described in Masiuk et al, and viral titers were calculated based on VCN[16].

LV infection in human BM CD34+ HSPCs

Human CD34+ HSPCs were isolated from healthy donor bone marrow (BM) aspirates using Ficoll-Hypaque gradient separation and a CD34 MicroBead Kit (Miltenyi Biotech, Bergisch Gladbach, Germany). The processed cells were cryopreserved in liquid nitrogen with BamBanker (Wako Chemicals, VA, USA).

CD34+ HSPCs were thawed at 37°C and plated at $1x10^6$ cells/mL in non-tissue culture treated plates coated with RetroNectin (20 μg/mL; Takara Shuzo Co., Otsu, Japan). The cells were

pre-stimulated for 24 h in X-Vivo-15 (Lonza, Basel, Switzerland) with 1 X L-glutamine-penicillin-streptomycin (Gemini BioProducts, West Sacramento, CA, USA), 50 ng/mL SCF, 50 ng/mL TPO, 50 ng/mL Flt3L and 20 ng/mL IL-3 (PeproTech, Rocky Hill, NJ, USA). Prestimulated cells were transduced with concentrated viral supernatants, and 24 h after transduction, cells were collected for *in vitro* myeloid differentiation cultures, as described below.

In vitro myeloid differentiation cultures

Transduced human BM CD34+ HSPCs were cultured in Basal BM Medium (BBMM: Iscove's Modified Dulbecco's Medium [IMDM] [Life Technologies, Grand Island, NY], 1 X L-glutamine-penicillin-streptomycin, 20% fetal bovine serum, 0.52% Bovine Serum Albumin) with recombinant human cytokines of 5 ng/ml interleukin-3, 10 ng/ml interleukin-6, and 25 ng/ml c*KIT* ligand (hSCF) (PeproTech) at 37°C, 5% CO_2. Cells were maintained in culture for 12 days with the addition of fresh BBMM and cytokines every 4 days. After 12 days, the cells were harvested for genomic DNA extraction and VCN analysis by ddPCR as described above.

Viral RNA analysis by ddPCR

RNA was extracted from either 2 x 10^6 293T cells or 140 uL unconcentrated viral supernatant three days after transfection for vector packaging. Cellular RNA was extracted using the RNeasy Plus Mini Kit (Qiagen, Hilden, Germany), and RNA from the viral supernatant was extracted using the QIAmp Viral RNA Mini Kit (Qiagen). Equal masses of RNA were treated with DNAse I (Invitrogen, Waltham, MA) to remove any traces of genomic or plasmid DNA contamination and then reverse transcribed using random primers, M-MLV reverse transcriptase, and RNAseOUT Recombinant Ribonuclease Inhibitor (all from Invitrogen), following the manufacturer's protocol. Amplification of R/U5, PBS, and U3/R regions by ddPCR

were conducted to quantify the Initial, Intermediate, and Complete viral RNA. The cycling conditions were 95°C for 10 min for one cycle, (94°C for 30 s and 60°C for 1 min) for 40 cycles, 10 min at 98°C for one cycle, and a 12°C hold.

p24 Assay

p24 antigen concentration in vector supernatants was measured by the UCLA/CFAR (Center for AIDS Research) Virology Core using the Alliance HIV-1 p24 Antigen ELISA Kit (cat# NEK050, PerkinElmer, Waltham, MA), following the manufacturer's manual.

RNA-Seq

Total RNA was extracted from raw viral supernatant using the QIAmp Viral RNA Mini Kit (Qiagen). Viral RNA was treated with TurboDNAse (Invitrogen) and sent to the UCLA Technology Center for Genomics and Bioinformatics Core for downstream library preparation. cDNA library was prepared using the KAPA RNA HyperPrep Kit with RiboErase (Roche Sequencing, Pleasanton, CA) following the manufacturer's manual without rRNA depletion to avoid bias. Briefly, RNA was fragmented into ~400 bp fragments; 1st strand cDNA was synthesized with random priming followed by 2nd strand synthesis. 150 bp paired-end reads were sequenced on HiSeq 3000 (Illumina, San Diego, CA). The reads were aligned to the designed vectors via Burrows-Wheeler Aligner (version 0.7.17) using parameters "bwa mem -t 16 -k 100 -A 1 -B 30 -O 10 -E 10". Bigwig files were generated on the bam files using the bamCoverage function from deepTools. The numbers of reads for each location were extracted from the bigwig files into R, and the average of the upstream and downstream 450 bp was calculated as the coverage score. The coverage scores were then normalized to the maximum value for each sample.

Reverse Transcription Assay

Raw viral supernatants of EFS-ADA, Lenti/βAS3-FB, and BGH-ADA vectors with the same amounts of Initial RNA were used to transduce KG1a cells. Benzonase, 50 U/mL (MilliporeSigma, Burlington, MA) and transduction enhancers, Poloxamer 1 mg/mL (Kolliphor P338; BSAF, Ludwigshafen, Germany) and PGE2 10 µM (Cayman Chemicals, Ann Arbor, MI, USA) were added to the cells at the same time as the addition of LV. The preparation of transduction enhancers was previously described in Masiuk et al[16]. Cells were harvested 24 hours after transduction, and DNA was extracted using Qiagen Blood and Cell Culture DNA Mini Kit (Qiagen).

The copies of reverse-transcribed DNA products were measured by ddPCR, calculated as the ratio of the copies of the viral genomes to the copies of the SDC4 endogenous reference gene. Different PCR primers were used to quantify early, intermediate and late reverse transcribed products. The R/U5 primers and probe were used to quantify early reverse transcribed products, and the U3/R primer and probe were used to quantify intermediate reverse transcribed products, as described earlier. The cycling conditions for ddPCR consisted of 95°C for 10 min for one cycle, (94°C for 30 s and 60°C for 1 min) for 40 cycles, 10 min at 98°C for one cycle, and a 12°C hold.

Statistical Analysis

Descriptive statistics such as the number of observations, mean and standard error were reported and presented graphically for quantitative measurements. Unpaired t-tests were used to compare between vectors for outcome measures such as titers, VCN, copies, and percentage of Initial/Intermediate/Complete RNA. In the case of normality assumption violation, nonparametric Wilcoxon rank-sum tests were used. Evaluation of infectivity of vectors was

done by comparing the slopes of respective regression lines. Pearson's correlation was used to correlate the titer of the LVs with the proviral length. For all statistical investigations, significance tests were two-tailed. A p-value of less than the 0.05 significance level was considered to be statistically significant. All statistical analyses were carried out using statistical software SAS version 9.4 (SAS Institute Inc. 2013) and GraphPad Prism version 8.3.0 (GraphPad Software, San Diego, California, USA).

Data and Code Availability

The RNA sequencing data can be accessed via the GEO repository number GEO: GSE158252

AUTHOR CONTRIBUTIONS

J.H., R.P.H., and D.B.K. conceived and designed all experiments. M.P. and M.M provided advice on portions of experiments. J.H. executed and analyzed all experiments. J.H., K.T., C.T., B.A., and J.Q. helped execute portions of experiments. R.P.H. provided research materials. R.P.H and D.B.K designed experiments. F.M and X.W. performed bioinformatics analysis. D.B.K. provided financial and administrative support. J.H. and D.B.K. wrote the manuscript. J.H. and D.B.K. approved the final manuscript.

CONFLICTS OF INTEREST The authors declare no competing interests.

ACKNOWLEDGMENTS

This work was supported by NIH T32 Interdisciplinary Training in Virology and Gene Therapy Training grant (T32 AI060567, J.H.). The Flow Cytometry Core of the UCLA Eli & Edythe Broad Center of Regenerative Medicine and Stem Cell Research, the Virology Core of the UCLA Center for AIDS Research (5P30 AI028697), and the UCLA Technology Center for Genomics & Bioinformatics were used to support studies.

REFERENCES

1. Aiuti, A., Cattaneo, F., Galimberti, S., Benninghoff, U., Cassani, B., Callegaro, L., Scaramuzza, S., Andolfi, G., Mirolo, M., Brigida, I., et al. (2009). Gene therapy for immunodeficiency due to adenosine deaminase deficiency. N. Engl. J. Med. *360*, 447–58.

2. Biffi, A., Bartholomae, C.C., Cesana, D., Cartier, N., Aubourg, P., Ranzani, M., Cesani, M., Benedicenti, F., Plati, T., Rubagotti, E., et al. (2011). Lentiviral vector common integration sites in preclinical models and a clinical trial reflect a benign integration bias and not oncogenic selection. Blood *117*, 5332–5339.

3. Cartier, N., Hacein-Bey-Abina, S., Bartholomae, C.C., Bougnres, P., Schmidt, M., Von Kalle, C., Fischer, A., Cavazzana-Calvo, M., and Aubourg, P. (2012). Lentiviral hematopoietic cell gene therapy for X-linked adrenoleukodystrophy. In Methods in Enzymology (Academic Press Inc.), pp. 187–198.

4. De Ravin, S.S., Wu, X., Moir, S., Anaya-O'Brien, S., Kwatemaa, N., Littel, P., Theobald, N., Choi, U., Su, L., Marquesen, M., et al. (2016). Lentiviral hematopoietic stem cell gene therapy for X-linked severe combined immunodeficiency. Sci. Transl. Med. *8*.

5. Kumar, M., Keller, B., Makalou, N., and Sutton, R.E. (2001). Systematic determination of

the packaging limit of lentiviral vectors. Hum. Gene Ther. *12*, 1893–905.

6. Morgan, R.A., Unti, M.J., Aleshe, B., Brown, D., Osborne, K.S., Koziol, C., Smith, O.B., O'Brien, R., Tam, C., Miyahira, E., et al. (2019). Title: Improved Titer and Gene Transfer by Lentiviral Vectors Using Novel, Small β-Globin Locus Control Region Elements. Mol. Ther.

7. Morgan, R.A., Gray, D., Lomova, A., and Kohn, D.B. (2017). Hematopoietic Stem Cell Gene Therapy: Progress and Lessons Learned. Cell Stem Cell *21*, 574–590.

8. Kanter, J., Walters, M.C., Hsieh, M., Krishnamurti, L., Kwiatkowski, J.L., Kamble, R., von Kalle, C., Joseney-Antoine, M., Pierciey, F.J., Shi, W., et al. (2017). Interim Results from a Phase 1/2 Clinical Study of Lentiglobin Gene Therapy for Severe Sickle Cell Disease. Blood *130*.

9. Counsell, J.R., Asgarian, Z., Meng, J., Ferrer, V., Vink, C.A., Howe, S.J., Waddington, S.N., Thrasher, A.J., Muntoni, F., Morgan, J.E., et al. (2017). Lentiviral vectors can be used for full-length dystrophin gene therapy. Sci. Rep. *7*, 79.

10. Romero, Z., Urbinati, F., Geiger, S., Cooper, A.R., Wherley, J., Kaufman, M.L., Hollis, R.P., De Assin, R.R., Senadheera, S., Sahagian, A., et al. (2013). β-globin gene transfer to human bone marrow for sickle cell disease. J. Clin. Invest. *123*, 3317–3330.

11. Modell, B., and Darlison, M. (2008). Global epidemiology of hemoglobin disorders and derived service indicators. Bull. World Health Organ. *86*, 480–487.

12. HARRIS, J.W. (1950). Studies on the destruction of red blood cells. VIII. Molecular orientation in sickle cell hemoglobin solutions. Proc. Soc. Exp. Biol. Med. *75*, 197–201.

13. Nash, G.B., Johnson, C.S., and Meiselman, H.J. (1986). Influence of oxygen tension on the viscoelastic behavior of red blood cells in sickle cell disease. Blood *67*, 110–8.

14. Pauling, L., Itano, H.A., Singer, S.J., and Wells, I.C. (1949). Sickle Cell Anemia, a Molecular Disease. Science (80-.). *110*, 543–548.

15. Lisowski, L., and Sadelain, M. (2008). Current status of globin gene therapy for the treatment of β-thalassemia. Br. J. Haematol. *141*, 335–345.

16. Masiuk, K.E., Zhang, R., Osborne, K., Hollis, R.P., Campo-fernandez, B., and Kohn, D.B. (2019). PGE2 and Poloxamer Synperonic F108 Enhance Transduction of Human HSPCs with a b -Globin Lentiviral Vector. Mol. Ther. Methods Clin. Dev. *13*, 390–398.

17. Heffner, G.C., Bonner, M., Christiansen, L., Pierciey, F.J., Campbell, D., Smurnyy, Y., Zhang, W., Hamel, A., Shaw, S., Lewis, G., et al. (2018). Prostaglandin E 2 Increases Lentiviral Vector Transduction Efficiency of Adult Human Hematopoietic Stem and Progenitor Cells. Mol. Ther. *26*, 320–328.

18. Editing, G., Human, I., Stem, H., Petrillo, C., Thorne, L.G., Unali, G., Naldini, L., Towers, G.J., Kajaste-rudnitski, A., Petrillo, C., et al. (2018). Cyclosporine H Overcomes Innate Immune Restrictions to Improve Lentiviral Transduction and Article Cyclosporine H Overcomes Innate Immune Restrictions to Improve Lentiviral Transduction and Gene Editing In Human Hematopoietic Stem Cells. Stem Cell *23*, 820-832.e9.

19. Carbonaro, D.A., Zhang, L., Jin, X., Montiel-Equihua, C., Geiger, S., Carmo, M., Cooper, A., Fairbanks, L., Kaufman, M.L., Sebire, N.J., et al. (2014). Preclinical Demonstration of Lentiviral Vector-mediated Correction of Immunological and Metabolic Abnormalities in Models of Adenosine Deaminase Deficiency. Mol. Ther. *22*, 607.

20. Schambach, A., Bohne, J., Chandra, S., Will, E., Margison, G.P., Williams, D.A., and Baum, C. (2006). Equal potency of gammaretroviral and lentiviral SIN vectors for expression of O6-methylguanine-DNA methyltransferase in hematopoietic cells. Mol. Ther. *13*, 391–400.

21. Zufferey, R., Dull, T., Mandel, R.J., Bukovsky, A., Quiroz, D., Naldini, L., and Trono, D. (1998). Self-Inactivating Lentivirus Vector for Safe and Efficient In Vivo Gene Delivery. J. Virol. *72*, 9873–9880.

22. Zhang, Z., Klatt, A., Henderson, A.J., and Gilmour, D.S. (2007). Transcription termination factor Pcf11 limits the processivity of Pol II on an HIV provirus to repress gene expression. Genes Dev. *21*, 1609–14.

23. Koeffler, H., Billing, R., Lusis, A., Sparkes, R., and Golde, D. (1980). An undifferentiated variant derived from the human acute myelogenous leukemia cell line (KG-1). Blood *56*.

24. Kao, S.Y., Calman, A.F., Luciw, P.A., and Peterlin, B.M. (1987). Anti-termination of transcription within the long terminal repeat of HIV-1 by tat gene product. Nature *330*, 489–493.

25. Feinberg, M.B., Baltimore, D., and Frankel, A.D. (1991). The role of Tat in the human immunodeficiency virus life cycle indicates a primary effect on transcriptional elongation. Proc. Natl. Acad. Sci. U. S. A. *88*, 4045–4049.

26. Laspia, M.F., Rice, A.P., and Mathews, M.B. (1989). HIV-1 Tat protein increases transcriptional initiation and stabilizes elongation. Cell *59*, 283–92.

27. Cullen, B.R. (1990). The HIV-1 Tat protein: An RNA sequence-specific processivity factor? Cell *63*, 655–657.

28. Maetzig, T., Galla, M., Brugman, M.H., Loew, R., Baum, C., and Schambach, A. (2010). Mechanisms controlling titer and expression of bidirectional lentiviral and gammaretroviral vectors. Gene Ther. *17*, 400–411.

29. Urbinati, F., Campo Fernandez, B., Masiuk, K.E., Poletti, V., Hollis, R.P., Koziol, C., Kaufman, M.L., Brown, D., Mavilio, F., and Kohn, D.B. (2018). Gene Therapy for Sickle

Cell Disease: A Lentiviral Vector Comparison Study. Hum. Gene Ther. *29*, 1153–1166.

30. Cooper, A.R., Lill, G.R., Gschweng, E.H., and Kohn, D.B. (2015). Rescue of splicing-mediated intron loss maximizes expression in lentiviral vectors containing the human ubiquitin C promoter. Nucleic Acids Res. *43*, 682–690.

31. Levasseur, D.N., Ryan, T.M., Pawlik, K.M., and Townes, T.M. (2003). Correction of a mouse model of sickle cell disease: Lentiviral/ antisickling β-globin gene transduction of unmobilized, purified hematopoietic stem cells. Blood *102*, 4312–4319.

CHAPTER 3

CRISPR-Cas9-mediated Knock Out Screen to Identify Host Restriction Factors

ABSTRACT

A major obstacle for clinical applications of lentiviral vectors (LV) is the capability to produce a large number of vectors with high titer and infectivity. Improvements in the packaging platform or protocol that can be applied to the production of many different LVs are needed. In this study, we identified three host restriction factors that impeded LV production, PKR, OAS1, and LDLR. Knocking out these three genes separately led to a 2~5-fold increase in viral titer. We created a monoclonal cell line by knocking out OAS1, LDLR, and PKR. The resulting cell line led to a 4~8-fold increase in viral titer, full-length viral RNA, and physical particles. We named this cell line CRISPRed HEK293T to Disrupt Antiviral Responses (CHEDAR). CHEDAR can be applied to improve the production of various LVs, especially the vectors with low titers or with internal promoters in the reverse orientation.

INTRODUCTION

Hematopoietic stem cell transplant in combination with lentiviral-based gene therapy has successfully treated various genetic blood cell diseases in clinical trials[1–4]. Lentiviral vectors (LVs) allows the integration of viral DNA into the host cell genomes of both dividing and nondividing cells, providing long-term stable expression of the gene of interest. However, we and others have observed that titer and infectivity decrease with increasing proviral length, resulting in barriers for scaling up Good Manufacturing Practices (GMP)-grade vector production and high costs for clinical and commercial applications. While optimizing the expression cassette is a viable strategy to create LVs with optimal titer, infectivity, and expression[5,6], this process requires years of redesigning and testing for individual LVs. Improvements on the packaging platform or protocol that can provide a global solution to the production of many different LVs are needed.

Recent research has shown that many cellular restriction factors (RFs) inhibit specific steps of the lentiviral life cycle[7–9]. Some RFs are inducible by sensing viral components and activating the interferon (IFN) signaling cascade, while other RFs are ubiquitously expressed for direct antiviral functions. Ferreira et al reported that LV production titer is not limited by induced intracellular innate immunity in HEK293T cells, because there was no detectable IFN cytokine release during the packaging process[10]. This is likely due to the large T-antigen (TAg) and adenovirus E1A expressed in HEK293T, which inactivate the tumor suppressors p53, IRF3, and other IFN-dependent transcription downstream of RNA and DNA sensing[11–14]. On the other hand, constitutively expressed antiviral effectors appeared to regulate vector production in HEK293T cells. An example is protein kinase R (PKR), an interferon-stimulated gene that regulates protein synthesis. PKR is constitutively expressed in all tissues in an inactive form and is upregulated by type I and type III IFNs[15]. PKR can be activated by TAR sequence or double-stranded RNA to inhibit general translation and therefore viral protein production[16,17]. Based on these previous studies, it is conceivable that the constitutively expressed antiviral effectors can still restrict LV production in HEK293T cells.

Moreover, RFs are not only limited to antiviral effectors but also include genes that regulate the lentiviral lifecycle. To date, the most common envelope glycoprotein used to pseudotype LVs remains to be vesicular stomatitis virus spike protein G (VSVG) due to its robust and pantropic infectivity. The low-density lipoprotein receptor (LDLR) serves as the major entry port of VSVG-pseudotyped LVs, while other LDLR family members serve as alternative receptors[20,21]. Otahal et al showed that LDLR prematurely interacts with VSVG in ER-Golgi intermediate compartment and reroutes the LDLR-VSVG complex to aggresome/autophagosome degradation prior to particle release[22]. Therefore, LDLR is likely to be an RF that regulates the VSVG level. The effects of RFs that regulate antiviral responses as well as the lentiviral lifecycle on vector production remain to be explored.

Herein we conducted a CRISPR-Cas9-mediated knockout (KO) screen in HEK293Ts to negate restriction factors (RFs) inhibiting specific steps of the lentiviral life cycle. We showed that knocking out PKR, OAS1, and LDLR additively increased the titer of various LVs, particularly complex and lengthy LVs with low titers. In addition, overexpressing transcription elongation factors, SPT4 and SPT5, improved vRNA completeness, thereby increasing the titer of LVs and infectivity in CD34+ HSPCs.

RESULTS

Knocking out *PKR* in packaging cells rescued vector protein production and increased titer and infectivity of reverse orientation vectors

In Chapter 2, we observed that Lenti/βAS3-FB had defective particle formation, resulting in low titer. It is conceivable that Lenti/βAS3-FB, but not EFS-ADA and MND-GFP, triggered a cellular response to inhibit p24 production. Protein kinase-R (PKR) is an interferon-induced, double-stranded RNA-activated protein kinase that protects cells against viral infections (Pindel et al., 2011). Vectors with internal expression cassette in the reverse orientation were shown by Kafri and colleagues to trigger PKR response to inhibit protein translation[18]. To test whether PKR was activated by Lenti/βAS3-FB, we knocked out *PKR* in 293T cells via CRISPR-Cas9, generated an isogenic *PKR-/-* cell clone, and confirmed the allelic disruption by TIDE sequencing and protein expression by western blot (Fig. 1A, B).

Two forward-oriented vectors bearing expression cassettes in the sense direction, MND-GFP, and EFS-ADA, and two reverse-oriented vectors bearing expression cassettes in the antisense direction, Lenti/βAS3-FB, and roUBC, were packaged in either parental 293T cells or *PKR-/-* 293T cells. roUBC (4.2-kb) consists of a reverse-oriented GFP expression cassette driven by the Ubiquitin C (UBC) promoter.

Knocking out *PKR* restored the p24 production by both reverse-oriented vectors (unpaired t test, ***p<0.001) (Fig. 1C). In addition, packaging in *PKR-/-* cells significantly increased the level of all three RNA species from either reverse-oriented vectors without changing the percentage of RNA (unpaired t test, *p<0.05, **p<0.01, ***p<0.001) (Fig. 1D, E). Packaging in *PKR-/-* cells led to a 5-fold increase in titer for Lenti/βAS3-FB and an 11-fold increase in titer for roUBC, and the titer of the reverse-oriented GFP vector roUBC matched to the titer of the forward-oriented GFP vector MND-GFP (unpaired t test, *p<0.05, **p<0.01, ***p<0.001) (Fig. 1F). Notably, packaging in *PKR-/-* cells also increased the titer of the forward-oriented vectors by 2~3 fold (unpaired t test, MND-GFP p=0.002, EFS-ADA p=0.02). These data strongly suggest that PKR was activated and inhibited the p24 production in reverse-oriented vectors. The increase in titer of forward-oriented vectors was likely caused by overcoming the antiviral effect of PKR recognizing single-stranded viral RNA species from these vectors, such as HIV TAR [43, 44].

Lastly, we characterized the infectivity of the LVs packaged in *PKR-/-* cells in human BM CD34+ cells. We observed an increase in infectivity of both EFS-ADA and Lenti/βAS3-FB LVs that were packaged in *PKR-/-* cells compared to the LVs packaged in parental 293T cells (linear regression, comparison of the slopes, EFS-ADA p=0.29, Lenti/βAS3-FB p=0.0016) (Fig. 1G).

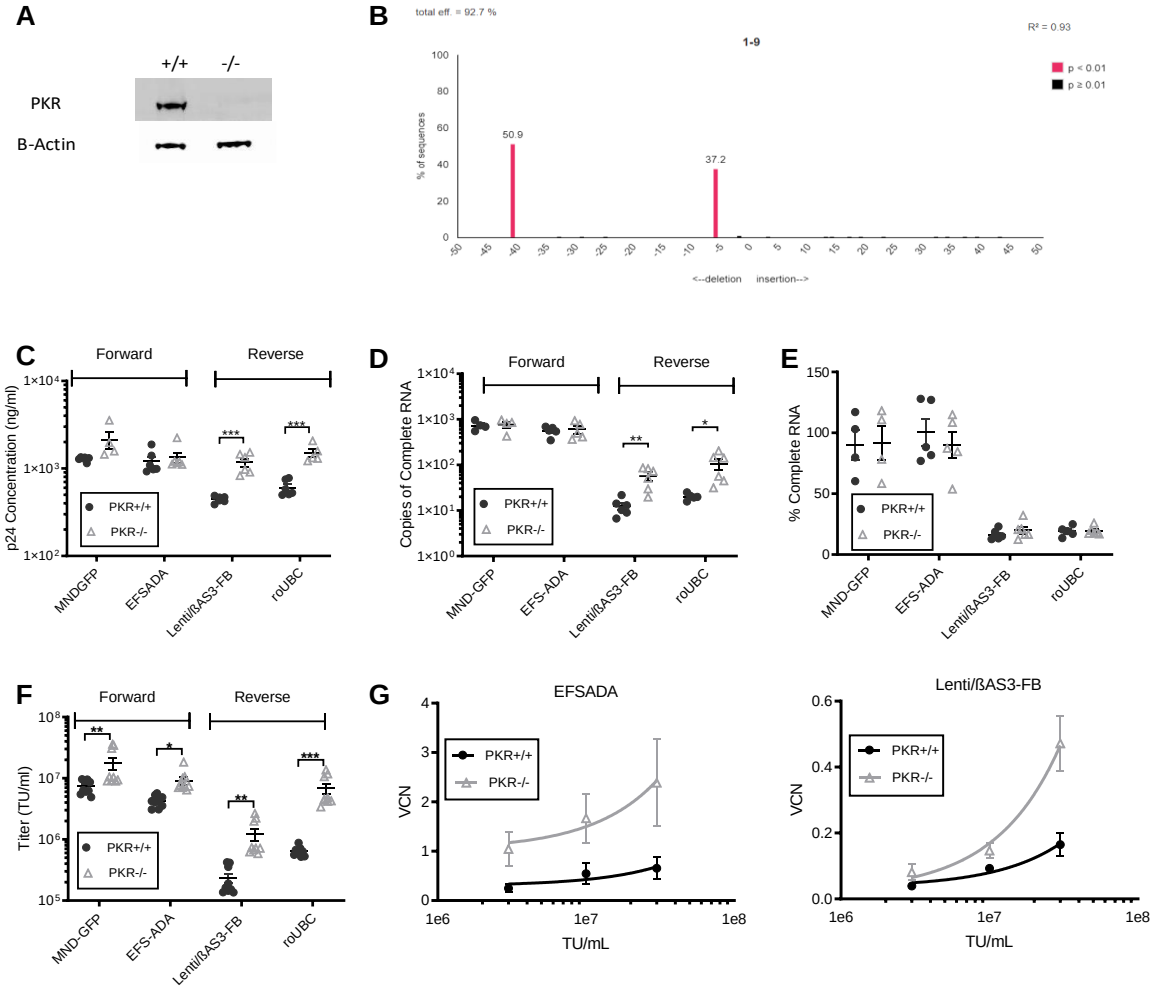

Figure 1. Knocking out PKR in 293T cells rescued p24 production and increased vector titers and CD34+ cell infectivity. (A) PKR protein expression in parental and PKR-/- cells measured by Western blot. PKR was knocked out by CRISPR-Cas 9, and a single cell clone with no parental PKR alleles was expanded for protein expression analysis by Western blot. ß-actin was used as the loading control. LVs were packaged in either parental (Par) or PKR-/- (KO) 293T cells. Viral supernatant was harvested for (B) Assessment of genome disruption by TIDE sequencing of the PKR-/- isogenic 293T cell line. Cas9 and guide RNA was introduced to the cells by lipofection of PX330 plasmids bearing the Cas9 and guide RNA sequence targeting PKR. Cells were sorted for single cell clones, and the isogenic cell clones were harvested three weeks later for genomic DNA extraction and Tide sequencing analysis. (C) p24 concentration, (D) the absolute quantification of Complete RNA, and (E) the percentage of Complete RNA (F) viral titers (bars represent mean with SEM; unpaired t test, *p<0.05, **p<0.01, ***p<0.001; n=4-9 dishes of identical cultures from 3 independent experiments). (G) Infectivity of EFS-ADA and Lenti/ßAS3-FB packaged either in parental or PKR-/- 293T cells in three independent human BM CD34+ HSPCs (bars represent mean with SEM; n=3 independent experiments; linear regression, comparison of the slopes, EFS-ADA p=0.29, Lenti/βAS3-FB p=0.0016). 1e6 cells/mL of HSPCs were transduced at MOI=3, 10, 30.

Knocking out IFNAR1, ATR, OAS1, and LDLR in 293T cells increased titers

To identify other RFs that restrict LV production, we conducted a targeted CRISPR-Cas9 knockout screen in HEK293T cells with a focus on 16 genes, each of which regulates one of the following biological properties: the immune response, DNA damage response, receptor-mediated virus entry, and transcription. The Cas9 and single-guide RNAs (sgRNAs) were delivered to HEK293T cells as ribonucleoprotein (RNP) via electroporation, and the edited cells were sorted for single-cell clones (Fig. 2A). Knockout (KO) or knockdown (KD) clones were validated on the genomic level by ICE analysis and the protein level by western blot or flow cytometry. The sequences of the sgRNAs used in this study and the genomic profile of the clones were listed in Table 1. These single-cell clones were expanded to test whether they increased the titer of Lenti/βAS3-FB, which is known to have low titer and infectivity. In addition, Lenti/βAS3-FB contains the Woodchuck Hepatitis Virus post-transcriptional regulatory element (wPRE) and a 77-bp insulator in the U3 region of the 3' LTR, termed as FB (FII-BEAD). *PKR-/-* cells were used as a positive control for the packaging process because we previously showed that knocking out PKR increased the titer of reverse-oriented LVs[24].

Because homozygous deletion of *ATR* leads to chromosome breaks and proliferative failure in culture[25–27], we selected an *ATR* knockdown (KD) clone with 63% indel and 63% KO score that showed a significant reduction in protein expression (Table 1 and Fig. 2B). IFNAR1, OAS1, and LDLR were successfully knocked out as shown in Fig. 2B and C. Unstimulated CD34+ HSPCs are known to have no or low expression of LDLR[28] and therefore were used as a negative control when measuring LDLR expression in the LDLR KO cells by flow cytometry (Fig. 2C).

The targeted CRISPR-Cas9 screen revealed that the disruption of *PKR*, *IFNAR1*, *OAS1*, *ATR* and *LDLR* genes increased titer by 2~3-fold (Fig. 2D; n=9-29 dishes of identical cultures from 3-10 independent experiments; bars represent mean with SD; unpaired t-test, $*p < 0.05$, $**p < 0.01$, $***p < 0.001$, $****p < 0.0001$)). The PKR-/- cells increased titer by 4.1 ± 1.1-fold.

The *IFNAR1-/-* cells increased titer by 2.4 ± 0.7 -fold. The OAS1-/- cells increased titer by 2.3 ± 0.8-fold. The ATR knockdown cells increased titer by 2.2 ± 0.8-fold. The LDLR-/- cells increased titer by 2.8 ± 0.9-fold. Knocking out RLR, RIG-I, MDA5, STING, TLR3, APOBEC, TRIM5a, TRIM56, ZAP, TASOR, and PCF11 in HEK293T cells did not increase the titer of Lenti/βAS3-FB more than 2-fold (Fig. 2E; n=3-22 dishes of identical cultures from 1-6 independent experiments; bars represent mean with SD). A potential explanation is that HEK293T cells do not have intact cellular pathways of these genes. Nonetheless, we decided to not prioritize these targets for this study.

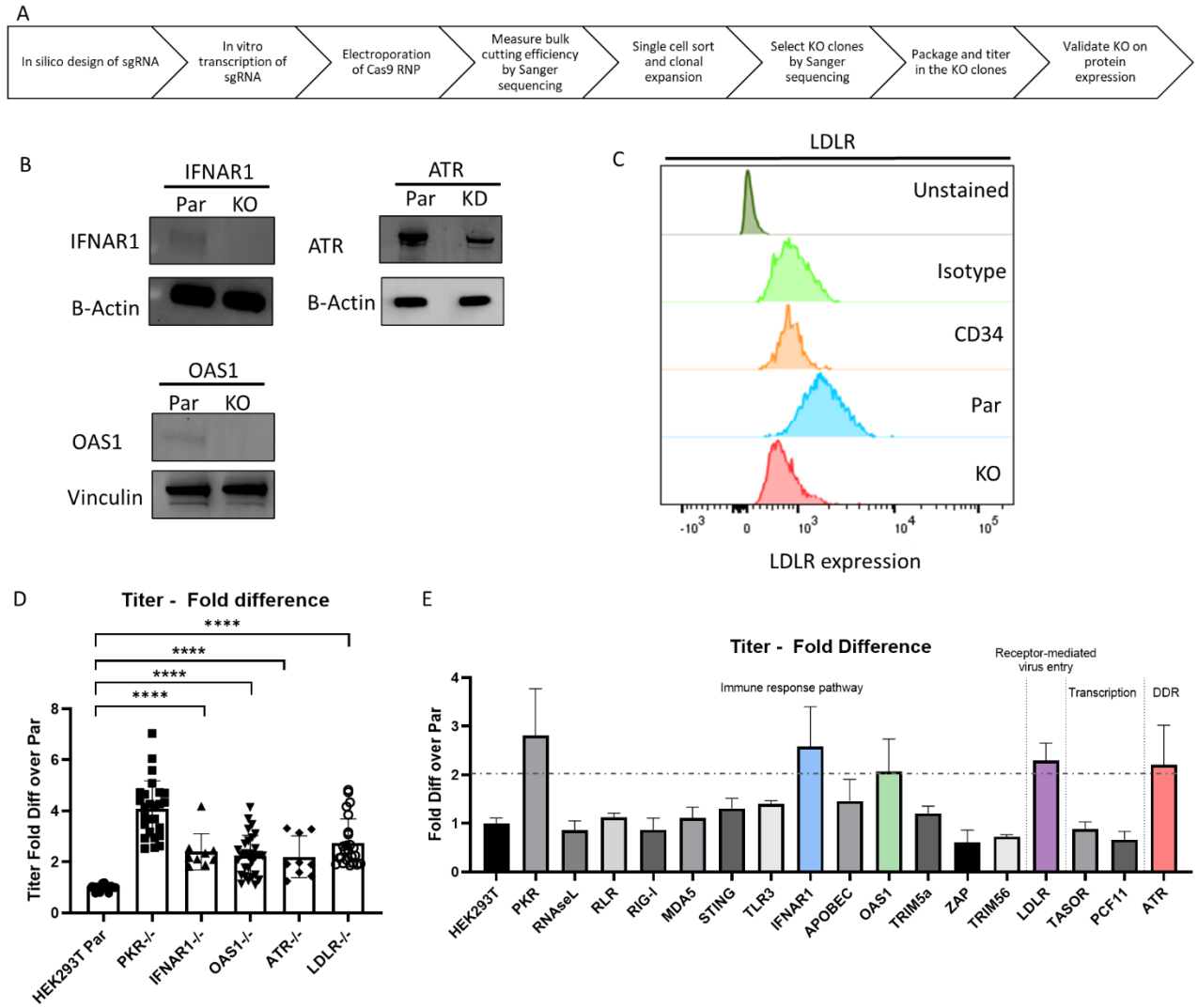

Figure 2. Targeted restriction factor knockout screen in HEK 293T cells. A) The workflow of the CRISPR-Cas9 screen. Single guide RNAs (sgRNA) were designed using the Benchling CRISPR online tool, and oligonucleotides were synthesized by Integrated DNA Technologies (San Diego, CA). The oligos were in vitro transcribed into the RNA form. Cas9 and sgRNA were delivered to 293T cells as RNP via electroporation. A portion of the edited cells was pelleted for gDNA extraction, PCR, Sanger sequencing, and ICE analysis for the KO score 24-48 hours after electroporation. The edited cells with greater than 20% indel were single-cell sorted. After two weeks of clonal expansion, the KO clones were selected by Sanger sequencing and then used for packaging to test whether they increased the titer of Lenti//βAS3-FB. If the KO clones successfully increased titer, the gene disruption was further validated on the protein level by western blot or flow cytometry. B) IFNAR1, ATR, and OAS1 protein expression in parental and gene-edited cells measured by western blot. HEK293T cells were edited by CRISPR-Cas9 targeting each of the genes. The edited cells were sorted for single-cell clones, and an isogenic clone with no parental allele, except ATR, was expanded for protein expression analysis. Because ATR is an essential gene for cell survival, an ATR knockdown (KD) clone with 33% parental allele remaining was selected. β-Actin and Vinculin were used as the loading controls. C) LDLR protein expression in parental, LDLR-/- 293T cells, and unstimulated CD34+ hematopoietic stem and progenitor cells (HSPCs) measured by flow cytometry. Unstimulated CD34+ HSPCs are known to not express LDLR and were used as a negative control. A mouse IgG1 antibody was used as the isotype control. D) Titers of Lenti/βAS3-FB packaged in parental and gene-edited cells (n=9-2931 dishes of identical cultures from 3-10 independent experiments; bars represent mean with SD; unpaired t-test, $*p < 0.05$, $**p < 0.01$, $***p < 0.001$, $****p < 0.0001$). E) Titers of Lenti//βAS3-FB in KO or KD clones (n=3-22 dishes of identical cultures from 1-6 independent experiments; bars represent mean with SD).

Table 1. Genomic profile of KO/KD clones measured by ICE Analysis.

Gene	sgRNA sequence	Indel %	Knockout Score	Indel Pattern
IFNAR1	AAACACTTCTTCATGGTATG	99	99	99% +1
OAS1	CTGAAGGAAAGGTGCTTCCG	96	96	49% +2 47% +1
ATR	AAAGTGCTAGCTGGTTGTGC	63	63	35% -2 33% 0 28% -13
LDLR	GACAACGGCTCAGACGAGCA	93	93	48% +1 45% -11
STING	CGGGCCGACCGCATTTGGGA	96	96	39% -20 21% -11 16% -8 8% -11 6% -8 4% -11 2% -8
RNAseL	TTATCCTCGCAGCGATTGCG	95	76	52% +1 20% -6 23% -1
RLR3	TGGACCGTGACAACCCTGAG	97	97	32% +1 29% -4 22% -20 6% -4 5% -20 3% -20
RIG-I	AAACAACAAGGGCCCAATGG	99	99	99% +1
MDA5	CGAATTCCCGAGTCCAACCA	100	100	100% -4
TASOR	GATAGGCAAAAAAGCACGAG	98	98	98% +1
PCF11	TCTGCTCTGACATTGCGCCG	57	57	57% -8
TLR3	GTACCTGAGTCAACTTCAGG	95	95	37% -20 23% -11 16% -11 7% -11 7% -20 3% -20 2% -11
TRIP12	GGTCACTGCGACGTTCACAG	98	98	98% +1
TRIM5a	GATCTGAGATGAGCTCTCTC	100	100	71% -4 29% -4
TRIM56	GAAGAAGTTGGTCTTGAAGG	95	95	47% +1 30% -11 18% -11
ZAP	GCAACTATTCGCAGTCCGAG	97	97	33% -2 32% -4 32% -13
APOBEC3G	CTGTCCTAAAACCAGAAGCT	94	94	73% -13 21% -14

Decreased Titers Are Associated with Rescued LDLR and OAS1 Expressions

To validate these RFs that increased titer, we restored the protein expressions of the four RFs in the KO clones. The WT cDNA of the longest open reading frame was cloned into a lentiviral backbone with ires-GFP driven by an MND promoter. The KO cells were transduced with a lentivirus encoding the wildtype (WT) cDNA linked to ires-GFP or a lentivirus encoding MND-GFP as a transduction control. The cells were subsequently sorted for the GFP+ population to exclude the non-transduced cells.

We first confirmed the restoration of the protein expressions of LDLR, OAS1, ATR, and IFNAR1 in the KO/KD cells by western blot or flow cytometry (Fig. 3A, B, D; Fig. 4A, C). The cells transduced with lentivirus encoding the WT cDNAs showed protein expressions that were comparable to the expressions in the parental HEK293T cells, while the cells transduced with MND-GFP did not show restoration of the target proteins. Next, we packaged Lenti/βAS3-FB in the parental HEK293T, KO cells, KO cells transduced with MND-GFP, and KO cells transduced with lentivirus encoding the corresponding cDNA. Restoring the LDLR expression decreased the titer to the wild-type level, while the LDLR-/- cells transduced with MND-GFP still showed an increase in titer (Fig. 3C; n=9 dishes of identical cultures from 3 independent experiments; bars represent mean with SD; unpaired t-test, $*p < 0.05$, $**p < 0.01$, $***p < 0.001$, $****p < 0.0001$)). Restoring the OAS1 expression decreased titer compared to the *OAS1-/-* cells and *OAS1-/-* cells transduced with MND-GFP (Fig. 3E; n=12 dishes of identical cultures from 4 independent experiments; bars represent mean with SD; unpaired t-test, $*p < 0.05$, $**p < 0.01$, $***p < 0.001$, $****p < 0.0001$). The decrease in titer in the LDLR and OAS1 restored cells suggested that the titer changes were associated with these genes. Although we observed titer increase in multiple *IFNAR1-/-* clones (data not shown), restoring IFNAR1 and ATR did not decrease titer (Fig. 4B, D; n=8-9 dishes of identical cultures from 3 independent experiments; bars represent mean with SD; unpaired t-test; ns, not significant). This could be due to a different isoform of the protein,

which was not responsible for the antiviral activity, was re-expressed. Nonetheless, we decided not to prioritize IFNAR1 and ATR in the rest of the study.

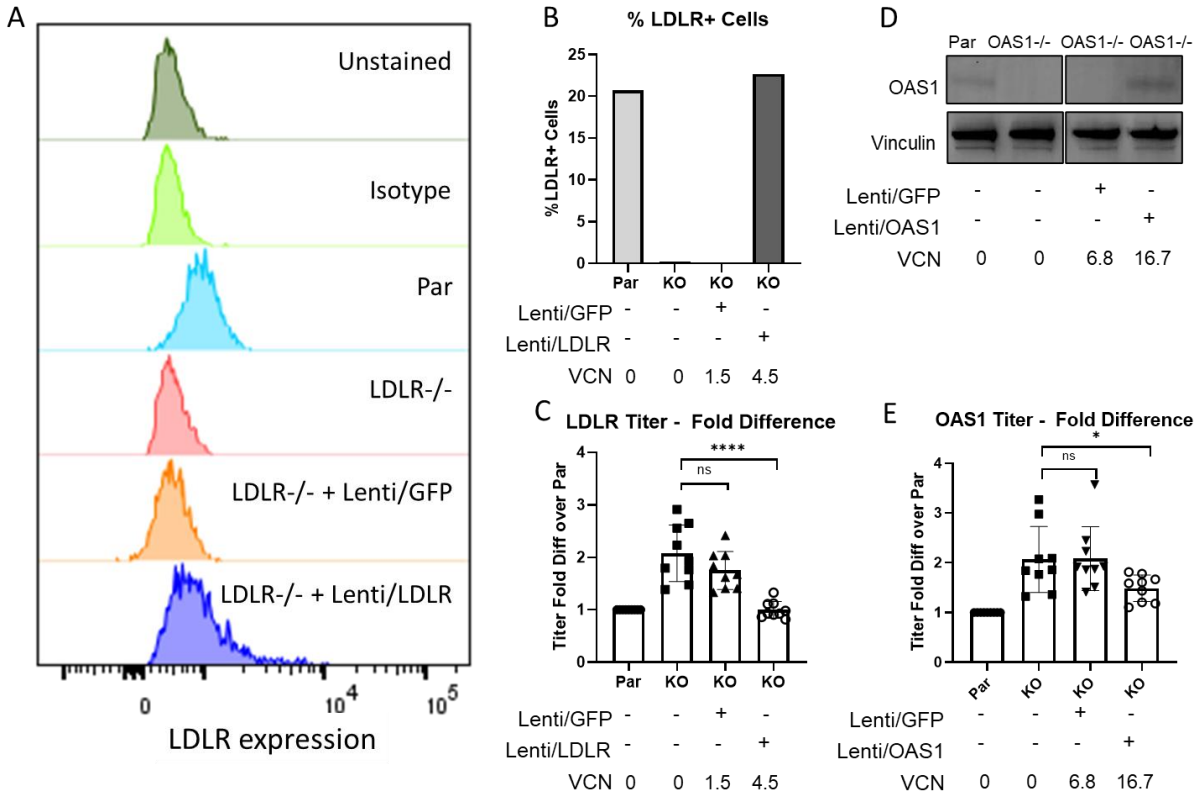

Figure 3. Restoring protein expression of LDLR and OAS1 decreased titers. A) LDLR protein expression in parental 293T, LDLR-/- 293T, LDLR-/- 293T transduced with Lenti/GFP, and LDLR-/- 293T transduced with Lenti/LDLR measured by flow cytometry. LDLR-/- cells were transduced with an LV encoding LDLR gene to restore the LDLR expression or an LV encoding GFP as a transduction control. B) Percentage of LDLR+ cells in parental, LDLR-/-, and LDLR restored cells measured by flow cytometry. C) Titers of Lenti/βAS3-FB packaged in parental 293T, LDLR-/- 293T, LDLR-/- 293T transduced with Lenti/GFP, and LDLR-/- 293T transduced with Lenti/LDLR. Because Lenti/LDLR carries an ires-GFP cassette, all transduced cells were sorted for the GFP+ population. The sorted GFP+ cells were expanded for VCN analysis by ddPCR and packaging (n=9 dishes of identical cultures from 3 independent experiments; bars represent mean with SD; unpaired t-test, ∗p < 0.05, ∗∗p < 0.01, ∗∗∗p < 0.001, ∗∗∗∗p < 0.0001). D) OAS1 protein expression in parental 293T, OAS1-/- 293T, OAS1-/- 293T transduced with Lenti/GFP, and OAS1-/- 293T transduced with Lenti/OAS1 measured by western blot. E) Titers of Lenti/βAS3-FB packaged in parental 293T, OAS1-/- 293T, OAS1-/- 293T transduced with Lenti/GFP, and OAS1-/- 293T transduced with Lenti/OAS1 (n=12 dishes of identical cultures from 3 independent experiments; bars represent mean with SD; unpaired t-test, ∗p < 0.05, ∗∗p < 0.01, ∗∗∗p < 0.001, ∗∗∗∗p < 0.0001).

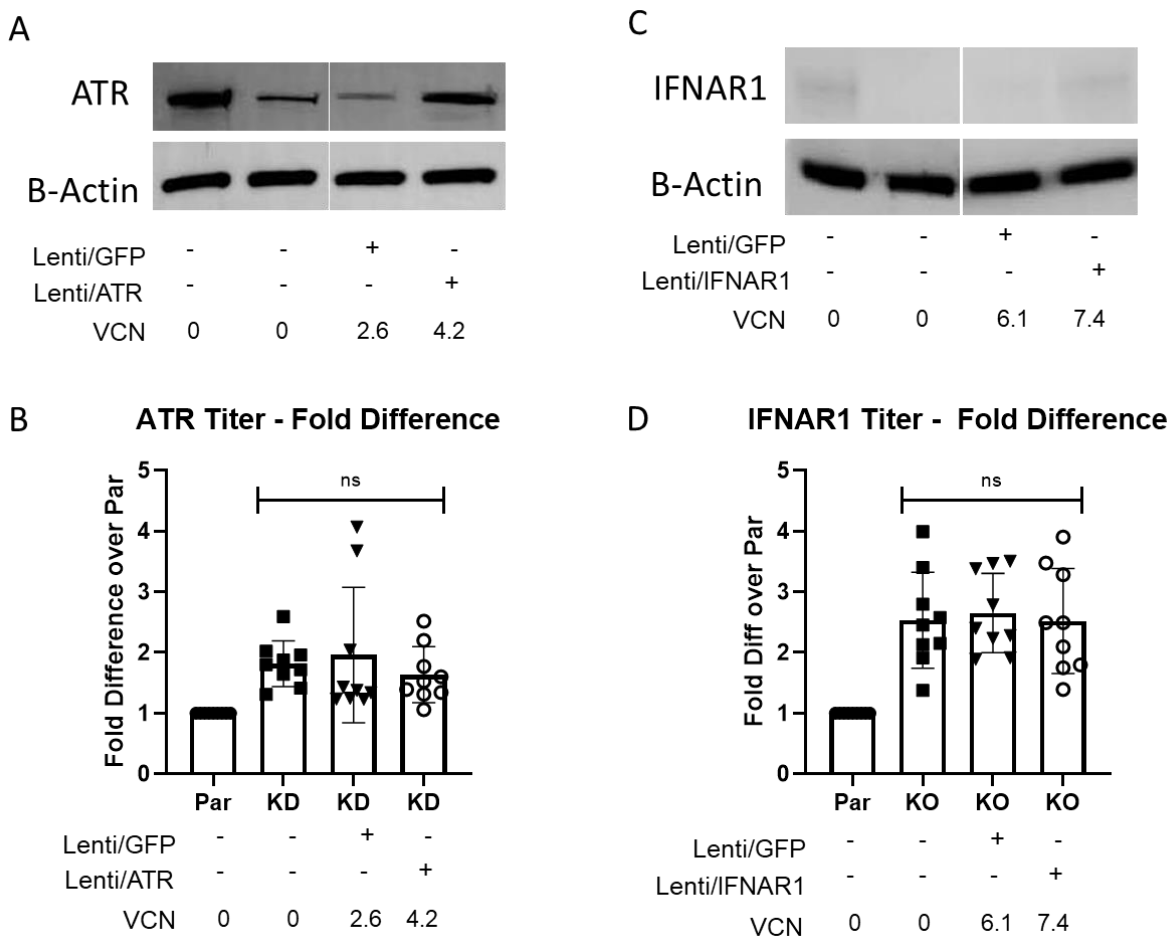

Figure 4. Restoring protein expressions of IFNAR1 and ATR did not decrease titer. A) ATR protein expression in parental HEK293T, ATR KD 293T, ATR KD 293T transduced with Lenti/GFP, and ATR KD 293T transduced with Lenti/ATR measured by western blot. B-actin was used as a loading control. ATR KD cells were transduced with an LV encoding MND-ATR-ires-GFP or an LV encoding MND-GFP as a transduction control. Two days after transduction, the transduced cells were sorted for the GFP+ population. The GFP+ cells were rested for an additional 12 days, measured for VCN analysis by ddPCR, and used for packaging of Lenti/βAS3-FB. B) Titers of Lenti/βAS3-FB packaged in parental HEK293T, ATR KD 293T, ATR KD 293T transduced with Lenti/GFP, and ATR KD 293T transduced with Lenti/ATR. (n=9 dishes of identical cultures from 3 independent experiments; bars represent mean with SD; one-way ANOVA; ns, not significant). C) Protein expression of IFNAR1 in parental 293T, IFNAR1-/- 293T, IFNAR1-/- 293T transduced with Lenti/GFP, and IFNAR1-/- 293T transduced with Lenti/IFNAR1 measured by western blot. B-Actin was used as a loading control. D) Titers of Lenti/βAS3-FB packaged in parental 293T, IFNAR1-/- 293T, IFNAR1-/- 293T transduced with Lenti/GFP, and IFNAR1-/- 293T transduced with Lenti/IFNAR1 (n=9 dishes of identical cultures from 3 independent experiments; bars represent mean with SD; one-way ANOVA; ns, not significant).

Combining OAS1, LDLR, and PKR knockouts improved titer, RNA production, and physical particle formation

Because OAS1, LDLR, and PKR are likely to have nonredundant functions, it is conceivable that knocking out multiple restriction factors may additively improve the vector production process. Next, we consecutively knocked out these restriction factors to study the effect on titer. Cas9 and sgRNA targeting *OAS1* were electroporated into the *PKR-/-* isogenic clone. After confirming the cutting efficiency, some of the edited cells were sorted for single-cell clones, and the other cells were electroporated with Cas9 and sgRNA targeting *LDLR*. These cells were used again to further knock out IFNAR1 and in the end, knock down ATR. Electroporation of two sgRNAs simultaneously was avoided to prevent chromosome translocation. The sgRNAs were introduced in the following order—PKR, OAS1, LDLR, IFNAR1, and ATR—to generate single, double, triple, quadruple, and quintuple KO/KD cells.

Lenti/βAS3-FB was packaged in the single, double, and triple KO cells in parallel and titered the unconcentrated viruses in HT-29 cells. As shown in Fig. 5A (n=9 dishes of identical cultures from 3 independent experiments; bars represent mean with SD; unpaired t-test, $*p < 0.05$, $**p < 0.01$, $***p < 0.001$, $****p < 0.0001$), the *OAS1 PKR* double KO cells increased titer by 5.9 ± 1.8-fold over the parental 293T cells. The *OAS1 PKR* double KO cells slightly increased titer compared to the *PKR-/-* cells (4.5 ± 1.5-fold over the parental 293T cells). Furthermore, the *OAS1 PKR LDLR* triple KO cells showed a significant increase in titer compared to the single KO cells, resulting in a 6.7 ± 0.7-fold increase over parental 293T cells. *OAS1 PKR LDLR IFNAR1* quadruple KO cells as well as *OAS1 PKR LDLR IFNAR1 ATR* quintuple KO/KD cells did not further increase titer (Fig. 6; n=3 dishes of identical culture from 1 independent experiment; base represent mean with SD). These data suggest that OAS1, PKR and LDLR triple KO led to the highest titer, and the data were reproducible in more than one clone (Fig. 6). We also showed that these edited cells shared a similar morphology and growth rate as the parental 293T cells (Fig. 7).

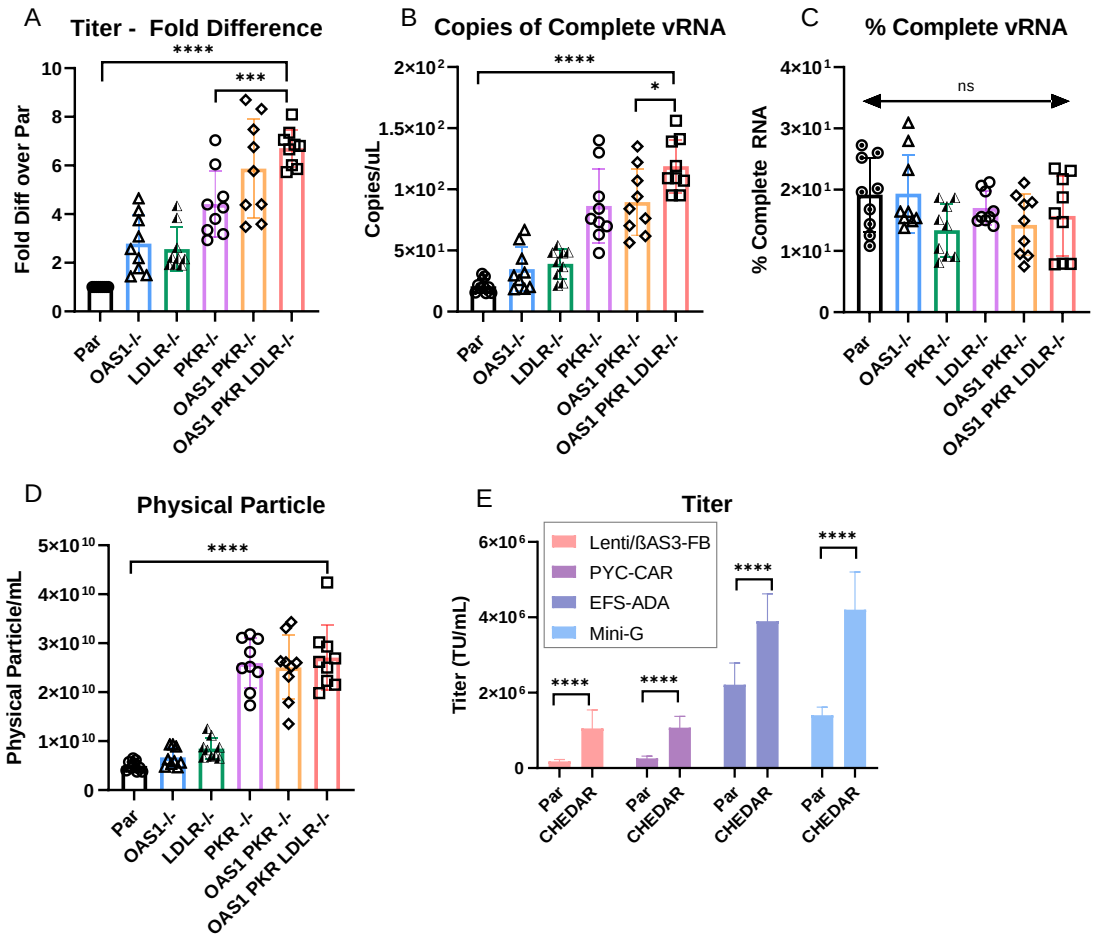

Figure 5. Knocking out PKR, OAS1, and LDLR in 293T cells additively increased titer, RNA, and physical particles. A) OAS1, PKR, LDLR protein expression in parental, OAS1 and PKR double KO, and OAS1, PKR, and LDLR triple KO cells measured by western blot and flow cytometry. The double KO isogenic clones were created by electroporating RNP targeting the OAS1 gene in the PKR-/- isogenic clones and selecting an isogenic clone with OAS1 and PKR knocked out. The triple KO isogenic clones were created by electroporating RNP targeting LDLR gene in the PKR and OAS1 double KO clone and selecting an isogenic clone with OAS1, PKR, and LDLR knocked out. B) Fold difference of titers of Lenti/βAS3-FB packaged in single, double, and triple KO cells (n=12 dishes of identical cultures from 4 independent experiments; bars represent mean with SD; unpaired t-test, ∗p < 0.05, ∗∗p < 0.01, ∗∗∗p < 0.001, ∗∗∗∗p < 0.0001). C, D) The absolute quantification and percentage of complete viral RNA in Lenti/βAS3-FB viral particles measured by ddPCR (n=9 dishes of identical cultures from 3 independent experiments; bars represent mean with SD; unpaired t-test, ∗p < 0.05, ∗∗p < 0.01, ∗∗∗p < 0.001, ∗∗∗∗p < 0.0001). E) Concentrations of physical particles in Lenti/βAS3-FB unconcentrated virus quantified by by p24 ELISA (n=9 dishes of identical cultures from 3 independent experiments; bars represent mean with SD; unpaired t-test, ∗p < 0.05, ∗∗p < 0.01, ∗∗∗p < 0.001, ∗∗∗∗p < 0.0001). F) Titers of Lenti/βAS3-FB, PYC-CAR, EFS-ADA, and Mini-G packaged in parental 293T and OAS1, PKR and LDLR KO cells (n=9 dishes of identical cultures from 3 independent experiments; bars represent mean with SD; unpaired t-test, ∗p < 0.05, ∗∗p < 0.01, ∗∗∗p < 0.001, ∗∗∗∗p < 0.0001).

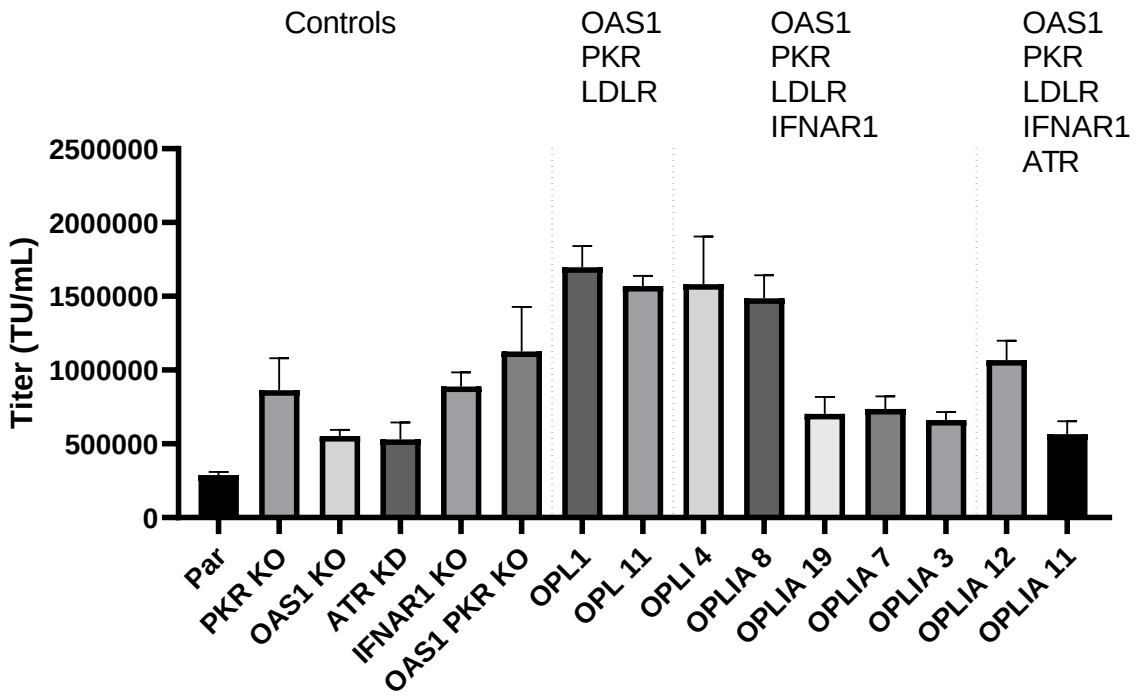

Figure 6. Additional KO of IFNAR1 and ATR did not increase titer. To create double KO, Cas9 and sgRNA targeting OAS1 were electroporated into the PKR-/- isogenic clone. After confirming the cutting efficiency, some of the edited cells were sorted for single-cell clones, and the other cells were electroporated with Cas9 and sgRNA targeting LDLR. This process was repeated to further knock out IFNAR1 and at the end knock down ATR. Electroporation of two sgRNA simultaneously was avoided to prevent chromosome translocation. The sgRNA were introduced in the following order—PKR, OAS1, LDLR, IFNAR1, and ATR—to generate single, double, triple, quadruple, and quintuple KO/KD cells. All the edited cells were sorted for single-cell clones. The clones with no parental allele or 30% parental allele for ATR were expanded for packaging of Lenti//βAS3-FB. OPL, OAS1 PKR LDLR. OPLI, OAS1, PKR, LDLR, IFNAR1. OPLIA, OAS, PKR, LDLR, IFNAR1, ATR. The numbers after the names are the clone numbers.

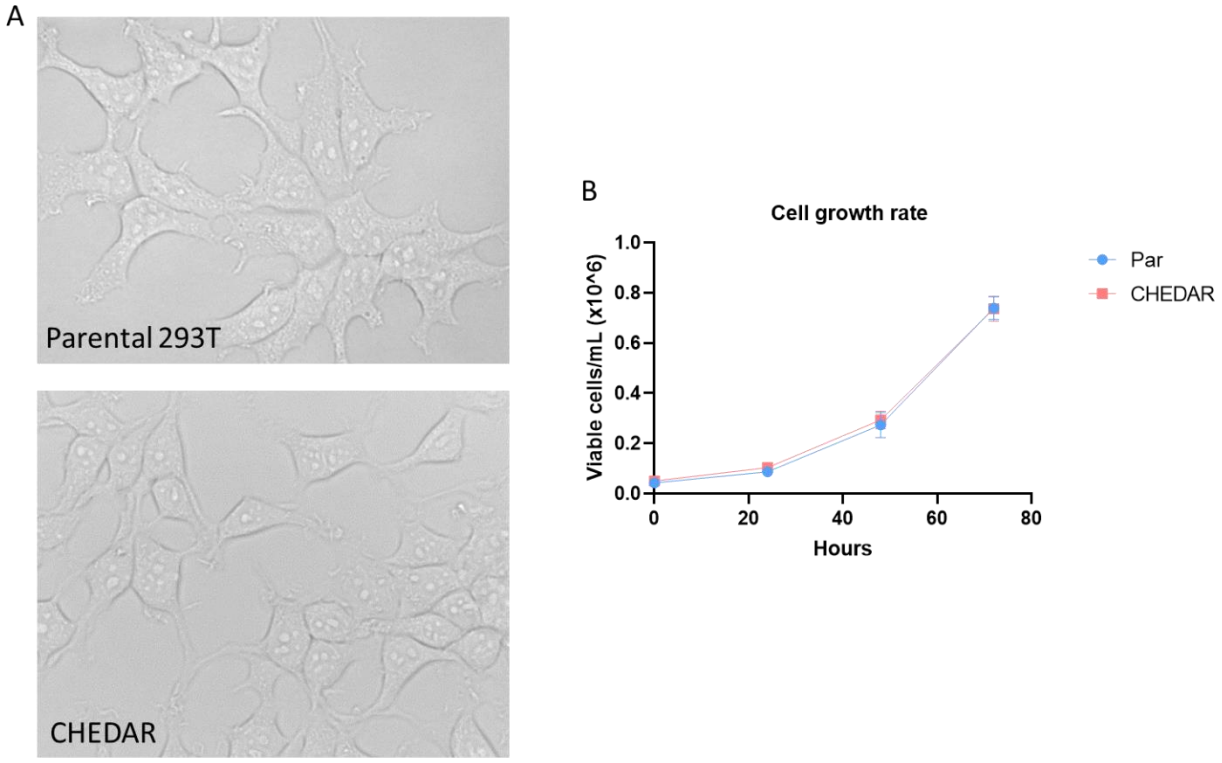

Figure 7. Morphology and growth rate of CHEDAR. A) The morphology of parental HEK293T cells and the CHEDAR cell line at 40X. B) The growth rate of parental HEK293T cells and the OAS1, PKR, LDLR triple KO cells. The cells were plated at equal density, and the cell number was monitored every 24 hours for three days (n=3 dishes of identical cultures).

Next, we investigated the viral RNA completeness and physical particle formation of the LVs produced from these genome-engineered cells. Using the method previously described in Han et al[24] to quantify Complete vRNA, we observed that the *OAS1 PKR LDLR* triple KO cells led to the highest level of Complete vRNA, which was significantly more than the double KO cells and the parental cells (Fig. 5B; n=9 dishes of identical cultures from 3 independent experiments; bars represent mean with SD; unpaired t-test, $*p < 0.05$, $**p < 0.01$, $***p < 0.001$, $****p < 0.0001$). All the different genome modifications did not affect the RNA completeness (Fig. 5C, n=9 dishes of identical cultures from 3 independent experiments; bars represent mean with SD; unpaired t-test, $*p < 0.05$, $**p < 0.01$, $***p < 0.001$, $****p < 0.0001$). All the genome modifications on the packaging cell improved physical particle formation, especially PKR KO (Fig. 5D, n=9 dishes of identical cultures from 3 independent experiments; bars represent mean

with SD; unpaired t-test, $*p < 0.05$, $**p < 0.01$, $***p < 0.001$, $****p < 0.0001$). The triple KO cells did not further increase physical particles compared to the PKR KO alone. These data suggested that the *OAS1 PKR LDLR* triple KO cells produced LVs with higher titer, higher absolute Complete vRNA yet the similar percentage of Complete vRNA, and more physical particles.

To test whether the engineered packaging cell can be used to improve the titer of other LVs, we packaged four different LVs in the *OAS1 PKR LDLR* triple KO cells. The vector maps are shown in Fig. 8. PYC-CAR is an LV encoding a chimeric antigen receptor (CAR) that targets B-cell maturation antigen (BCMA), an antigen that presents on multiple myeloma cells[29]. The CAR was constructed with four anti-BCMA single-chain variable fragments, fused to the CD137 (4-1BB) co-stimulatory and CD3ζ signaling domains under the control of an MND promoter[29]. Mini-G is a reverse-oriented β-globin vector with redefined enhancer element boundaries of the β-globin locus control region[6]. The EFS-ADA vector consists of the human elongation factor-α gene "short" promoter (EFS) driving the expression of a codon-optimized human ADA gene cassette followed by the wPRE, all in the sense (forward) orientation[30].

Our engineered cell line was able to improve the titer of all four LVs (Fig. 5E). We were able to improve the titer of Lenti/βAS3-FB by 5.9 ± 1.7-fold, PYC-CAR by 4.2 ± 0.9-fold, EFS-ADA by 1.8 ± 0.3-fold, and Mini-G by 3 ± 0.5-fold (n=9 dishes of identical cultures from 3 independent experiments; bars represent mean with SD; unpaired t-test, $*p < 0.05$, $**p < 0.01$, $***p < 0.001$, $****p < 0.0001$). These data suggest that the *OAS1 PKR LDLR* triple KO cells can be used to improve the packaging process for different LVs, especially LVs with low titer and LVs in reverse orientation. We decided to name the OAS PKR LDLR triple KO cells as **C**RISPRed **HE**K293T to **D**isrupt **A**ntiviral **R**estrictions or in short CHEDAR.

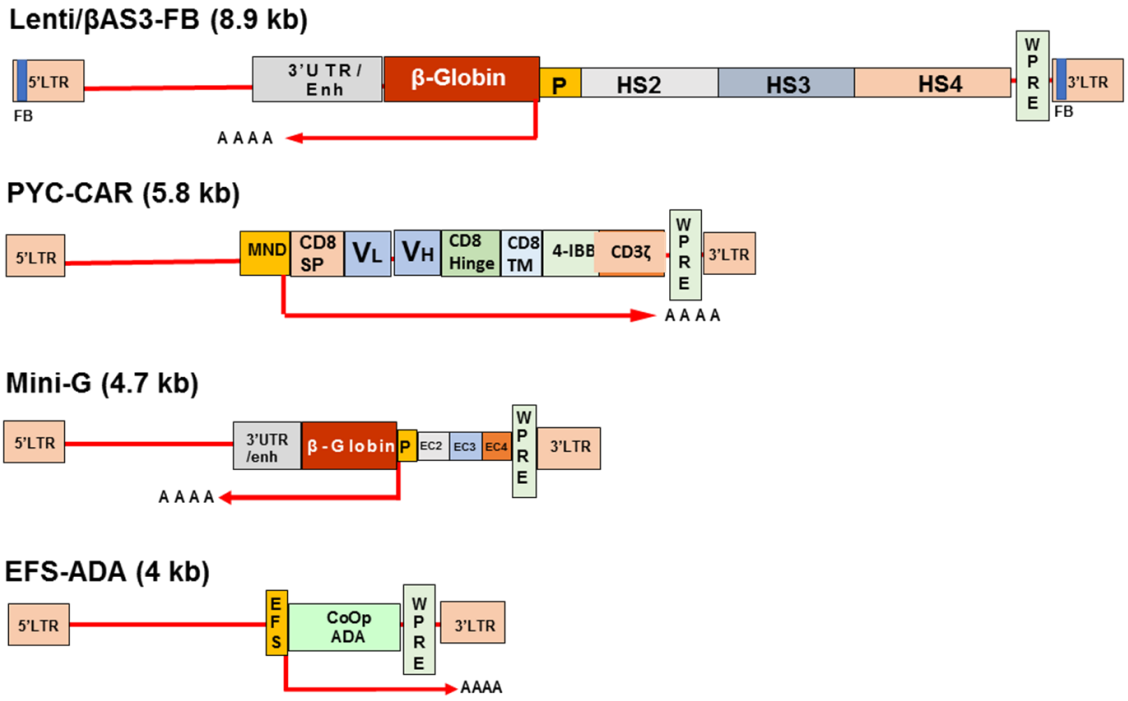

Figure 8. Maps of lentiviral vector proviruses. Long terminal repeats (LTR) include the ΔU3, R, U5 sequences. FB, FII-BEAD insulator. 3' UTR, ß-globin gene 3' UTR enhancer elements. P, promoter. HS2, HS3, HS4, ß-globin locus hypersensitive sites 2, 3, and 4. EC2, EC3, EC4, enhancer core elements. WPRE, mutated woodchuck hepatitis virus post-transcriptional regulatory element. ß-Globin, ß-Globin gene cassette. EFS, elongation factor 1 alpha promoter. ADA, codon-optimized adenosine deaminase cDNA. PYC-CAR encodes the CD8 signal peptide, V_L, linker, V_H, CD8-alpha hinge, and transmembrane (TM), CD137 (4-1BB) co-stimulatory cytoplasmic signaling domain, and CD3-zeta cytoplasmic signaling domain expressed under the control of the MND promoter.

DISCUSSIONS

Low titer and infectivity of complex lentiviral vectors, like β-globin LVs and CAR-T LVs, create barriers for clinical and commercial applications of gene and cell therapy. We elucidated the mechanisms leading to low titer and infectivity: 1) restriction factors impeding various steps of the lentiviral lifecycle; 2) viral RNA truncations. In this chapter, we focused on negating restriction factors to rescue titer and infectivity. Restriction factors are not only interferon-dependent genes in innate immunity but also cellular proteins inhibiting the lentiviral lifecycle. We first conducted a CRISPR-Cas9 mediated KO screen focusing on genes in the immune

response, receptor-mediated virus entry, transcription, and DNA damage response pathway. We showed that knocking out OAS1, LDLR, and PKR in the HEK293T cells increased the titer of lentiviral vectors and knocking out all three genes in a monoclonal cell line, CHEDAR, further increased titer of Lenti/βAS3FB 4~8-fold higher than the titer of the vectors produced from the parental HEK293T cells.

We observed that Lenti/βAS3-FB triggered an antiviral response mediated by PKR to inhibit virion formation. Double-stranded RNA (dsRNA)-activated PKR inactivates the eukaryotic translation initiation factor 2A, resulting in the inhibition of mRNA translation initiation[43, 44]. Although LVs are single-stranded RNA viruses, non-lineage-specific activation of the internal β-globin promoter in the reverse orientated Lenti/βAS3-FB may lead to the production of viral RNA in the anti-sense orientation; hybridization of the sense RNA driven by the CMV promoter and anti-sense RNA driven by the internal promoter can lead to the production of dsRNA and PKR response. Our observations were consistent with others that bidirectional vectors had low titer due to the formation of dsRNA[45].

Previous studies have shown that knocking out certain cellular factors improved the production of LVs[18,46]. In this study, we showed that knocking out PKR in the packaging cells restored p24 production in the reverse-oriented vectors, suggesting that PKR was activated to inhibit P24 production in reverse-oriented LVs. Furthermore, we demonstrated potentially additive effects of combining the three strategies: shortening the vector, packaging with Tat, and knocking out PKR to increase titer by ~30-fold and infectivity by 3-fold for the β-globin vector. These modifications were able to increase the production of viral substrates that are essential for the remaining steps of the lentiviral lifecycle.

LDLR serves as the major cellular entry port of VSVG-pseudotyped LVs, and other LDLR family proteins serve as the alternative, yet less effective, binding target[34]. One initial hypothesis of the LDLR-dependent decrease of vector titer is that LVs interact with HEK293T

LDLR at the plasma membrane and re-enter the packaging cells, resulting in the loss of LVs. However, Otahal *Et al*. showed that VSVG granules colocalized with LDLR in the ER-Golgi intermediate compartment (ERGIC) and aggresome/autophagosome[35]. They proposed a model that LDLR and VSVG interact prematurely in ERGIC, and these VSVG-LDLR complex are subsequently rerouted to be degraded in aggresome/autophagosome[35]. We also observed that the *LDLR-/-* cells were equally infected as the parental HEK293T cells (data not shown), suggesting that knocking out LDLR did not prevent LVs from reentering the cells. The latter hypothesis of aggresome/autophagosome degradation of LDLR-VSVG complex is more likely to explain the increase in titer in the *LDLR-/-* cells.

The 2'-5' oligoadenylate synthetases (OAS) are a family of antiviral proteins consisting of *OAS1*, *OAS2*, *OAS3*, and *OASL*. The OAS proteins are expressed at low levels and are augmented upon IFN induction[36]. The OAS1, OAS2, and OAS3 proteins can be activated upon detecting double-stranded RNA (dsRNA) to produce 2'-5' oligoadenylates (2-5As)[37], which subsequently activates RNAse L[38]. RNAse L degrades both cellular and viral RNA, thereby inhibiting viral replication[39]. While OAS1-3 proteins are well known for their RNAseL-dependent activity, recent evidence suggests that OAS1 can directly inhibit viral replication independent of RNAse L[40]. Kristiansen et al reported that OAS can be released to the extracellular space and acts as a paracrine antiviral agent without activation of RNAseL. In our study, we did not observe an increase in titer packaging in *RNAseL* KD 293T cells, suggesting that the RNAse L independent antiviral activity may explain the increase in titer with the *OAS1-/-* 293T cells. Future studies to explore the mechanisms leading to the titer increase in *OAS1-/-* cells are needed. Although the interferon signaling is uncoupled from cytokine secretion in 293T cells, we showed that some of the antiviral effectors, such as OAS1 and PKR, are still active in 293T cells, and knocking them out improved packaging efficiency.

In summary, we present a new packaging cell line, CHEDAR, with OAS1, LDLR and PKR knocked out to prevent the antiviral responses and inhibition on the lentiviral lifecycle. CHEDAR increased the titer of Lenti/βAS3FB 4~8-fold higher than the titer of the vectors produced from the parental HEK293T cells.

ACKNOWLEDGMENTS

The PYC-CAR vector was created by Dr. Yvonne Chen and kindly provided by Dr. Satiro De Oliveira. The Flow Cytometry Core of the UCLA Eli & Edythe Broad Center of Regenerative Medicine and Stem Cell Research and the Virology Core of the UCLA Center for AIDS Research (5P30 AI028697) supported these studies.

METHODS

LV Production and Titration

The LVs used in this study include roUBC[47], EFS-ADA[30], Lenti/βAS3-FB[23], Mini-G[6], and PYC-CAR[48]. The LV packaging and titration protocols were previously described in Han et al[24]. Briefly, genetically modified and wild-type 293T cells were plated in 6-well plates and transiently transfected with a fixed amount of HIV Gag/Pol, Rev, VSV-G expression plasmids, and equimolar amounts of transfer plasmids with TransIT-293 (Mirus Bio, Madison, WI). For certain experiments, SPT4 and SPT5 expression plasmids or a non-packageable GFP plasmid were added to the transfection mix. About 20 hours after transfection, transfected cells were incubated in D10 containing 10 mM sodium butyrate and 20 mM HEPES for 6-8 hours. Cells were then washed with PBS and cultured in fresh D10 for approximately 40 hours. Viral supernatants were collected and filtered through a 0.45 μm filter. If needed, viral supernatants

were concentrated by ultracentrifugation at 26,000 rpm for 90 min. Both raw and concentrated viruses were kept at -80°C for long-term storage.

Viral titers were determined by transducing HT-29 human colon carcinoma cells with different dilutions of the LVs and pelleted the cells ~60 hours after transduction. Genomic DNA was extracted using either the PureLink Genomic DNA Mini Kit (Invitrogen, Waltham, MA) or QuickExtract DNA Extraction Solution (Lucigen, Middleton, WI). Viral titers were calculated as VCN x cell number at the time of transduction x dilution factor. VCN was defined as the ratio of the copies of the HIV-1 PBS region to the copies of the *SDC4* endogenous reference gene and measured by Droplet Digital PCR (ddPCR). The droplet generation process was described in Hindson et al[41], and the ddPCR cycling conditions and protocols were described previously in Han et al[24].

Single Guide RNAs Construction

Single guide RNAs (sgRNA) were designed using the Benchling CRISPR online tool, and oligonucleotides were synthesized by Integrated DNA Technologies (San Diego, CA). sgRNAs were in vitro transcribed following the protocol as previously described[42]. Briefly, sgRNA was assembled as DNA and PCR amplified to generate enough DNA templates. The DNA template was in vitro transcribed into sgRNAs using the HiScribe T7 Quick High Yield RNA Synthesis Kit (New England Biolabs; Ipswich, MA). RNA was purified using the RNeast MinElute Cleanup Kit (Qiagen; Valencia, CA), following the manufacturer's protocol.

Electroporation

2×10^5 cells per condition were pelleted at 100 xg for 10 minutes at room temperature, resuspended in 10 ul of SF solution with supplements (Lonza; Basel, Switzerland). 100 pmol of Cas9 was added to 240 pmol of sgRNA to form the ribonucleoprotein (RNP) complex, and the RNP was incubated on ice for 10-20 minutes. The cells and RNP were combined and electroporated with the Lonza 4D Nucleofector system (program CM-130). After electroporation, cells were recovered at room temperature for ten minutes and then transferred to a 24 well plate. To analyze the cutting efficiency, cells were pelleted for DNA extraction 24-48 hours after electroporation using the PureLink Genomic DNA Mini Kit (Invitrogen/ThermoFisher Scientific; Carlsbad, CA). DNA regions around the cut site were PCR amplified, and the PCR products were sent for Sanger sequencing. The cutting efficiencies were analyzed using Synthego Performance Analysis, ICE Analysis. 2019. v2.0. Synthego. After confirming the cutting efficiency, electroporated cells were single-cell sorted at the UCLA Broad Stem Cell Research Center Flow Cytometry Core. About two weeks after sorting, isogenic cell clones were collected for genomic DNA extraction, PCR amplification, Sanger sequencing, and ICE Analysis to identify knockout or knockdown clones.

Flow Cytometry

All flow cytometry analyses were performed on BD LSRFortessa and BD FACS Aria II. The cells were harvested and washed with PBS and stained for 30 min at 4°C or 15 min at room temperature with the anti-LDLR antibody (R&D Systems, Minneapolis, MN) and DAPI. For FACS-sorting of single cells, cells were stained with DAPI, and live cells were sorted into one cell per well in 96-well plates.

Western Blot

The western blot protocol was previously described by Crowell et al[43]. All samples except OAS1 did not require prior treatments. To induce OAS1 expression, cells were incubated with 10 ng/mL recombinant human IFN-beta protein (R&D Systems, Minneapolis, MN) at 37°C for 24 hrs prior to harvesting the cells. 2×10^6 cells were collected and lysed in RIPA buffer (50 mM Tris-HCL pH8.0, 150 mM NaCl, 1% NP-40, 0.5% Sodium Deoxycholate, 0.1% SDS) with HALT protease inhibitor cocktail (ThermoFisher, Waltham, MA). To determine the protein concentration, the BCA assay was conducted using the Pierce BCA Protein assay kit (ThermoFisher, Waltham, MA) following the manufacturer's protocol. An equal amount of proteins was run on NuPAGE 4%-12% Bis-Tris Gel (Novex), transferred onto PVDF membranes (Millipore Sigma), and incubated with the primary antibodies at 4°C overnight. The primary antibodies used in this study include anti-SPT4 (Cell Signaling Technology, Product #648285, Danvers, MA), anti-SPT5 (Santa Cruz Biotechnology, sc-390961, Dallas, Texas), anti-ATR (Cell Signaling Technology, Product #13934, Danvers, MA), anti-IFNAR1 (Abcam, ab124764, Cambridge, MA), anti-β-Actin (Cell Signaling Technology, Product #3700, Danvers, MA), anti-OAS1 (Cell Signaling Technology, Product #14498, Danvers, MA), and anti-tubulin (company, product number). The primary antibodies were then detected with HRP-conjugated secondary antibodies followed by HRP chemiluminescence.

Viral RNA Analysis by ddPCR

RNA was extracted from 140 ul unconcentrated viral supernatant using the QIAmp Viral RNA Mini Kit (Qiagen), treated with DNAse I (Invitrogen, Waltham, MA), reverse transcribed with M-MLV reverse transcriptase (Invitrogen, Waltham, MA), as previously described in Han et al[24].

The abundance of Initial, Intermediate and Complete RNA was quantified by ddPCR using different primer and probe sets. Initial RNA was quantified by the amplification with the R/U5 primers and probe: forward primer 5'- GCTAACTAGGGAACCCACTGCT-3', reverse primer 5'-GGGTCTGAGGGATCTCTAGTTACCA-3', and probe 5'-FAM-CTTCAAGTAGTGTGTGCCCGTCTGT-31ABFQ-3' (Integrated DNA Technologies). Intermediate RNA was quantified by the amplification with the PBS primers and probe: forward primer 5'- AAGTAGTGTGTGCCCGTCTG-3', reverse primer 5'- CCTCTGGTTTCCCTTTCGCT-3', and probe 5'-FAM-CCCTCAGACCCTTTTAGTCAGTGTGGAAAATCTCTAG-31ABFQ-3'. Complete RNA was quantified by the amplification with the U3/R primers and probe: forward primer 5'-AGCAGTGGGTTCCCTAGTTAG-3', reverse primer 5'-GGGACTGGAAGGGCTAATTC-3', and probe 5'-FAM-AGAGACCCAGTACAAGCAAAAAGCAG-31ABFQ-3'. The cycling conditions were 95°C for 10 min for one cycle, (94°C for 30 s and 60°C for 1 min) for 40 cycles, 10 min at 98°C for one cycle, and a 12°C hold.

P24 Assay

UCLA/CFAR (Center for AIDS Research) Virology Core kindly conducted all the p24 ELISA to quantify p24 antigen concentration in unconcentrated viral supernatants using the Alliance HIV-1 p24 Antigen ELISA Kit (cat# NEK050, PerkinElmer, Waltham, MA), following the manufacturer's manual.

Statistical Analysis

Descriptive Statistics, such as a number of observations, mean and standard deviation were reported and presented graphically for quantitative measurements. Unpaired t-tests were

used to compare between columns for outcome measures, such as titers, the concentration of physical particles, copies, and percentage of RNA. In the case of normality assumption violation, nonparametric Wilcoxon rank-sum tests were used. For all statistical investigations, tests for significance were two-tailed. A p-value of less than 0.05 significance level was considered to be statistically significant. All statistical analyses were conducted using GraphPad Prism version 8.0 (GraphPad Software, San Diego, CA, USA).

REFERENCES

1. Kohn, D.B., Booth, C., Shaw, K.L., Xu-Bayford, J., Garabedian, E., Trevisan, V., Carbonaro-Sarracino, D.A., Soni, K., Terrazas, D., Snell, K., et al. (2021). Autologous Ex Vivo Lentiviral Gene Therapy for Adenosine Deaminase Deficiency. New England Journal of Medicine, NEJMoa2027675.

2. Aiuti, A., Cattaneo, F., Galimberti, S., Benninghoff, U., Cassani, B., Callegaro, L., Scaramuzza, S., Andolfi, G., Mirolo, M., Brigida, I., et al. (2009). Gene therapy for immunodeficiency due to adenosine deaminase deficiency. The New England journal of medicine *360*, 447–58.

3. Cartier, N., Hacein-Bey-Abina, S., von Kalle, C., Bougnères, P., Fischer, A., Cavazzana-Calvo, M., and Aubourg, P. (2010). [Gene therapy of x-linked adrenoleukodystrophy using hematopoietic stem cells and a lentiviral vector]. Bulletin de l'Academie nationale de medecine *194*, 255–64; discussion 264-8.

4. de Ravin, S.S., Wu, X., Moir, S., Anaya-O'Brien, S., Kwatemaa, N., Littel, P., Theobald, N., Choi, U., Su, L., Marquesen, M., et al. (2016). Lentiviral hematopoietic stem cell gene therapy for X-linked severe combined immunodeficiency. Science Translational Medicine *8*.

5. Morgan, R.A., Ma, F., Unti, M.J., Brown, D., Ayoub, P.G., Tam, C., Lathrop, L., Aleshe, B., Kurita, R., Nakamura, Y., et al. (2020). Creating New β-Globin-Expressing Lentiviral Vectors by High-Resolution Mapping of Locus Control Region Enhancer Sequences. Molecular Therapy - Methods and Clinical Development *17*, 999–1013.

6. Morgan, R.A., Unti, M.J., Aleshe, B., Brown, D., Osborne, K.S., Koziol, C., Smith, O.B., O'Brien, R., Tam, C., Miyahira, E., et al. (2019). Title: Improved Titer and Gene Transfer by Lentiviral Vectors Using Novel, Small β-Globin Locus Control Region Elements. Molecular Therapy.

7. Strebel, K., Luban, J., and Jeang, K.T. (2009). Human cellular restriction factors that target HIV-1 replication. BMC Medicine *7*, 48.

8. Kajaste-Rudnitski, A., Pultrone, C., Marzetta, F., Ghezzi, S., Coradin, T., and Vicenzi, E. (2010). Restriction factors of retroviral replication: The example of Tripartite Motif (TRIM) protein 5α and 22. Amino Acids *39*, 1–9.

9. Kajaste-Rudnitski, A., and Naldini, L. (2015). Cellular innate immunity and restriction of viral infection: Implications for lentiviral gene therapy in human hematopoietic cells. Human Gene Therapy *26*, 201–209.

10. Ferreira, C.B., Sumner, R.P., Rodriguez-Plata, M.T., Rasaiyaah, J., Milne, R.S., Thrasher, A.J., Qasim, W., and Towers, G.J. (2020). Lentiviral Vector Production Titer Is Not Limited in HEK293T by Induced Intracellular Innate Immunity. Molecular Therapy - Methods and Clinical Development *17*, 209–219.

11. Juang, Y.T., Lowther, W., Kellum, M., Au, W.C., Lin, R., Hiscott, J., and Pitha, P.M. (1998). Primary activation of interferon A and interferon B gene transcription by interferon regulatory factor 3. Proceedings of the National Academy of Sciences of the United States of America *95*, 9837–9842.

12. Fonseca, G.J., Thillainadesan, G., Yousef, A.F., Ablack, J.N., Mossman, K.L., Torchia, J., and Mymryk, J.S. (2012). Adenovirus evasion of interferon-mediated innate immunity by direct antagonism of a cellular histone posttranslational modification. Cell Host and Microbe *11*, 597–606.

13. Ronco, L. v., Karpova, A.Y., Vidal, M., and Howley, P.M. (1998). Human papillomavirus 16 E6 oncoprotein binds to interferon regulatory factor-3 and inhibits its transcriptional activity. Genes and Development *12*, 2061–2072.

14. Levine, A.J. (2009). The common mechanisms of transformation by the small DNA tumor viruses: The inactivation of tumor suppressor gene products: p53. Virology *384*, 285–293.

15. Ank, N., West, H., Bartholdy, C., Eriksson, K., Thomsen, A.R., and Paludan, S.R. (2006). Lambda Interferon (IFN-λ), a Type III IFN, Is Induced by Viruses and IFNs and Displays Potent Antiviral Activity against Select Virus Infections In Vivo. Journal of Virology *80*, 4501–4509.

16. Williams, B.R.G. (1999). PKR; A sentinel kinase for cellular stress. Oncogene *18*, 6112–6120.

17. Garcia, M.A., Gil, J., Ventoso, I., Guerra, S., Domingo, E., Rivas, C., and Esteban, M. (2006). Impact of Protein Kinase PKR in Cell Biology: from Antiviral to Antiproliferative Action. Microbiology and Molecular Biology Reviews *70*, 1032–1060.

18. Hu, P., Bi, Y., Ma, H., Suwanmanee, T., Zeithaml, B., Fry, N.J., Kohn, D.B., and Kafri, T. (2018). Superior lentiviral vectors designed for BSL-0 environment abolish vector mobilization. Gene Therapy, 454–472.

19. Han, J., Tam, K., Ma, F., Tam, C., Aleshe, B., Wang, X., Quintos, J.P., Morselli, M., Pellegrini, M., Hollis, R.P., et al. (2021). β-Globin Lentiviral Vectors Have Reduced Titers due to Incomplete Vector RNA Genomes and Lowered Virion Production. Stem Cell Reports *16*, 198–211.

20. Finkelshtein, D., Werman, A., Novick, D., Barak, S., and Rubinstein, M. (2013). LDL receptor and its family members serve as the cellular receptors for vesicular stomatitis virus. Proceedings of the National Academy of Sciences of the United States of America *110*, 7306–7311.

21. Amirache, F., Lévy, C., Costa, C., Mangeot, P.E., Torbett, B.E., Wang, C.X., Nègre, D., Cosset, F.L., and Verhoeyen, E. (2014). Mystery solved: VSV-G-LVs do not allow efficient gene transfer into unstimulated T cells, B cells, and HSCs because they lack the LDL receptor. Blood *123*, 1422–1424.

22. Otahal, A., Fuchs, R., Al-Allaf, F.A., and Blaas, D. (2015). Release of Vesicular Stomatitis Virus Spike Protein G-Pseudotyped Lentivirus from the Host Cell Is Impaired upon Low-Density Lipoprotein Receptor Overexpression. Journal of Virology *89*, 11723–11726.

23. Romero, Z., Urbinati, F., Geiger, S., Cooper, A.R., Wherley, J., Kaufman, M.L., Hollis, R.P., de Assin, R.R., Senadheera, S., Sahagian, A., et al. (2013). β-globin gene transfer to human bone marrow for sickle cell disease. Journal of Clinical Investigation *123*, 3317–3330.

24. Han, J., Tam, K., Ma, F., Tam, C., Aleshe, B., Wang, X., Quintos, J.P., Morselli, M., Pellegrini, M., Hollis, R.P., et al. (2021). β-Globin Lentiviral Vectors Have Reduced Titers

due to Incomplete Vector RNA Genomes and Lowered Virion Production. Stem Cell Reports.

25. Ruzankina, Y., Pinzon-Guzman, C., Asare, A., Ong, T., Pontano, L., Cotsarelis, G., Zediak, V.P., Velez, M., Bhandoola, A., and Brown, E.J. (2007). Deletion of the Developmentally Essential Gene ATR in Adult Mice Leads to Age-Related Phenotypes and Stem Cell Loss. Cell Stem Cell *1*, 113–126.

26. Brown, E.J., and Baltimore, D. (2003). Essential and dispensable roles of ATR in cell cycle arrest and genome maintenance. Genes and Development *17*, 615–628.

27. Cortez, D., Guntuku, S., Qin, J., and Elledge, S.J. (2001). ATR and ATRIP: Partners in checkpoint signaling. Science *294*, 1713–1716.

28. Baldwin, K., Urbinati, F., Romero, Z., Campo-Fernandez, B., Kaufman, M.L., Cooper, A.R., Masiuk, K., Hollis, R.P., and Kohn, D.B. (2015). Enrichment of human hematopoietic stem/progenitor cells facilitates transduction for stem cell gene therapy. Stem Cells *33*, 1532–1542.

29. Friedman, K.M., Garrett, T.E., Evans, J.W., Horton, H.M., Latimer, H.J., Seidel, S.L., Horvath, C.J., and Morgan, R.A. (2018). Effective Targeting of Multiple B-Cell Maturation Antigen-Expressing Hematological Malignances by Anti-B-Cell Maturation Antigen Chimeric Antigen Receptor T Cells. Human Gene Therapy *29*, 585–601.

30. Carbonaro, D.A., Zhang, L., Jin, X., Montiel-Equihua, C., Geiger, S., Carmo, M., Cooper, A., Fairbanks, L., Kaufman, M.L., Sebire, N.J., et al. (2014). Preclinical Demonstration of Lentiviral Vector-mediated Correction of Immunological and Metabolic Abnormalities in Models of Adenosine Deaminase Deficiency. Molecular Therapy *22*, 607.

31. Fitz, J., Neumann, T., and Pavri, R. (2018). Regulation of RNA polymerase II processivity by Spt5 is restricted to a narrow window during elongation . The EMBO Journal *37*.

32. Bernecky, C., Plitzko, J.M., and Cramer, P. (2017). Structure of a transcribing RNA polymerase II-DSIF complex reveals a multidentate DNA-RNA clamp. Nature Structural and Molecular Biology *24*, 809–815.

33. Ehara, H., Yokoyama, T., Shigematsu, H., Yokoyama, S., Shirouzu, M., and Sekine, S.I. (2017). Structure of the complete elongation complex of RNA polymerase II with basal factors. Science *357*, 921–924.

34. Finkelshtein, D., Werman, A., Novick, D., Barak, S., and Rubinstein, M. (2013). LDL receptor and its family members serve as the cellular receptors for vesicular stomatitis virus. Proceedings of the National Academy of Sciences of the United States of America *110*, 7306–7311.

35. Otahal, A., Fuchs, R., Al-Allaf, F.A., and Blaas, D. (2015). Release of Vesicular Stomatitis Virus Spike Protein G-Pseudotyped Lentivirus from the Host Cell Is Impaired upon Low-Density Lipoprotein Receptor Overexpression. Journal of Virology *89*, 11723–11726.

36. Baglioni, C., Minks, M.A., and Clercq, E. de (1981). Structural requirements of polynucleotides for the activation of (2′-5′)An polymerase and protein kinase. Nucleic Acids Research *9*, 4939–4950.

37. Dong, B., and Silverman, R.H. (1997). A bipartite model of 2-5A-dependent RNase L. Journal of Biological Chemistry *272*, 22236–22242.

38. Clemens, M.J., and Williams, B.R.G. (1978). Inhibition of cell-free protein synthesis by pppA2′ p5′ A2′ p5′ A: a novel oligonucleotide synthesized by interferon-treated L cell extracts. Cell *13*, 565–572.

39. Kristiansen, H., Scherer, C.A., McVean, M., Iadonato, S.P., Vends, S., Thavachelvam, K., Steffensen, T.B., Horan, K.A., Kuri, T., Weber, F., et al. (2010). Extracellular 2′-5′ Oligoadenylate Synthetase Stimulates RNase L-Independent Antiviral Activity: a Novel Mechanism of Virus-Induced Innate Immunity. Journal of Virology *84*, 11898–11904.

40. Hindson, B.J., Ness, K.D., Masquelier, D.A., Belgrader, P., Heredia, N.J., Makarewicz, A.J., Bright, I.J., Lucero, M.Y., Hiddessen, A.L., Legler, T.C., et al. (2011). High-Throughput Droplet Digital PCR System for Absolute Quantitation of DNA Copy Number. 8604–8610.

41. Dewitt, M., and Wong, J. (2015). Cas9 RNP nucleofection for cell lines using Lonza 4D Nucleofector V.1 Nature Communications.

42. Crowell, P.D., Fox, J.J., Hashimoto, T., Diaz, J.A., Navarro, H.I., Henry, G.H., Feldmar, B.A., Lowe, M.G., Garcia, A.J., Wu, Y.E., et al. (2019). Expansion of Luminal Progenitor Cells in the Aging Mouse and Human Prostate. Cell Reports *28*, 1499-1510.e6.

43. Samuel, C. E. Antiviral Actions of Interferons.pdf. **14**, 778–809 (2001)

44. Pindel, A. & Sadler, A. The Role of Protein Kinase R in the Interferon Response. *J. Interf. Cytokine Res.* **31**, 59–70 (2011).

45. Maetzig, T., Galla, M., Brugman, M. *et al.* Mechanisms controlling titer and expression of bidirectional lentiviral and gammaretroviral vectors. *Gene Ther* **17,** 400–411 (2010).

46. Park, Hee Ho et al. “DROSHA Knockout Leads to Enhancement of Viral Titers for Vectors Encoding miRNA-Adapted shRNAs.” *Molecular therapy. Nucleic acids* vol. 12: 591-599 (2018).

47. Cooper, A.R., Lill, G.R., Gschweng, E.H., and Kohn, D.B. (2015). Rescue of splicing-mediated intron loss maximizes expression in lentiviral vectors containing the human ubiquitin C promoter. Nucleic Acids Res. *43*, 682–690.

48. Friedman, K.M., Garrett, T.E., Evans, J.W., Horton, H.M., Latimer, H.J., Seidel, S.L., Horvath, C.J., and Morgan, R.A. (2018). Effective Targeting of Multiple B-Cell Maturation Antigen-Expressing Hematological Malignances by Anti-B-Cell Maturation Antigen Chimeric Antigen Receptor T Cells. Hum. Gene Ther. *29*, 585–601.

CHAPTER 4

Strategies to Improve Viral RNA Production

ABSTRACT

In this chapter, we explored strategies to rescue viral RNA truncation and combined methods reported in both Chapters 3 and 4 to further increase titer and infectivity. Shortening β-globin LV led to higher percentages of complete viral RNA genomes and higher titers. Expression of TAT protein during packaging increased vector RNA initiation, resulting in a modest increase of titers, but did not improve the completion of the viral genome. By combining three modifications to vector design and production (shortening the vector length to 5.3-kb; expressing TAT protein during packaging; and packaging in *PKR-/-* cells) there was a 30-fold increase in vector titer and a 3-fold increase in vector infectivity in HSPC. In addition, overexpressing transcription elongation factors, SPT4 and SPT5, improved the production of Complete viral RNA, thereby increasing titer by 2~3-fold. Packaging with SPT4 and SPT5 in CHEDAR cell line led to a 11-fold increase in titer. These approaches may improve the manufacturing of β-globin and other complex LVs for enhanced gene delivery and may facilitate clinical applications.

INTRODUCTION

A lentiviral vector (LV) typically contains a gene of interest under the control of human *cis*-regulatory promoters and enhancers to drive stable robust and lineage-specific expression. The identifications of these *cis*-regulatory elements have been historically challenging, especially in the realm of β-globin vectors. In the past, researchers knocked out specific sequences in mice to study their effects and define the boundaries of these elements[1–3]. However, these early studies fail to provide the exact base pair boundaries of the enhancer elements. This has led to excessive sequences in the lentiviral transgenes.

In Chapter 2, we showed that the lengthy and complex genome of LVs leads to lower titer and gene transfer efficiency. We also reported that vRNA was truncated in a length-

dependent manner in packaging cells and was exported into the viral particles. These truncated vRNAs failed reverse transcription at the first strand transfer step due to the absence of the 3' LTR and cannot form the double-stranded viral DNA to be integrated into the host cell genome. Because we did not observe any "hot" truncation sites and the RNA truncations happen in a length-dependent manner, it is conceivable that the vRNA truncations are caused by the low processivity of RNA polymerase II (RNA POL II).

One rational way to avoid exhausting RNA POL II is to shorten the vector length by removing non-essential sequences. Morgan et al redefined the functional elements in the locus control region of the endogenous human β-globin genomic sequences by employing existing genomic and epigenomic databases and created a 5.3-kb β-globin LV[4]. Another way to identify the minimal length of functional elements is the massively parallel reporter assay (MPRA). The *cis*-regulatory sequences of interest are dissected into small fragments, for example, 100 base pairs, and each fragment is cloned into a reporter cassette followed by a specific barcode sequence. If the sequence is a promoter, it will lead to the transcription of the barcode sequence. Although the method has been successfully used to generate vectors with minimal enhancer and promoter, these elements provide lower expressions compared to the larger core fragments[5]. Therefore, finding the balance between titer, infectivity, and expression is still challenging.

Alternatively, improving the processivity of RNA POL II is a viable strategy to improve titer and infectivity without reducing the expression. Tat is an accessory protein encoded in the genomes of wild-type HIV-1 that plays a pivotal role in transcription activation and elongation. Upon binding to the TAT-responsive element (TAR) hairpin from the 5' end of the HIV transcript, Tat recruits the transcriptional elongation factor pTEFb to phosphorylate the C-terminal domain of RNA Pol II, thereby enhancing the processivity of the polymerase[6–10]. In addition to Tat, cellular transcription elongation factors are also feasible targets that regulate RNA POL II

processivity. SPT4 and SPT5 are components of the DRB sensitivity-inducing factor complex (DSIF complex), which regulates transcription elongation by RNA polymerase II (RNA Pol II). SPT4-SPT5 complex promotes Pol II processivity by traveling with Pol II throughout transcription elongation[11]. Recent evidence suggests that the SPT4-SPT5 complex binds to the DNA exit region on Pol II, assisting the rewinding of DNA and preventing aberrant backtracking of Pol II[12,13].

In this chapter, we explored various strategies to improve vRNA production, including shortening the vector length, packaging with Tat, and packaging with the transcription elongation factors. We also assessed the combinatorial effects of the strategies discussed in Chapter 3 and Chapter 4.

RESULTS

Shortening the vector length increased viral RNA, titer, and gene transfer

We sought methods to improve titer and infectivity of the complex β-globin vector by rescuing the viral RNA truncation. Because the level of Complete RNA decreases with increasing vector length, we hypothesized that shortening the vector can rescue RNA production, thereby increasing titer and infectivity. Morgan *et al*. reported a 5.3-kb β-globin vector “Mini-G”, where the major size reductions are from using short LCR enhancer regions identified from the ENCODE database[4]. To test our hypothesis, we packaged Mini-G and Lenti/βAS3-FB concurrently and measured the RNA content in viral particles, titer, and infectivity in CD34+ BM cells (Fig. 1A).

Shortening the vector successfully rescued the RNA production and increased titer and infectivity in CD34+. Mini-G showed 27-fold more Complete RNA than Lenti/βAS3-FB (unpaired t test, p=0.0003) (Fig. 1B). The percentage of Complete RNA increased from 5.4% in

Lenti/βAS3-FB to 84% in Mini-G, which led to a 15.5-fold increase in the percentage of Complete RNA (unpaired t test, p<0.0001). In addition, the viral titer of the unconcentrated virus was 7.6-fold higher for Mini-G (unpaired t test, p=0.0004) (Fig. 1C). Mini-G also showed an improvement in the infectivity of human BM CD34+ HSPCs (linear regression, comparison of the slopes, p=0.0007) (Fig. 1D).

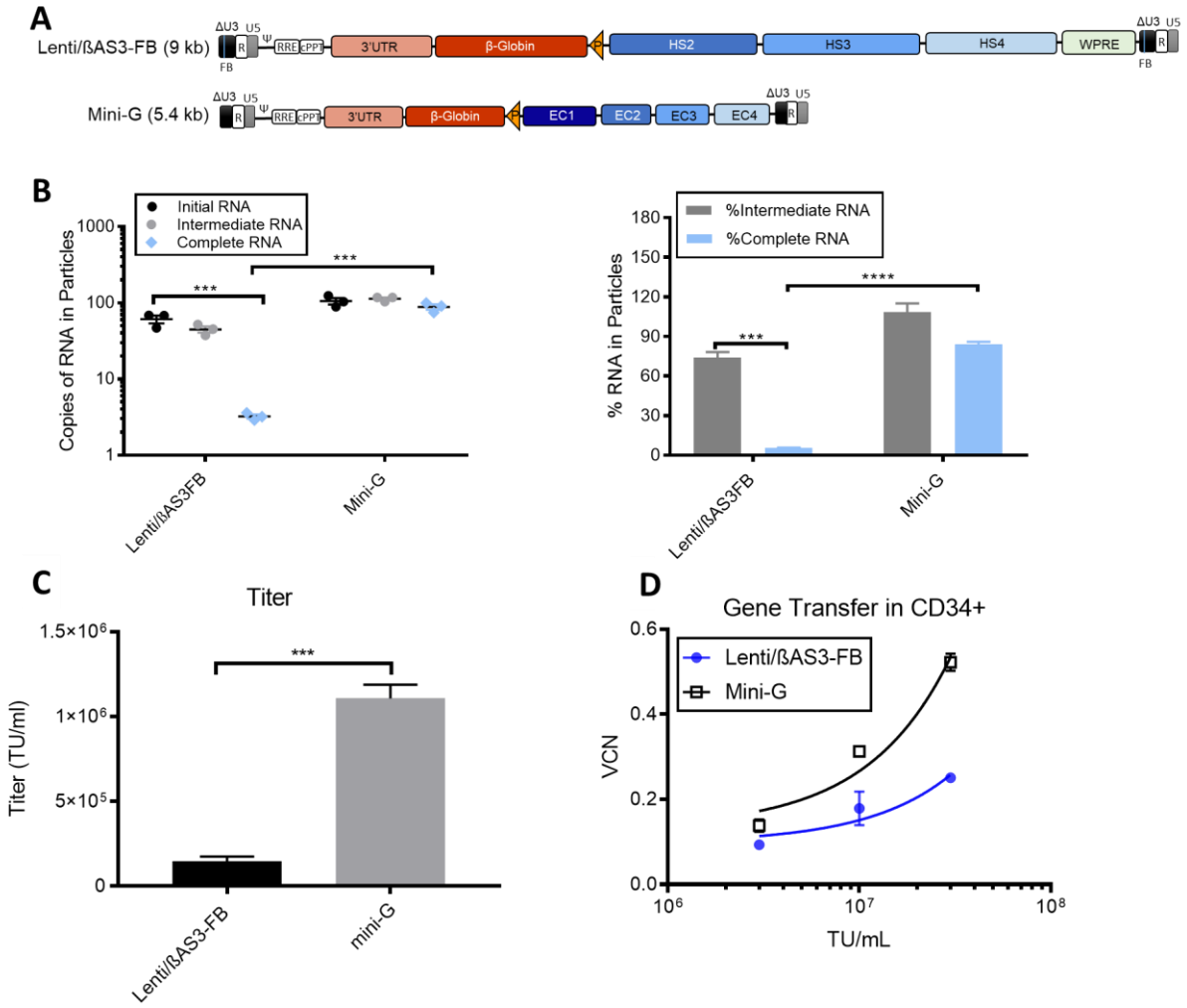

Figure 1. Shortening the vector length increased viral RNA completeness, vector titer, and CD34+ cell infectivity. (A) The schematic representation of the provirus of Lenti/ßAS3-FB and mini-G. (B) The absolute quantification and percentage of viral RNA in viral particles measured by ddPCR. (C) Viral titers of Lenti/ßAS3-FB and mini-G (bars represent mean with SEM; n=3 independent experiments; unpaired t test, *p<0.05, **p<0.01, ***p<0.001, ****p<0.0001). (D) Infectivity of Lenti/ßAS3-FB and mini-G LVs in 1e6 cells/mL of BM CD34+ HSPCs at MOI=3, 10, 30 (bars represent mean with SEM; n=3 independent experiments; linear regression, comparison of the slopes, p=0.0007). Data represent measurements from three independent human BM CD34+ HSPCs donors.

Packaging with Tat increased viral RNA

We hypothesized that packaging with Tat will increase the production of Complete RNA in LV. To test our hypothesis, we packaged Lenti/βAS3-FB[14], EFS-ADA[15], and DL-βAS3[14] vectors with the addition of either a Tat expression plasmid or a filler plasmid (unpackageable GFP plasmid without lentiviral genome). The Lenti/βAS3-FB vector plasmid is driven by the CMV promoter, whereas DL-βAS3, the parent LV to Lenti/βAS3-FB, contains an intact 5' HIV-1 LTR and is thus Tat-dependent.

We first assessed the effect of Tat on viral RNA production. Packaging with the addition of the Tat plasmid increased the levels of all viral RNA species from all three vectors (Fig. 2A). In particular, we observed a 2~3-fold increase in the absolute quantity of Complete RNA from EFS-ADA and Lenti/βAS3-FB and a ~6-fold increase in Complete RNA from DL-βAS3 (unpaired t test, *p<0.05, **p<0.01, ***p<0.001). Tat significantly elevated the percentage of Complete RNA in DL- βAS3 (unpaired t test, p=0.02), confirming that Tat was necessary for efficient transcription elongation from LV with intact 5' HIV LTR in the packaging plasmid (Fig. 2B). However, Tat did not increase the percentage of Complete RNA from EFS-ADA or Lenti/βAS3-FB, suggesting that the CMV-driven LV packaging plasmids are not Tat-dependent for transcription elongation.

Nevertheless, we examined whether the increase in the absolute quantities of full-length viral RNA when packaged with Tat correlate with viral titer. The titers of EFS-ADA and Lenti/βAS3-FB increased by 2~3-fold, and the titer of DL-118 increased by ~6-fold (unpaired t test, EFS-ADA p=0.01, DL- βAS3 p=0.004, Lenti/βAS3-FB p=0.39) (Fig. 2C). Although the increase in titer for Lenti/βAS3-FB was not statistically significant, we observed a consistent 2-fold increase in titer in LVs packaged with Tat in each independent experiment. Furthermore, LVs packaged with Tat, especially DL- βAS3 and EFS-ADA, showed an improvement in their infectivity in human BM CD34+ HSPCs (linear regression, comparison of the slopes, EFS-ADA p=0.039, DL- βAS3 p=0.01, Lenti/βAS3-FB p=0.105) (Fig. 2D).

We tried to further increase the level of Complete RNA by manipulating the location of the rev-response element (RRE). The HIV-1 Rev protein binds to the RRE to facilitate the nuclear export of viral RNA[16–19]. Moving RRE from downstream of the 5' LTR to a position upstream of the 3' LTR modestly increased the copies of Complete RNA without changing the percentage of Complete RNA and had no significant effect on titer (Fig. 3).

By combining some of the modifications discussed above—shortening the vector length, packaging with Tat, and packaging in PKR-/- cells—we were able to increase the copies of Complete RNA from the Mini-G vector compared to Lenti/βAS3-FB packaged without Tat in PKR-replete cells by 149.9-fold and to improve the percentage of Complete RNA to 79.4%. These strategies resulted in a 29.3-fold increase in titer (Fig. 4) and increased the infectivity of the β-globin vector in human BM CD34+ HSPCs by 3.2-fold at the highest dose (bars represent mean with SEM; n=3 independent experiments; linear regression, comparison of slopes, p=0.0009).

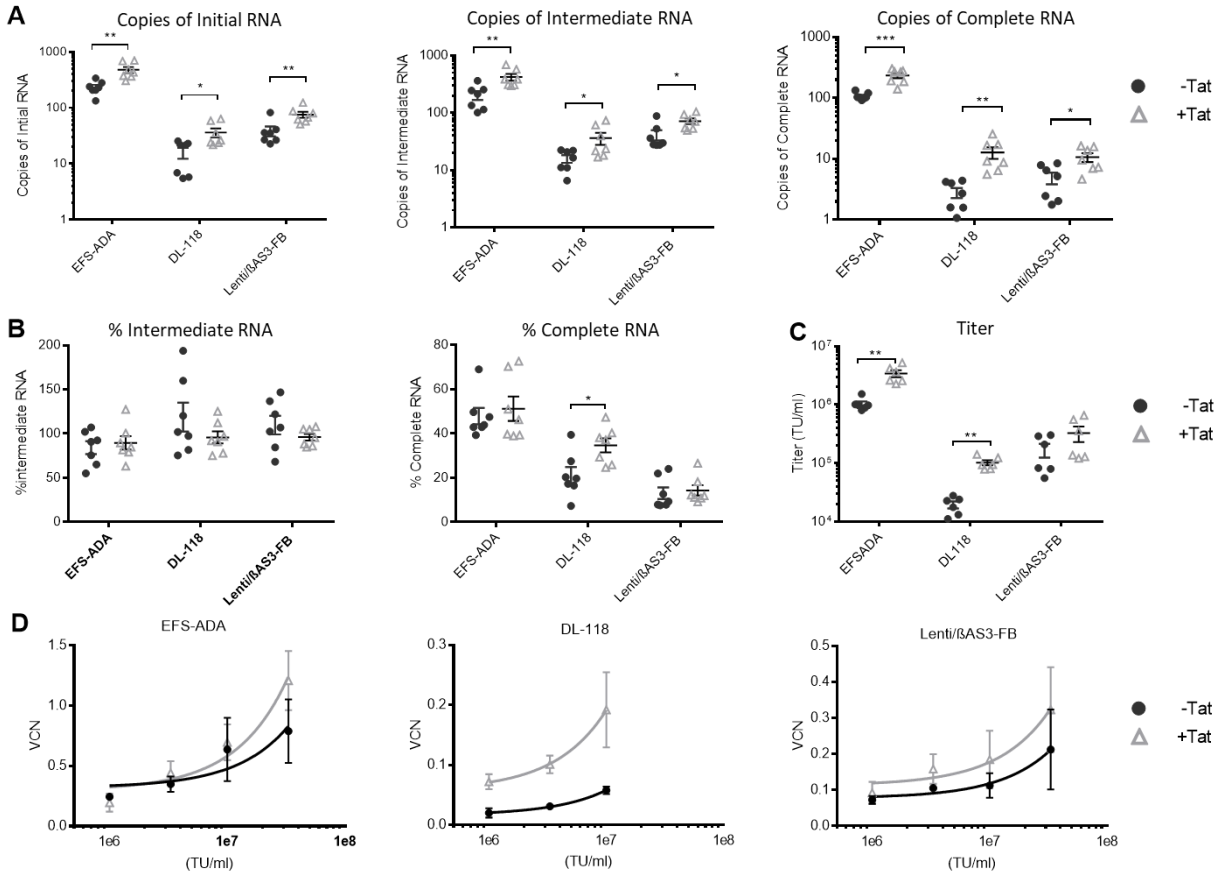

Figure 2. Packaging with Tat increased viral RNA amounts but not completeness, vector titer, and CD34+ cell infectivity. (A) The absolute quantification and (B) the percentage of Initial, Intermediate, and Complete RNA in EFS-ADA, DL- ßAS3, Lenti/ßAS3-FB LVs. DL-ßAS3 (a parental ß-globin vector to Lenti/ßAS3-FB) contains an intact 5' HIV LTR and is dependent on Tat for full-length RNA transcription. Vectors were packaged with either Tat plasmids or a filler plasmid (an unpackageable GFP plasmid without lentiviral sequences) and harvested three days post-transfection. Viral RNA was extracted from vector particles. (C) Titers of LVs packaged +/- Tat plasmids (bars represent mean with SEM; n=6 dishes of identical cultures from 3 independent experiments; unpaired t test, *p<0.05, **p<0.01, ***p<0.001). (D) Infectivity of CCLAS3 and Globe LVs +/- Tat in 1e6 cells/mL of BM CD34+ HSPCs at MOI=1, 3, 10, 30 (bars represent mean with SEM; n=3 independent experiments; linear regression, comparison of the slopes, EFS-ADA p=0.039, DL- βAS3 p=0.01, Lenti/βAS3-FB p=0.105). Data represent measurements from three independent human BM CD34+ HSPCs donors.

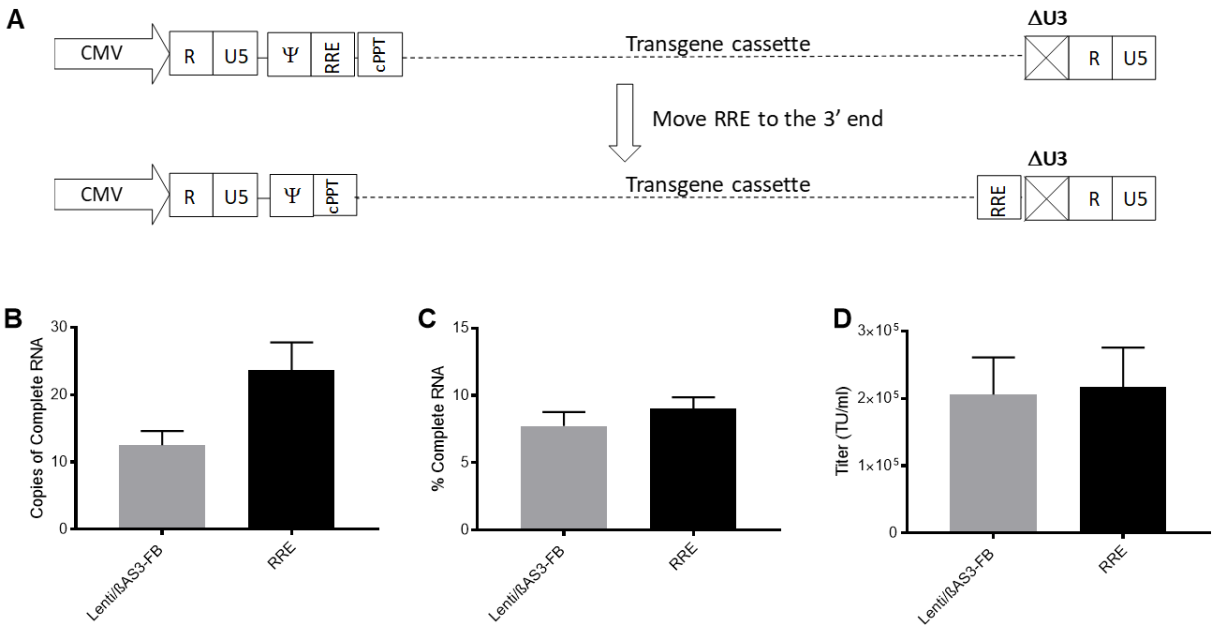

Figure 3. Moving the RRE element to the 3' LTR did not increase the viral titer. (A) Schematic representation of the vector constructs. The RRE element in Lenti/ßAS3-FB was moved from a site downstream of the 5' LTR to a site upstream of the 3' LTR to generate a new vector termed as Lenti/ßAS3-FB-RRE. (B) Absolute quantification and (C) percentage of viral RNA from unconcentrated viral supernatant of Lenti/ßAS3-FB-RRE and Lenti/ßAS3-FB measured by ddPCR with R/U5 and U3/R primers and probes (n=3 dishes of identical cultures treated and analyzed in two independent experiments). (D) Viral titers of Lenti/ßAS3-FB-RRE and Lenti/ßAS3-FB LVs (n=3 dishes of identical cultures treated and analyzed in two independent experiments; bars represent mean with SEM).

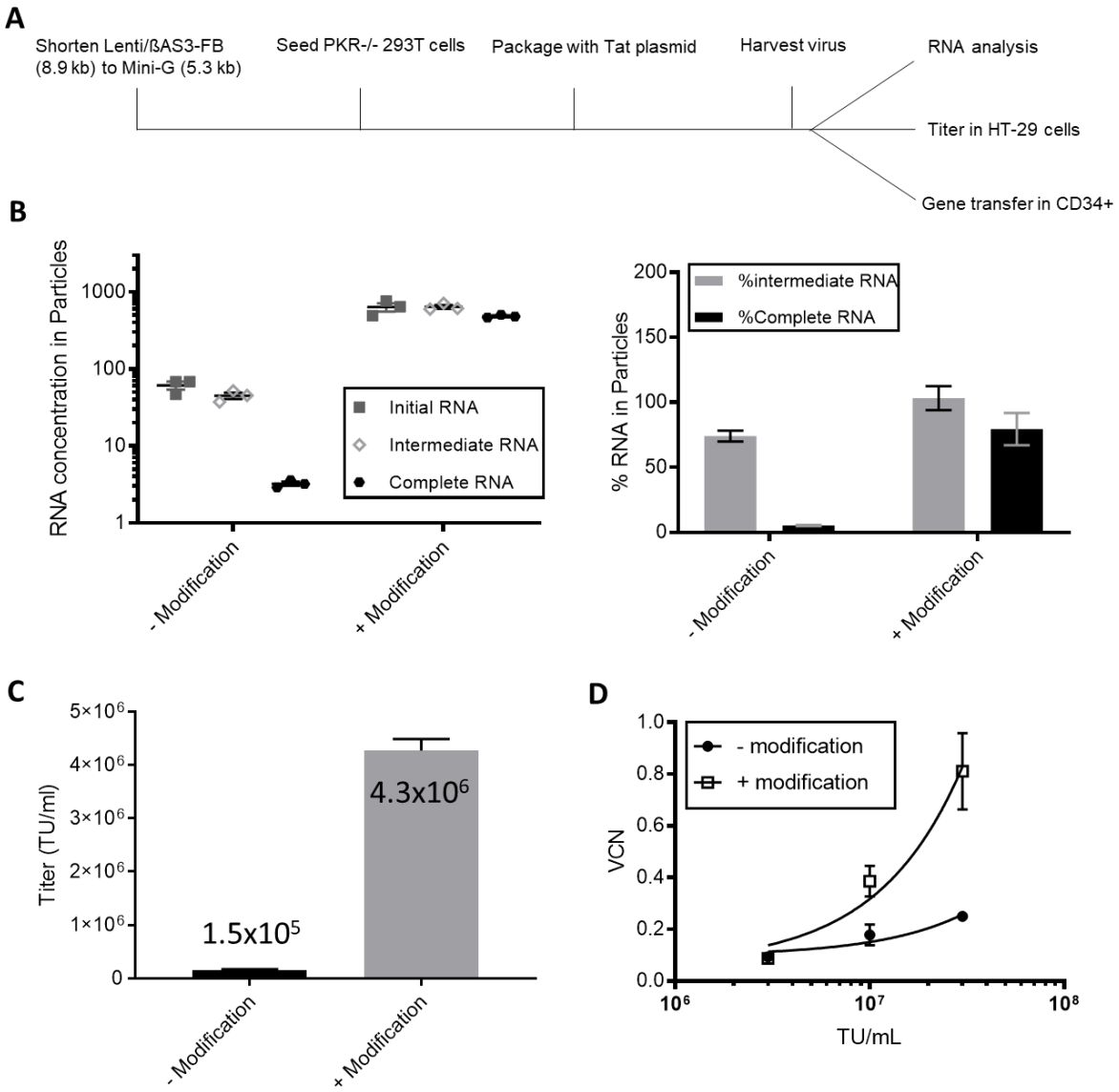

Figure 4. Combining the three modifications for the production of ß-globin vectors increased viral RNA, vector titer and CD34+ cell infectivity. (A) The schematic representation of the three modifications: shortening the vector length, packaging with TAT plasmids and packaging in PKR-/- cells. (B) The absolute quantification and percentage of viral RNA in viral particles measured by ddPCR. (C) Titers of unconcentrated ß-globin vectors +/- 3 modifications (bars represent mean with SEM; n=3 dishes of identical cultures treated and analyzed in 2 independent experiments). (D) Infectivity of ß-globin vectors +/- 3 modifications in BM CD34+ HSPCs (bars represent mean with SEM; n=3 independent experiments; linear regression, comparison of the slopes, p=0.0009). Data represent measurements from three independent human BM CD34+ HSPCs donors.

Packaging with transcription elongation factors improved RNA completeness and titer

In our previous study, we reported that Lenti/βAS3-FB viral RNA is truncated during RNA production, and the truncated RNA cannot be reverse transcribed and integrated into the host cell genome. We hypothesized that packaging with transcription elongation factors, SPT4 and SPT5, may result in more Complete viral RNA. SPT4 and SPT5 are components of the DRB sensitivity-inducing factor complex (DSIF complex), which regulates transcription elongation by RNA polymerase II (RNA Pol II). SPT4-SPT5 complex promotes Pol II processivity by traveling with Pol II throughout transcription elongation[11]. Recent evidence suggests that the SPT4-SPT5 complex binds to the DNA exit region on Pol II, assisting the rewinding of DNA and preventing aberrant backtracking of Pol II[12,13].

To test our hypothesis, we packaged Lenti/βAS3-FB with the addition of SPT4/5 expression plasmids. SPT4 and SPT5 were cloned into expression plasmids under the control of an MND promoter and transiently transfected into the 293T cells with the rest of the packaging plasmids 24 hours after plating the cells. Four conditions were tested: 5 μg of GFP plasmids alone, 2.5 μg of SPT4 plasmids with 2.5 μg of GFP plasmids, 2.5 μg of SPT5 plasmids with 2.5 μg of GFP plasmids, and 2.5 μg of SPT4 plasmids with 2.5 μg of SPT5 plasmid. GFP plasmids were used as fillers to ensure an equal mass of plasmids were transfected in each condition.

We first assessed the effect of SPT4 and SPT5 on viral RNA production (Fig. 5A; n=9 dishes of identical cultures from 3 independent experiments; bars represent mean with SD; unpaired t-test, $*p < 0.05$, $**p < 0.01$, $***p < 0.001$, $****p < 0.0001$). Compared to the transfection control, adding SPT5 alone increased the level of Initial vRNA by 1.7 ± 0.4-fold, the level of Intermediate vRNA by 1.9 ± 0.5-fold, and the level of Complete vRNA by 2.4 ± 1.5-fold; adding SPT4 alone increased the level of Initial vRNA by 1.5 ± 0.4-fold, the level of Intermediate vRNA by 1.6 ± 0.5-fold, and the Complete vRNA by 2 ± 1.2-fold. These data suggest that there

was a gradual enrichment in vRNA level towards the 3' end when the transcription elongation factors were added. Moreover, adding both SPT4 and SPT5 expression plasmids during packaging increased the level of Initial vRNA by 2.2 ± 0.6-fold, the level of Intermediate vRNA by 2.4 ± 0.7-fold, and the level of Complete vRNA by 4.4 ± 2-fold compared to the transfection control. We did not observe an increase in the percentage of Intermediate RNA, probably because the primers and probes to detect the Initial vRNA (in RU5) and Intermediate vRNA (in the primer binding site sequence) are very close to each other (Fig. 5B; n=9 dishes of identical cultures from 3 independent experiments; bars represent mean with SD; unpaired t-test, $*p < 0.05$, $**p < 0.01$, $***p < 0.001$, $****p < 0.0001$). Nevertheless, we indeed observed a significant increase in the percentage of Complete vRNA when both SPT4 and SPT5 were added. These data suggest that SPT4 and SPT5 additively facilitate transcription elongation.

Next, we examined whether the increase in vRNA correlated with titer (Fig. 5C; n=9 dishes of identical cultures from 3 independent experiments; bars represent mean with SD; unpaired t-test, $*p < 0.05$, $**p < 0.01$, $***p < 0.001$, $****p < 0.0001$). Compared to the transfection control, adding SPT5 alone increased titer by 1.4 ± 0.2-fold, adding SPT4 alone increased titer by 1.3 ± 0.1-fold, and adding both SPT4 and SPT5 increased titer by 2.2 ± 0.4-fold.

We also observed increased levels of physical particles measured by p24 ELISA when SPT4 and SPT5 were added (Fig. 5D; n=9-12 dishes of identical cultures from 3-4 independent experiments; bars represent mean with SD; unpaired t-test, $*p < 0.05$, $**p < 0.01$, $***p < 0.001$, $****p < 0.0001$). This observation suggested that SPT4 and SPT5 potentially enhanced transcription elongation not only for the transfer plasmid but also the packaging and envelope plasmids. Moreover, we examined the ratio of infectious to physical particles, which reflects the fraction of virus particles that can complete an infectious cycle. Adding both SPT4 and SPT5 increased the ratio of infectious particles to physical particles by 1.6 ± 0.4-fold than the

transfection control (Fig. 5E; n=9 dishes of identical cultures from 3 independent experiments; bars represent mean with SD; unpaired t-test, ∗p < 0.05, ∗∗p < 0.01, ∗∗∗p < 0.001, ∗∗∗∗p < 0.0001). Therefore, adding SPT4 and SPT5 yielded more infectious particles and fewer empty particles, likely due to the increased in Complete vRNA.

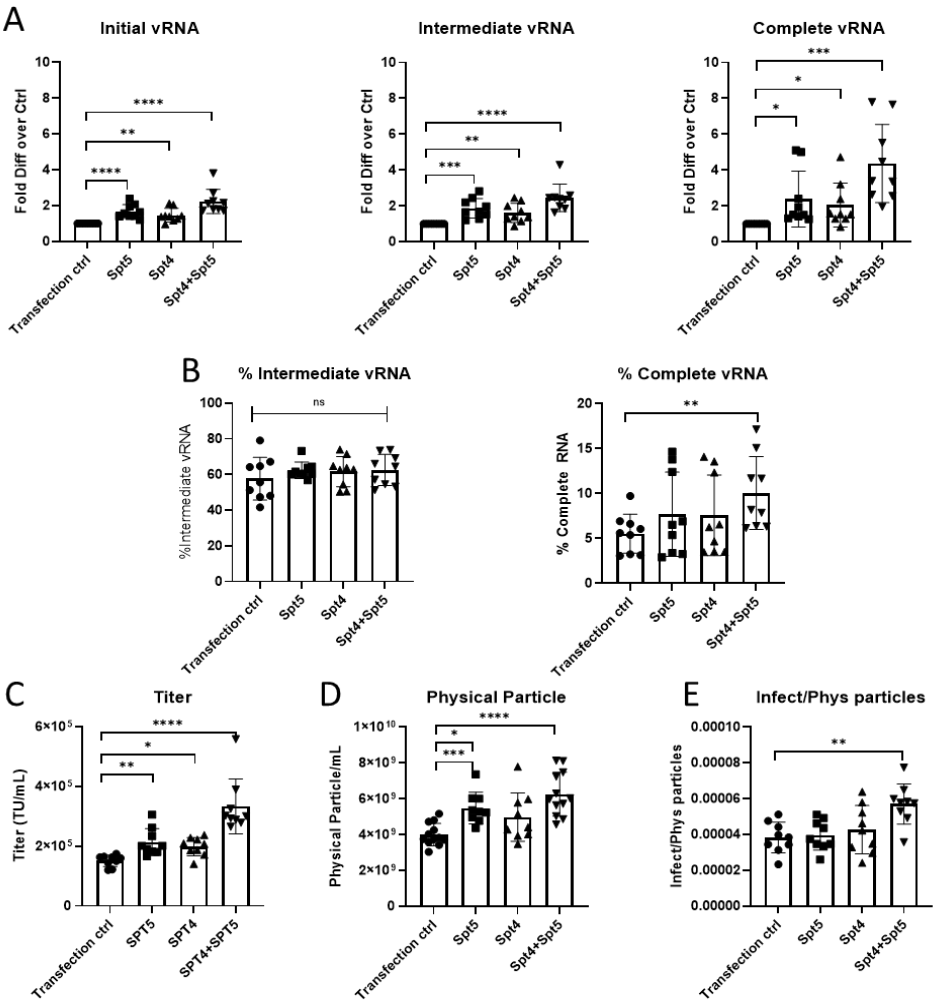

Figure 5. Packaging with transcription elongation factors SPT4/5 increased viral RNA completeness and vector titer. A) The fold difference of Initial, Intermediate and Complete vRNA compared to the transfection control and B) a percentage of Intermediate and Complete vRNA in parental HEK293T cells with SPT4/5 plasmids or a filler plasmid (n=9 dishes identical cultures from 3 independent experiments; bars represent mean with SD). The percentage of Intermediate vRNA was calculated as the copies of Intermediate vRNA divided by the copies of Initial RNA. The percentage of Complete vRNA was calculated as the copies of Complete vRNA divided by the copies of Initial vRNA. C) Titers of Lenti/βAS3-FB packaged in parental HEK293T cells with SPT4/5 plasmids or a filler plasmid as the transfection control (an unpackageable GFP plasmid without lentiviral sequences) (n=9 dishes identical cultures from 3 independent experiments; bars represent mean with SD). D) Concentration of physical particles measured by p24 ELISA (n=9 dishes identical cultures from 3 independent experiments; bars represent mean with SD). E) The ratio of infectious particles to physical particles (n=9 dishes identical cultures from 3 independent experiments; bars represent mean with SD).

Packaging with transcription elongation factors in the CHEDAR cell line increased titer, vRNA, and physical particles

Lastly, we explored the combinatorial effects of packaging with the transcription elongation factors in the CHEDAR cell line. As shown in Figure 6A, packaging in the parental HEK293T cells with the addition of SPT4 and SPT5 increased titer by 2 ± 0.4-fold compared to the parental HEK293T transfection control. Packaging in the CHEDAR cell line with the transfection control increased titer by 7 ± 1-fold over the parental HEK293T transfection control. Packaging in the CHEDAR cell line with the addition of SPT4 and SPT5 increased titer by 10.7 ± 3.2-fold over the parental HEK293T transfection control (n=9 dishes of identical cultures from 3 independent experiments; bars represent mean with SD; unpaired t-test, $*p < 0.05$, $**p < 0.01$, $***p < 0.001$, $****p < 0.0001$). We also observed a significant increase in the level of Complete vRNA and the percentage of Complete when SPT4 and SPT5 were added to the CHEDAR cell line (Fig. 6B, C; n=6-9 dishes of identical cultures from 2-3 independent experiments). Packaging with the addition of SPT4 and SPT5 in the CHEDAR cell line further improved titer and RNA production compared to the CHEDAR transfection control, suggesting that these two strategies work additively to increase titer.

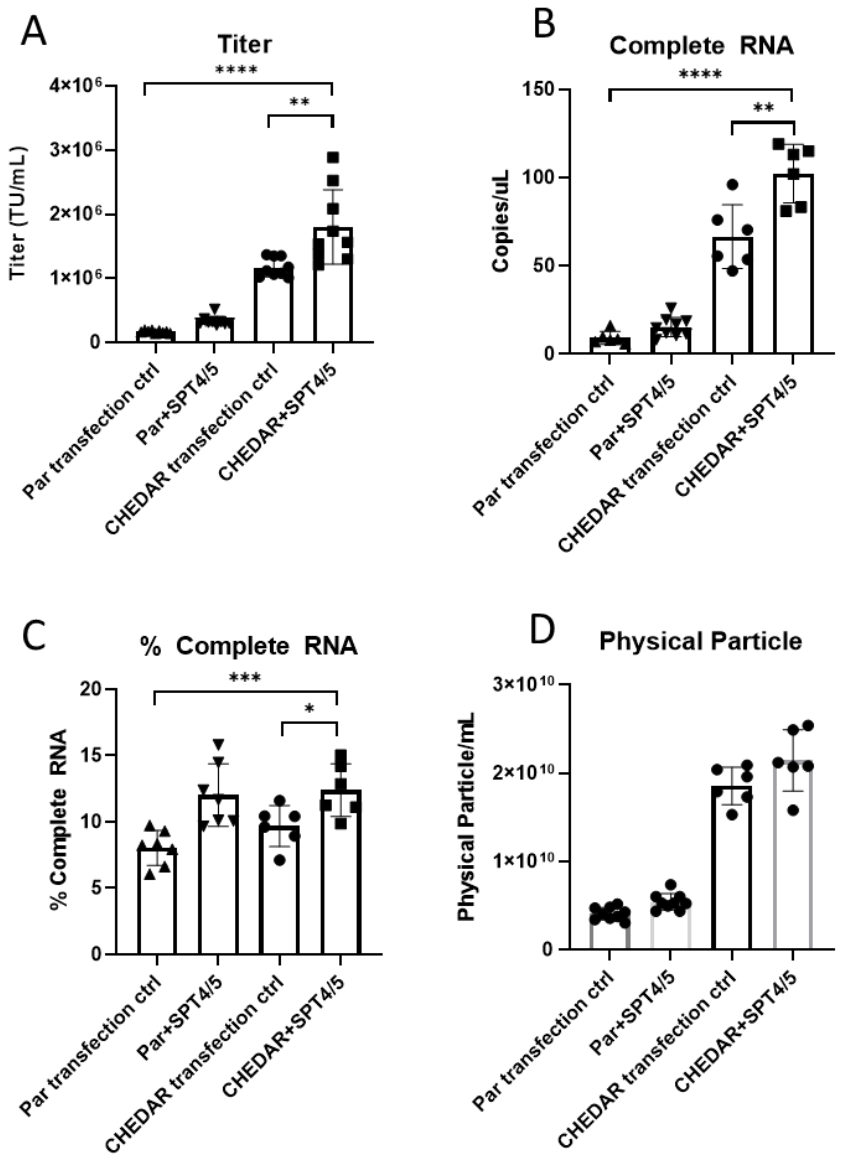

Figure 6. Packaging with SPT4 and SPT5 in the CHEDAR cell line increased titer, vRNA, and physical particles. A) Titers of Lenti/βAS3-FB packaged in parental HEK293T cells and CHEDAR cells with SPT4/5 plasmids or a filler plasmid as the transfection control (an unpackageable GFP plasmid without lentiviral sequences) (n=9-15 dishes identical cultures from 3-5 independent experiments; bars represent mean with SD). B) The absolute quantification of Complete vRNA and C) the percentage of Complete vRNA of Lenti/βAS3-FB packaged in parental HEK293T cells and CHEDAR cells with SPT4/5 plasmids or a filler plasmid as the transfection control (n=9-15 dishes identical cultures from 3-5 independent experiments; bars represent mean with SD). D) The concentration of physical particles measured by p24 ELISA.

DISCUSSIONS

Low titer and infectivity of complex lentiviral vectors, like β-globin LVs and CAR-T LVs, create barriers for clinical and commercial applications of gene and cell therapy. We elucidated the mechanisms leading to low titer and infectivity: 1) restriction factors impeding various steps of the lentiviral lifecycle; 2) viral RNA truncations. We first used three strategies to increase viral RNA production: shortening the vector length to ensure that viral RNA can be fully transcribed; packaging with HIV Tat and transcription elongation factors to enhance the processivity of RNA Pol II. Shortening the 8.9-kb Lenti/βAS3-FB vector to the 5.3-kb mini-G vector rescued the production of Complete RNA, resulting in a 7.6-fold increase in titer and a 2-fold increase in CD34+ cell infectivity at the highest dose. Packaging LVs with Tat improved RNA initiation but not Pol II processivity from CMV-driven lentiviral vector packaging plasmids. Nonetheless, a two-fold increase in titer and infectivity at the high dosage of TU was observed in Lenti/βAS3-FB when packaged with Tat. Future studies to improve RNA Pol II processivity or to identify additional problematic sequences that truncate RNA are needed.

In addition to exploring the lentiviral restriction factors, we overexpressed transcription elongation factors, SPT4 and SPT5, to enhance the production of Complete vRNA. Expressing either SPT4 or SPT5 led to a ~2-fold increase in Complete vRNA. SPT4 and SPT5 worked synergistically, because expressing both transcription elongation factors led to a ~4-fold increase in Complete vRNA and a 2-fold increase in the percentage of Complete RNA. Moreover, the transcription elongation factors showed an additive effect with the CHEDAR KO cell line to further increase Complete vRNA by 1.5-fold, resulting in a 1.2-fold increase in titer. These results suggest that overexpressing transcription elongation factors facilitates the vRNA production in both parental HEK293T and the triple KO cells. Future studies are needed to explore the addition of other transcription elongation factors.

Furthermore, we demonstrated the additive effects of improving vRNA production and removing restriction factors. Shortening the vector, packaging with Tat, and knocking out PKR together increased titer by ~30-fold and infectivity by 3-fold for the β-globin vector. Packaging with the transcription elongation factors, SPT4 and SPT5, in the *OAS1-/- LDLR-/- PKR-/-* CHEDAR cell line improved titer by 10.7 ± 3.2-fold. These modifications should be able to increase the production of viral substrates that are essential for the remaining steps of the lentiviral lifecycle, resulting in increased titer and infectivity.

METHODS

LV production and titration

The LV packaging and titration protocol were previously described in Chapter 2 and Chapter 3. Briefly, LVs were packaged by transient transfection of 293T cells with fixed amounts of HIV Gag/Pol, Rev, and VSV-G expression plasmids and equimolar amounts of each of the different vector transfer plasmids using TransIT-293 (Mirus Bio, Madison, WI). For some experiments, cells were co-transfected with one or more of the following plasmis: the HIV-1 pSV2-TAT expression plasmid (NIH AIDS Reagent Program (Rockville, MD), SPT4 expression plasmid, SPT5 expression plasmid, and a GFP expression plasmid lacking vector elements so that it would not be packaged. About 72 hours after transfection, raw virus or concentrated virus was collected for titer measurements.

LV infection in human BM CD34+ HSPCs

Human CD34+ HSPCs were isolated from healthy donor bone marrow (BM) aspirates using Ficoll-Hypaque gradient separation and a CD34 MicroBead Kit (Miltenyi Biotech, Bergisch

Gladbach, Germany). CD34+ HSPCs were plated at $1x10^6$ cells/mL in non-tissue culture treated plates coated with RetroNectin (20 µg/mL; Takara Shuzo Co., Otsu, Japan). The cells were pre-stimulated for 24 h in X-Vivo-15 (Lonza, Basel, Switzerland) with 1 X L-glutamine-penicillin-streptomycin (Gemini BioProducts, West Sacramento, CA, USA), 50 ng/mL SCF, 50 ng/mL TPO, 50 ng/mL Flt3L and 20 ng/mL IL-3 (PeproTech, Rocky Hill, NJ, USA). Prestimulated cells were transduced with viral supernatants, and 24 h after transduction, cells were collected for *in vitro* myeloid differentiation cultures. Transduced human BM CD34+ HSPCs were cultured in Basal BM Medium (BBMM: Iscove's Modified Dulbecco's Medium [IMDM] [Life Technologies, Grand Island, NY], 1 X L-glutamine-penicillin-streptomycin, 20% fetal bovine serum, 0.52% Bovine Serum Albumin) with recombinant human cytokines of 5 ng/ml interleukin-3, 10 ng/ml interleukin-6, and 25 ng/ml c*KIT* ligand (hSCF) (PeproTech) at 37°C, 5% CO_2. Cells were maintained in culture for 12 days with the addition of fresh BBMM and cytokines every 4 days. After 12 days, the cells were harvested for genomic DNA extraction and VCN analysis by ddPCR as described above.

Viral RNA analysis by ddPCR

RNA was extracted using either the RNeasy Plus Mini Kit (Qiagen, Hilden, Germany) or the QIAmp Viral RNA Mini Kit (Qiagen). 1 ug of RNA were treated with DNAse I (Invitrogen, Waltham, MA) and then reverse transcribed using random primers, M-MLV reverse transcriptase, and RNAseOUT Recombinant Ribonuclease Inhibitor (all from Invitrogen), following the manufacturer's protocol. Amplification of R/U5, PBS and U3/R regions by ddPCR were conducted to quantify the Initial, Intermediate, and Complete viral RNA. The sequences of the primers and probes are listed in Chapter 2. The cycling conditions were 95°C for 10 min for one cycle, (94°C for 30 s and 60°C for 1 min) for 40 cycles, 10 min at 98°C for one cycle, and a 12°C hold.

p24 Assay

p24 antigen concentration in vector supernatants was measured by the UCLA/CFAR (Center for AIDS Research) Virology Core using the Alliance HIV-1 p24 Antigen ELISA Kit (cat# NEK050, PerkinElmer, Waltham, MA), following the manufacturer's manual.

Statistical Analysis

Descriptive statistics such as the number of observations, mean and standard error were reported and presented graphically for quantitative measurements. Unpaired t tests were used to compare between vectors for outcome measures such as titers, VCN, copies, and percentage of Initial/Intermediate/Complete RNA. In the case of normality assumption violation, nonparametric Wilcoxon rank-sum tests were used. Evaluation of infectivity of vectors was done by comparing the slopes of respective regression lines. For all statistical investigations, tests for significance were two-tailed. A p-value of less than the 0.05 significance level was considered to be statistically significant. All statistical analyses were carried out using statistical software SAS version 9.4 (SAS Institute Inc. 2013) and GraphPad Prism version 8.3.0 (GraphPad Software, San Diego, California, USA).

REFERENCES

1. Ryan, T.M., Behringer, R.R., Martin, N.C., Townes, T.M., Palmiter, R.D., and Brinster, R.L. (1989). A single erythroid-specific DNase I super-hypersensitive site activates high levels of human beta-globin gene expression in transgenic mice. Genes Dev. *3*, 314–323.

2. Peterson, K.R., Clegg, C.H., Navas, P.A., Norton, E.J., Kimbrough, T.G., and Stamatoyannopoulos, G. (1996). Effect of deletion of 5′HS3 or 5′HS2 of the human β-

globin locus control region on the developmental regulation of globin gene expression in β-globin locus yeast artificial chromosome transgenic mice. Proc. Natl. Acad. Sci. U. S. A. *93*, 6605–6609.

3. Grosveld, F., van Assendelft, G.B., Greaves, D.R., and Kollias, G. (1987). Position-independent, high-level expression of the human β-globin gene in transgenic mice. Cell *51*, 975–985.

4. Morgan, R.A., Unti, M.J., Aleshe, B., Brown, D., Osborne, K.S., Koziol, C., Smith, O.B., O'Brien, R., Tam, C., Miyahira, E., et al. (2019). Improved Titer and Gene Transfer by Lentiviral Vectors Using Novel, Small β-Globin Locus Control Region Elements. Mol. Ther.

5. Morgan, R.A., Ma, F., Unti, M.J., Brown, D., Ayoub, P.G., Tam, C., Lathrop, L., Aleshe, B., Kurita, R., Nakamura, Y., et al. (2020). Creating New β-Globin-Expressing Lentiviral Vectors by High-Resolution Mapping of Locus Control Region Enhancer Sequences. Mol. Ther. - Methods Clin. Dev. *17*, 999–1013.

6. Parada CA, R.R. (1996). Enhanced processivity of RNA polymerase II triggered by Tat-induced phosphorylation of its carboxy-terminal. Nature.

7. Kao, S.Y., Calman, A.F., Luciw, P.A., and Peterlin, B.M. (1987). Anti-termination of transcription within the long terminal repeat of HIV-1 by tat gene product. Nature *330*, 489–493.

8. Romani, B., Engelbrecht, S., and Glashoff, R.H. (2010). Functions of Tat: the versatile protein of human immunodeficiency virus type 1. J. Gen. Virol. *91*, 1–12.

9. Feinberg, M.B., Baltimore, D., and Frankel, A.D. (1991). The role of Tat in the human immunodeficiency virus life cycle indicates a primary effect on transcriptional elongation.

Proc. Natl. Acad. Sci. U. S. A. *88*, 4045–4049.

10. Laspia, M.F., Rice, A.P., and Mathews, M.B. (1989). HIV-1 Tat protein increases transcriptional initiation and stabilizes elongation. Cell *59*, 283–92.

11. Fitz, J., Neumann, T., and Pavri, R. (2018). Regulation of RNA polymerase II processivity by Spt5 is restricted to a narrow window during elongation . EMBO J. *37*.

12. Bernecky, C., Plitzko, J.M., and Cramer, P. (2017). Structure of a transcribing RNA polymerase II-DSIF complex reveals a multidentate DNA-RNA clamp. Nat. Struct. Mol. Biol. *24*, 809–815.

13. Ehara, H., Yokoyama, T., Shigematsu, H., Yokoyama, S., Shirouzu, M., and Sekine, S.I. (2017). Structure of the complete elongation complex of RNA polymerase II with basal factors. Science (80-.). *357*, 921–924.

14. Romero, Z., Urbinati, F., Geiger, S., Cooper, A.R., Wherley, J., Kaufman, M.L., Hollis, R.P., De Assin, R.R., Senadheera, S., Sahagian, A., et al. (2013). β-globin gene transfer to human bone marrow for sickle cell disease. J. Clin. Invest. *123*, 3317–3330.

15. Carbonaro, D.A., Zhang, L., Jin, X., Montiel-Equihua, C., Geiger, S., Carmo, M., Cooper, A., Fairbanks, L., Kaufman, M.L., Sebire, N.J., et al. (2014). Preclinical Demonstration of Lentiviral Vector-mediated Correction of Immunological and Metabolic Abnormalities in Models of Adenosine Deaminase Deficiency. Mol. Ther. *22*, 607.

16. Cullen, B.R. (2005). Nuclear RNA export unwound. Nature *433*, 26–27.

17. Mann, D.A., Mikaélian, I., Zemmel, R.W., Green, S.M., Lowe, A.D., Kimura, T., Singh, M., Butler, P.J.G., Gait, M.J., and Karn, J. (1994). A molecular rheostat: Co-operative rev binding to stem I of the rev-response element modulates human immunodeficiency virus type-1 late gene expression. J. Mol. Biol. *241*, 193–207.

18. Battiste, J.L., Mao, H., Rao, N.S., Tan, R., Muhandiram, D.R., Kay, L.E., Frankel, A.D., and Williamson, J.R. (1996). α Helix-RNA major groove recognition in an HIV-1 Rev peptide-RRE RNA complex. Science (80-.). *273*, 1547–1551.

19. Pollard, V.W., and Malim, M.H. (1998). THE HIV-1 REV PROTEIN. Annu. Rev. Microbiol. *52*, 491–532.

20. Masiuk, K.E., Zhang, R., Osborne, K., Hollis, R.P., Campo-fernandez, B., and Kohn, D.B. (2019). PGE2 and Poloxamer Synperonic F108 Enhance Transduction of Human HSPCs with a b -Globin Lentiviral Vector. Mol. Ther. Methods Clin. Dev. *13*, 390–398.